# MASTERARBEIT

**A comparison of ducted and ductless personalized ventilation
by means of a calibrated CFD simulation model**

Ausgeführt zum Zwecke der Erlangung des akademischen
Grades eines Diplom-Ingenieur

unter der Leitung von
**Univ.-Prof. Dipl.-Ing. Dr.techn. Ardeshir Mahdavi**
E 259-3 Abteilung für Bauphysik und Bauökologie
Institut für Architekturwissenschaften

eingereicht an der
**Technischen Universität Wien**
Fakultät für Architektur und Raumplanung

von
**Sepehr Hayatqaiby**
Matrikelnr. 1228544

Wien, im November 2021

# Kurzfassung

In dieser Arbeit werden zwei Varianten von persönlicher Lüftung ( engl. Personalized-Ventilation/PV) verglichen und ihre Wirkung auf die Raumluftqualität in Bürogebäuden untersucht. PV stellt dem Nutzer frische Luft direkt in der „Breathing Zone" (BZ) am Arbeitsplatz zur Verfügung. Darüber hinaus haben PV-Systeme das Potenzial, die Innenraumluftqualität (engl. Indoor Air Quality/IAQ) beim Nutzer zu verbessern und ermöglichen diesem ebenfalls eine individuelle Kontrolle der Frischluftmenge am Ausblasdiffusor. Normale PV-Systeme erfordern einen direkten Anschluss an eine zentrale Luftführungsanlage, was die Installationskosten erhöht und die Innenraumästhetik und die Flexibilität des Bürolayouts beeinträchtigt. Neue anschlusslose (engl. ductless) PV-Systeme ermöglichen die gewünschte Flexibilität durch Kombination einer klassischen Verdrängungslüftung (engl. displacement-Ventilation - DV), um so Frischluft dem Raum und den unabhängigen ductless PV-Systemen bodennahe zuzuführen. Ob PV-Systeme in der Praxis alleine komfortable thermische Bedingungen im Nutzerbereich speziell bei Raumkühlung gewährleisten können, ist nicht sicher. Darüber hinaus könnte entsprechend der einschlägigen Literatur durch die zusätzlich nötige Verdrängungslüftung auch lokal unkomfortable Bedingungen durch den kalten Luftzug in Bodennähe entstehen.

In dieser Arbeit werden beide Varianten vergleichend untersucht, um folgenden Fragen zu beantworten und Zweifel an der Funktionalität auszuräumen. Lohnt es sich, ductless PV zu wählen , um dadurch mehr Flexibilität bei der architektonischen Gestaltung zu haben? Ist eines der Systeme im Bezug auf thermischen Komfort und IAQ im Nutzerbereich überlegen? Inwieweit beeinflusst die Qualität der Verdrängungslüftung die Wirksamkeit von ductless-PV?

Für den Vergleich der Systeme wurde ein kalibriertes CFD-Modell und das Konzepts des Luftalters benutzt. Die Möglichkeit, Frischluft zuzuführen und

Luftschadstoffe durch das Lüftungssysteme zu entfernen, wurde anhand von fünf verschiedenen Szenarien beurteilt. Zusätzlich wurde anhand eines realen Beispiels, die Wirkung der Verdrängungslüftung und der zugehörigen Einlassdiffusoren auf die Funktion der ductless PV untersucht. Basierend auf diesen Erkenntnissen wurden vier alternative Prototypen von Einlassdiffusoren vom Autor vorgeschlagen und mit derselben Methodik wie zuvor untersucht.

# Summary

This research aims to compare two variations of Personal Ventilation (PV) systems and address their effects on indoor environmental characteristics in office buildings. Personalized ventilation (PV) aims to supply clean air directly to the Breathing Zone (BZ) of the occupants, mostly in places with workstations and office cubicles. In addition, PV systems have the potential to improve Indoor Air Quality (IAQ) by increasing individual control over discharged air from inlet diffusers into the BZ. However, ducted PV requires additional duct work, which increases the cost of the installation and negatively affects indoor aesthetics and the flexibility of the room layout. Ductless PV is a design attempt to overcome those disadvantages. In contrast to ducted PV solutions ductless Systems can't be deployed individually and works only in conjunction with a classical Displacement Ventilation (DV). It is, nevertheless, not definitely clear that a PV system alone could provide the accepted level of thermal comfort in the occupant's position. Moreover, according to the literature, one problem of the DV systems could be the sensation of the cold draught at the feet level.

The performance of these two variants should be studied side by side to answer the following questions and to dispel doubts about their hypothetical shortcomings. Is it worth not having ductworks to have more architectural design flexibilities; Is any of these two systems superior to another in terms of providing thermal comfort in occupant's position and a better IAQ in the BZ; and to what extent could DV's performance affect the effectiveness of ductless PV?

This project implements this comparison by means of a calibrated CFD model and the concept of age of air. The ability to provide fresh air and remove air pollutants by ventilation systems is assessed in five different scenarios in which they operate individually or in conjunction with each other in an office mock-up. Additionally, in an attempt to examine the effect of the DV inlet diffuser on the performance of the ductless PV, four alternative prototypes of DV inlet diffusers are proposed by the researcher and studied with the same methodology.

# Acknowledgments

First and foremost, I would like to express my appreciation and thanks to my main advisor Univ.-Prof. Dr. Ardeshir Mahdavi for his guidance, and support during the project.

Secondly my special gratitude to my co-advisor Associate Prof. Dr. Matthias Schuss for his assistance, and presence throughout the project, and for his brilliant comments and suggestions. Without his help this work would not be possible.

I would also appreciate all highly motivated, supportive, and inspiring colleagues of the Department of Building Physics and Building Ecology, especially technical supports of dear Mr. Joseph Lechleitner, and caring Ms. Elisabeth Finz.

I would also like to thank Dr. Ondrej Sikula from Faculty of Civil Engineering of Brno University of Technology for his consultant and scientific support with CFD simulations.

Furthermore, I am extremely grateful to Dr. Mahnameh Taheri for her advice and encouragement.

I extend my gratitude to dear colleagues Dr. Hamidreza Shirdel for his intellectual support.

In particular, I am grateful to my beloved parents, whose support, inspiration and encouragement enabled me to complete this work.

for…

My Beloved Parents

V

# Contents

# Chapter 1

# Introduction

## *1.1  Overview*

Personalized ventilation (PV) aims to supply clean air directly to the Breathing Zone (BZ) of its users, mostly for the desk or workstations. On the other hand, PV systems have the potential to improve Indoor Air Quality (IAQ) by increasing individual control over discharged air from inlet diffusers into the BZ. The possibility of reducing energy consumption because of decreasing the conditioned air demand is also considerable.

Each personalized ventilation system may be controlled by the user at the local supply stations. Also, it can achieve an optimized microenvironment based on individual preferences. However, ducted PV requires additional duct work, which increases the cost of installation and negatively affects indoor aesthetics and the flexibility of room layout. Ductless PV has been developed in order to overcome those disadvantages.

Ductless PV is a variation of personalized ventilation systems which combines the advantages of PV with flexibility and simplicity of ventilation system design. Ductless PVs are installed at each workstation and transport the air which is distributed over the floor by the DV to the breathing zone of each user. Physical measurements in a climate chamber that were made with breathing thermal mannequin revealed that inhaled air supplied by ductless PV is as clean as that supplied by DV alone, and under some conditions even cleaner, depending on the type and location of pollution sources and disturbing factors present in the room (Halvonová B., 2010). Previous studies have shown that inhaled air temperature decreased with ductless PV compared to DV alone as ductless PV reduces the mixing of cool and clean displacement air with warm and polluted room air (Halvoňová B., 2010).

In practice, providing occupants with individual control over a cool personalized flow supplied at higher velocity makes it possible to allow increasing indoor air temperature without causing thermal discomfort. This strategy may contribute to a reduction in building energy use by reducing the cooling requirement. At the same time, ductless PV users benefit from a higher quality of inhaled air, as it can be filtered by the ductless PV (Dalewski, et al., 2012). Combining ductless PV with efficient air cleaning technologies may also be beneficial if ductless PV is used with Mixing Ventilation (MV) or natural ventilation. In this case ductless PV filters and may also disinfect polluted indoor air, therefor the inhaled air quality is better than what is provided by a desk fan, which can supply air at higher velocity without any possibility of filtering it.

A DV system consumes energy efficiently it removes exhaust air from space with a temperature that is several degrees above the room temperature in the occupied zone. This process allows a higher inlet air temperature at the same load compared to MV (Nielsen, 1995).

Regards to the short aforementioned introduction, this project is an attempt to compare the ducted and ductless variations of PV systems using quantitative methods and disambiguate the uncertainties about their performances.

## 1.2 *Motivation*

PV systems provide a potential for system efficiency over conventional systems which ventilate the whole space. Nonetheless they might result in a varied thermal environment. Consequently, the BZ reach to comfort temperature while the rest of the room might remain slightly warmer or cooler depending on the seasonal air conditioning program. In addition, there is speculation that the occupants could endure an unpleasant indoor air quality despite the immediate supply of fresh air at the workstations in less frequently used regions of the room such as storage areas. But, conversely, it might help to alleviate fatigue or thermal boredom associated with exposure to constant temperatures (Kwok, 2000). The supply of clean air near to the breathing zone has the potential to improve inhaled air quality which may help to improve worker performance. And, most importantly, it

gives occupants a degree of freedom to control over their personal thermal environment by allowing them to adjust air-flow rates and direction at any time. PV systems could also have the potential to reduce energy use by reducing the amount of conditioned air delivered to a workspace. They have been for many years suggested as an alternative to traditional air-conditioning systems.

The main motivation of this study was to assess the functionality of two variations of PV systems with regard to indoor air quality and thermal comfort. To this end the measured data and simulation results provide a basis to document the indoor conditions and their implications for the occupants. The study employs also the application of calibrated CFD models and the concept of age of air toward a better understanding of the ventilation effectiveness and estimation of the indoor air condition as an input data for calculation of predicted mean vote (PMV) values.

## 1.3 Objective

In spaces which cannot be ventilated through the manual operation of windows and are ventilated by means of mechanical ventilation systems, some laboratory experiments have been carried out testing these delivery systems. For instance, correctly designed PV can supply air to the breathing zone such that 100% of the breathed air comes from the outlet and not from mixed air in the space (Niu, et al., 2007). Moreover, greater control over the movement of air in the breathing zone can also contribute to improved occupant satisfaction (Bauman, et al., 1993), not to mention the fact that the design used in this study has already been tested (Halvoňová B., 2010). On the other hand results of some field studies suggest that ductless PV is prone to make some problems for the occupants such as supplying air from shoe level to the BZ (Taheri, et al., 2016).  However, some physical measurements confirmed the working principle of ductless PV in conjunction with DV.

Since the previously described facts produce disambiguation about some aspects of these systems, their performances should be studied side by side with a numerical methodology. There are few literatures available regarding the quantitative analyze of these systems, which are not enough to provide answers for the following uncertainties. The question is how near the thermal

comfort would be provided by a ductless PV together with DV versus the individual operation of PV; and does the compromise of having a potential lower IAQ in the occupant's BZ zone justify architectural flexibility and economical aspects of the ducted PV system.

This study is an effort to examine the effects of air distribution quality supplied by DV on the performance of ductless PV with the criteria of providing acceptable thermal comfort and perceived air quality in the BZ of the occupant. The project aims to provide reasonable answers for the hypothesis by simulating the condition of an occupant in an office mock-up under multiple ventilation scenarios.

## 1.4 Thesis Structure

After the introduction you will find this work consisting of 6 chapters as described below.

Chapter 2, background, provides general information about PV, and its functionality in conjunction with DV. Additionally, some information about the prediction of air quality by CFD, ventilation effectiveness and Thermal comfort is also provided.

Chapter 3 is the portrayal of the methodology which is used in order to implement this comparison project. The results of the physical experiments which are carried out in a laboratory under controlled condition are presented in this chapter as a part of the process of the calibration which leads to prepare a foundation for the final work.

Chapter 4 reports the results of a series of CFD simulations and discuss the findings in the discussion section.

Chapter 5 contains a final conclusion and assess the hypothesis of this research as the contribution of this work.

# Chapter 2
# Background

In this chapter you will find general information about PV and the associated ventilation system as well as some information on indoor air quality assessment by Computational Fluid Dynamics (CFD), ventilation efficiency and thermal comfort.

## *2.1  Personalized Ventilation*

Personalized Ventilation (PV) is a generic term used for desk- or workstation mounted air-conditioning that deliver conditioned air directly to the breathing zone of office workers. PV systems have the potential to improve occupant comfort by increasing individual control over air conditioning outlets as well as by improving indoor air quality at the point of use.

Positive effects of personalized ventilation on health, thermal comfort and performance of the occupants have been documented (Kaczmarczyk J., 2004), including its ability to protect occupants against infectious agents (Cermak R., 2006) (Nielsen, et al., 2007).

Depending on the seasonal HVAC scenario each personalized ventilation user has the ability to control local cooling or heating and is able to achieve an optimized microenvironment based on individual preferences. PVs are found in two forms of ducted and ductless. Ducted PV requires additional duct work, which increases the cost of installation and demands some additional construction and the flexibility of room layout. Nonetheless ductless PV do not have those disadvantages. Ductless PV is a more recent ventilation system which combines the advantages of ducted PV with flexibility and simplicity of design. This variation cannot nevertheless deliver fresh air to the destination independently. At each workstation it draws in the distributed air in ankle level by DV and brings it up to the BZ of each user. Physical measurements in a climate chamber that were made

with breathing thermal manikins revealed that inhaled air supplied by ductless PV is as clean as that supplied by ducted DV alone, and under some conditions even cleaner depending on the type and location of sources of pollution (Halvonová B., 2010) and disturbing factors present in the room (Halvoňová B., 2010). Previous studies have shown that inhaled air temperature decreased with ductless PV compared to DV alone as ductless PV reduces the mixing of cool and clean displacement air with warm and polluted room air (Halvoňová B., 2010).

In practice, providing occupants with individual control over a cool personalized flow supplied at elevated velocity makes it possible to allow indoor air temperature to increase without causing thermal discomfort. This strategy may contribute to a reduction in building energy use by reducing the cooling requirement. At the same time, ductless PV users benefit from a high quality of inhaled air, as it can filter air through its intake box (Dalewski, et al., 2012). Combining ductless PV with efficient air cleaning technologies may also be beneficial if ductless PV is used with mixing ventilation or natural ventilation. In this case ductless PV filters and may also disinfect polluted room air, so that the inhaled air quality is superior compared to what is provided by a desk fan, which can supply air at elevated velocity without any possibility of filtering it.

## 2.2  *Displacement Ventilation*

To distinguish the DV from the other varieties of ventilation systems it is necessary to understand its fundamentals. The ASHRAE Handbook Of Fundamentals (HOF) classifies room air diffusion systems as mixing, displacement, unidirectional, and underfloor (ASHRAE, 2001). The Mixing Ventilation (MV) systems are descried by HOF as those discharging the conditioned air from outlets near either the ceiling or floor at velocities much greater than those acceptable in the occupied zone to achieve a level of air mixing that creates relatively uniform air velocity, temperature, humidity, and air quality conditions in the occupied zone. In contrast, the principle of DV is based on the natural buoyancy forces which created by the convective flows from heat sources in the space. After the fresh air enters the room with a few degrees cooler than the room temperature, it will flow near the floor in the ankle level, interacts with heat sources and raise into the upper or

stratified zone. Typically, the supplied air from DV in the range of 18-20˚C versus the supplied air by MV is around 12˚C. Over time the indoor air forms layers with stratified temperature zones, with the warmest temperatures located near the ceiling. Thus, the air will be displaced towards the outlet and causes the contaminants exits the room without being mixed with the fresh air so much. Figure 1 summarizes the working principle of DV and the terminology is used to address different zones and regions of the air in the system. In contrast to MV, in the ventilated area, if the system is correctly designed, there are no zones of stagnant air. In general, the warmest layer contains the most impurities. By placing the recirculation point in or near the ceiling, we can maximize the removal of polluted air. This approach not only improves the air quality in the occupied zone, but also contributes to the maintenance of thermal comfort.
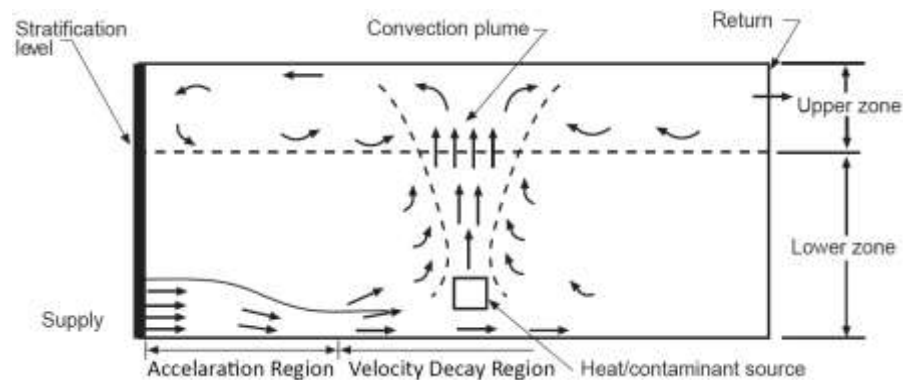


*Figure 1 Displacement Ventilation Principle (Titus-HVAC, 2021)*

Traditionally, DV is combined with a Dedicated Outdoor Air System (DOAS), however if the regional code allows, it can also be used in a variety of other HVAC designs. DV systems, as commonly used in Europe, do not use recirculation of exhaust air, although this is not discussed in the HOF. The recirculation is usually done because the flow rates required for ventilation are too low for heating or cooling purposes. Therefore, to meet the heating or cooling heat transfer rates and keep the supply temperatures within a reasonable range, higher supply flow rates are needed. Since the recirculation poses a problem for evaluating ventilation performance using measures derived from the concept of age-of-air, the design used in the laboratory for this project also provided fresh air through a DOAS system.

Because DVs remove pollutants from space according to the buoyancy principle, they perform better than MVs in this respect. According to table 6-2 of ASHRAE Standard 62.1-2004, the air change effectiveness, $E_z$, of DV is 1.2 versus 1.0 of MV. Therefore, the DV system should offer a better indoor air quality compared. DV system provide flexibility in design and since the volume of air supplied is smaller it has other advantages too as well as being quiet and energy-efficient. This makes DV ideal for applications in restaurants and cafeterias, schools, theaters, halls or conference rooms, places of worship, lobby areas, offices, casinos, and industrial spaces.

## 2.3 *Ventilation Performance Assessment*

The air is generally ventilated constantly in rooms due to a constant difference in pressure. This gradient could be also generated by a mechanical ventilation system. Engineers who are tasked with designing Heating, Ventilation, and Air-Conditioning (HVAC) systems for buildings will need to assess the indoor air quality to ensure meeting minimum regulatory, optimum health requirements, and thermal comfort for occupants. The regulations in every country draw guideline for them by studying the spaces from a comprehensive point of view considering minimum ventilation flow rates according to the typology, surface properties, contamination and heat sources and etcetera. In certain cases, despite fulfilling these prescriptive requirements, there are regions in the ventilated area with excessive or deficiency of supplied fresh air. Such cases, incidentally, are not rare, although predicting the air flow pattern in a space generated by a ventilation system in the design stage could preclude them from occurring. One of the useful tools for assessing the efficiency of a ventilation system in terms of distributing fresh air consistently in a room and removing contaminants effectively is measuring the local mean age of air throughout the space.

To comprehend the concept of age of air we may assume that the molecules of outdoor air begin their life in a room as they enter a building or a ventilation system. When they arrive at a given location in a room after a time that varies from one particle to the other. This variable is called the residence time of the particle in the room, or its age. However, the longer a small volume of air spends in a room, the more it will be contaminated by pollutants. The Local Mean Age (LMA) is a statistical value of the time that

all the particles of fresh air require to travel from the supply point to the point of study. The lower this value is it suggests the system has a better ability for air exchange rate at that point.

The dimension of the age of air is time and it is measured in seconds or minutes, hence it is not a technical ventilation effectiveness measure, but can describe or give indication of problems within a space or zone (PADILLA-MARCOS , et al., 2017). ASHRAE Handbook (1997) defines the Air Change Effectiveness (ACE) as a description of a system's ability to deliver air from ventilation system to a space, whereas ventilation effectiveness is a description of an air distribution system's ability to remove internally generated pollutants from a zone or space. However, ACE and the air change rate value are not individually sufficient to describe the air flow pattern in a space and cannot address the issues of the system comprehensively.

Furthermore, studying profiles of the age of the air alongside velocity and temperature is useful for the detection of possible shortcuts and dead zones and for the checking of the general airflow pattern in ventilated areas. In order to deliver fresh air effectively to the occupants, the airflow patterns should be principally designed in an organized way, thus the contaminants be evacuated efficiently as possible and not being mixed with indoor air.

## 2.4 Indoor air quality assessment by CFD

Considering the fact that in industrialized countries, people spend more than 90 percent of their time in an enclosed environment, providing an acceptable air quality for the inhabitants is a key component for the well-being of the inhabitants (H.B.AWBI, 1991). Therefore, one of the main concerns in building performance studies is supplying the occupants with a comfortable thermal condition. In order to interpret the level of comfort perceived by the building occupants, it is necessary to take into account the effects of the physical environmental parameters of the interior, human factors, physiological and psychological parameters. In this field, researchers typically use both experimental and computational methods. Surveys, for example, can be used to assess the indoor environmental conditions as perceived by the occupants. Furthermore, thermal comfort calculations that use measured environmental variables as input can aid in the assessment of

indoor climate and thermal comfort (Bordass & Leaman, 2009), It is therefore important to consider and address possible sources of error, such as distortions in the responses of the occupants in surveys or sampling errors in measurements (Lesbirel, 2012). An effective method to study indoor air environment is computational fluid dynamics (Wiercinski & Skotnicka-Siepsiak, 2008). Although CFD programs are designed for indoor air quality assessments but provision of empirical evidence is necessary to ensure the reliability of the outcomes (Chen & Srebric, 2002).

CFD is a practical tool to quantitatively predict thermal-fluid physical phenomena in indoor environmental modeling. Equation 1 is the common form of the Navier-Strokes, which is the governing equation of mass, momentum, and energy, that describes the airflow, convective heat transfer, and species dispersion in the indoor environment. It is derived from the physical phenomenon that the change in time of a variable at a location is equal to the amount of the variable flux as well as momentum, mass, thermal energy, etc.

$$\frac{\partial}{\partial t}(\rho\phi) \;+\; \frac{\partial}{\partial x_j}\big(\rho U_j\phi\big) \;=\; \frac{\partial}{\partial x_j}\big(\Gamma_\phi\frac{\partial\phi}{\partial x_j}\big) \;+\; S_\phi \qquad (1)$$

$$\text{Transient} \;+\; \text{Convection} \;=\; \text{Diffusion} \;+\; \text{Source}$$

To investigate airflow and heat transfer an indoor environment the boundary conditions need to be defined. Generally they describe the physical conditions for each case study, while the mathematical equations build the conceptual model. The CFD code, for instance the Autodesk CFD program which is used in this work use the governing equations to solve the problem. Although the computed results alone are not enough and need inspection and interpretation of an expert. Figure 2 illustrates the abstract blocks of the whole process.
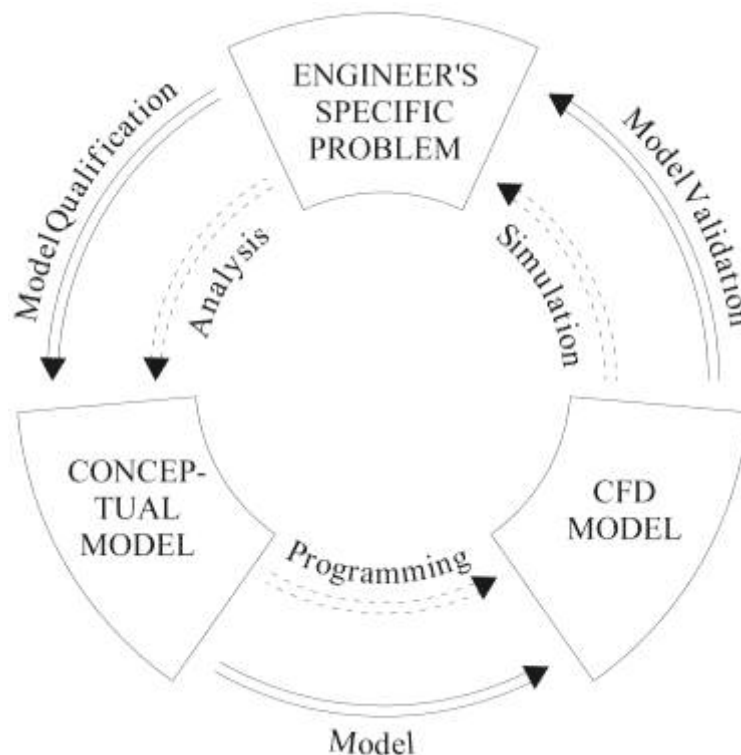
*Figure 2 Procedure for CFD Modeling of an Indoor Environment and Corresponding Phase (Modified from Schlesinger 1979)*

CFD is used to determine the fluid flow, heat transfer, and chemical species transport in a wide range of Architecture, Engineering and Construction (AEC) applications (Ladeinde F, Nearon M., 1997). CFD analysis is a practical and quick tool that designers and engineers benefit from throughout their work, especially in the early design phases. However, the cost, effort, and time of deployment, and expectations of its performance determine its usefulness in the specific application (Martin, 1999). Additionally, some studies show that its use does not necessarily guarantee the accuracy of the outcome results (Baker & Gordon, 1997) (Chen, 1997), it requires engineering judgment and depend highly on the experience of the user (Post, 1994). This leads to an instructive implementation of CFD analyses with **verification**, **validation**, and **reporting** the indoor environmental CFD simulation. However, the extent of CFD capabilities in modeling is not yet sufficiently developed to the extent in order to develop a written standards (AIAA, 1998). Nevertheless, some institutes already have provided guidance for performing CFD calculations. For instance the American Institute of Aeronautics and Astronautics (AIAA) defines verification as "The process of determining that a (physical/mathematical) model implementation

accurately represents the developer's conceptual description of the model and the solution on the model", and defines validation as "The process of determining the degree to which a (CFD) model is an accurate representation of the real world from the perspective of the intended uses of the model" (AIAA, 1998).

### 2.4.1 VERIFICATION

Verification is the process of determining whether a simulation computer program works as intended, comparable to the process of debugging programming errors. AIAA defines an error as "a recognizable deficiency in any phase or activity of modeling and simulation that is not due to lack of knowledge". The uncertainty, in contrary, is the product of lack of knowledge which may be remedied in the validation process.

The first step in the verification process is to define benchmark cases with one or more features of the four basic physical phenomena of the indoor environment, namely the airflow, heat transfer, mass transfer (species concentrations and solid and liquid particulates), and chemical reactions (combustion). Therefore, special attention should be paid to the following aspects:

• Basic flow and heat transfer (convection, diffusion, conduction, and/or radiation)

• Turbulence models

• Auxiliary heat transfer and flow models

• Numerical methods

• Assessing CFD predictions

Additionally, reviewing the code manual and fundamentals of the CFD program usually help the user to understand how to break down the problem and approach to a feasible process for the verification. Hence, the assessing of verification examples provided by the CFD developers can determine whether the program is basically able to simulate the indoor environment of interest. The data available for verification often comes from high-precision experimental measurements that are accurate with few human error (Chen & Srebric, 2002).

**Flow and Heat Transfer**

The heat transfer from available sources in the room including building envelopes, the residents, and the air supply through diffusers influence the airflow in space. Therefore, the flow in an office for example is a mixed convection combined with conductive, convective and radiating heat and mass transfer.

For Verification one or more cases that represent different flow characteristics should be investigated. Since mixed convection is the focus of this study, the parameters to be solved are air velocity and temperature.

**Turbulence Models**

The flow in the fluids can be laminar or turbulent. The unsteadiness in the flow pattern is called turbulence. Figure 3 illustrates how the flow pattern changes from laminar to turbulence in a classic flow over a flat plate. It displays schematically the eddies and circular motions that occur throughout the flow domain.
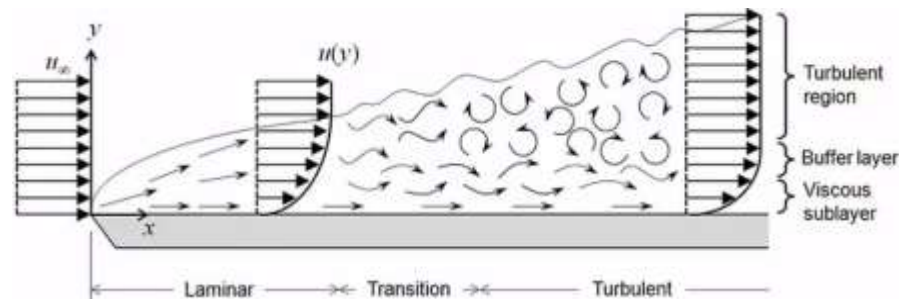


*Figure 3 transition of a flow over a flat plate*

*from Laminar to Turbulent (Comsol, 2021)*

The turbulence in the flow is determined with two parameters. The Rayleigh (Ra) and Reynolds (Re) number are dimensionless numbers that characterizes the flow regime. The higher value of these numbers denote the change in the flow from laminar to turbulent.

The Ra and Re numbers are defined correspondingly as equation (2 and equation (3. The Ra and Re numbers are in most indoor airflows are high, thus the overall flow pattern is turbulent, however, the airflow can be laminar or weakly turbulent in some regions of the space.

$$\text{Ra} = \frac{T_{Tdiff}}{T_{TconvU}} \tag{2}$$

*Ra = Rayleigh Number*
*$T_{Tdiff}$ = time scale for thermal transport via diffusion*
*$T_{TconvU}$ = time scale for thermal transport via convection at speed U*

$$\text{Re} = \frac{UL}{\upsilon} \tag{3}$$

*Re = Reynolds Number*
*U = flow speed*
*L = a characteristic linear dimension*
*$\upsilon$ = kinematic viscosity of the fluid*

There are mainly two approaches to solve the Navier-Stokes equations in CFD calculations. The first method is direct numerical simulation, a time-consuming attempt to solve the equations without approximations, which in practice is not feasible for indoor simulations with the processing power of current computers. In contrary using turbulence model approximations makes designers able to carry out the calculations with the current available processing power of computers. The turbulence models are divided into two groups of Large-Eddy Simulations (LES) and turbulent transport models or Reynolds averaged Navier-Stokes models (RANS). LES needs fewer assumptions comparing to RANS and are usually used for solving transient, time-dependent flow. To achieve convergence in the solution it calculates a mean of the time-dependent flow fields versus RANS, in which the mean flow variables are found by using turbulent-transport models. The less time consuming RANS model is usually preferred for indoor simulations, however the user should understand the differences between these models and choose the optimal model based on the accuracy and application required. It is also recommended to start with simpler models, such as the standard $k$-$\Sigma$, and proceed to a more complicated model if the satisfactory results are not achieved (Launder & Spalding, 1974).

**Auxiliary Heat Transfer and Flow Models**

The flow in the indoor environment consists of radiative, conductive, convective heat transfer phenomena, and also sometimes combustion, participating media radiation, and particle transport in air-liquid, air-solid,

and air-liquid-solid phases. Since the calculation of all those phenomena simultaneously will be very time consuming even for the computers, therefore, applying appropriate auxiliary heat transfer and flow models is necessary.

**Numerical Methods**

A CFD code commonly uses finite-difference, finite-volume, and finite-element methods, for discretization of the continuous space and time to compute variables at only grid points. To meet the requirements of different applications the discretization method of the space and type of the numerical grid should be chosen carefully. To verify the model in this step user should chose the discretization scheme based on the comparison of the obtained results. The grid size and time steps must be also refined to reduce the error to the acceptable level. Not to mention that the time step applies only to transient flow simulation. Doubling the grid number in each step and comparing the solutions is a common technique in this step (Wilcox, 1994). Essentially, the discretization leads to errors in the numerical solution that decrease as the grid size and time step approach zero.

**Assessing CFD Predictions**

Both qualitative and quantitative comparison of CFD results need to be assessed with data from the experiment, analytical solutions, and direct numerical simulations. Error analyses need to be detailed; the results should serve as a basis to judge whether the CFD code can be used for indoor environment modeling.

The goal of the verification process is to create a CFD model which is able to correctly calculate the airflow and heat transfer in an indoor environment. It should be noted that while the accuracy of the model depends on the criteria defined and the amount of effort required to enter the data by the user, the discrepancies between the results and the measured data depend on errors in the CFD code or its inherent inability to solve the problem.

## 2.4.2 VALIDATION

Validation is the process of determining whether the conceptual model is an accurate representation of the actual system being analyzed. Validation and

verification have rather similar definitions. To understand the difference between these two processes, they can be defined in simple terms, as verification checks that the model was built correctly, in contrast, validation proves that the model is the right model for the specific application. Reliable measurement data are therefore required to validate a model for the indoor environment. In order to calculate the level of error and uncertainty in the CFD simulation, a data set from an experiment is needed that includes all the important physical phenomena of the problem of interest. Basically validation confirms quantitatively all of the aspects of the model discussed in the verification process. Therefore the created model for this purpose should include all the important airflow and heat transfer features, and a full geometric configuration.

The measured data in an environmental chamber usually have a relatively high degree of uncertainty and large errors. They may also contain biased errors and random errors which should be reported as part of the validation.

To create the model of course not all of the initial and boundary condition information for a complete indoor environment are obtainable from on-site measurements, hence reasonable assumptions are needed to make a CFD simulation feasible. Furthermore, it is not necessary to start with a very complicated case and a subsystems or a system with some of the flow features can also be used for validation purpose (Chen & Srebric, 2002). For example, using simple geometry and convection alone instead of considering all three heat transfer disciplines can reduce the time and amount of calculations and consequently generate more reliable data with fewer errors for validation.

## 2.4.3 REPORTING OF CFD RESULTS

Systematic reporting during the entire verification and validation process of a CFD simulation is necessary so that readers can easily understand the work steps and the process of drawing conclusions.

From verification to validation, reporting the CFD results must include the information discussed in all sections, e. g. experimental design, CFD models and auxiliary heat transfer and flow models etc. and the assessment and the expert opinion based the calculated results. Since the indoor environment

systems are usually complicated, and the corresponding experimental data may contain biased errors and random errors, these errors should be reported as well.

## 2.5 Thermal Comfort

The human temperature determines the physiological thermal comfort of the occupant, as the human body exchanges heat with the environment. Heat is exchanged by radiation, convection and evaporation.

ASHRAE Standard 55-2004 defines Thermal Comfort as *"The condition of mind that expresses satisfaction with the thermal environment, and is assessed by subjective evaluation."*

Thermal comfort is an important consideration in the design and layout of dwellings that are occupied by people. It is a way to characterize specific conditions in which a known fraction of occupants will find the environment thermally acceptable. Several environmental and personal factors are considered when assessing thermal comfort, Table 1.

*Table 1 Environmental and Personal Factors of Thermal Comfort*

| Environmental Factors | Personal Factors |
|---|---|
| Temperature | Activity Level |
| Thermal Radiation | Clothing |
| Relative Humidity | |
| Ambient Air Velocity | |

Different concepts have been applied to derive a practical relation between the thermal environment and the physiological and psychological well-being of the occupant. The Predicted Mean Vote (PMV) is one of the most recognized thermal comfort models which is adopted as an ISO standard. The PMV index predicts the average response of a large group of people. ASHRAE defines a seven-point thermal sensation scale as Table 2.

*Table 2 PMV Thermal Sensation Scale*

| -3 | -2 | -1 | 0 | +1 | +2 | +3 |
|---|---|---|---|---|---|---|
| Cold | Cool | Slightly Cool | Neutral | Slightly Warm | Warm | Hot |

The PMV index is expressed as equation (4.

$$PMV = (0.303 \ e^{-0.036M} + 0.028) \ L \qquad (4)$$

*PMV = Predicted Mean Vote*
*M = metabolic rate*
*L = thermal load*

Thermal Load is defined for a person at comfort skin temperature and evaporative heat loss by sweating at the actual activity level as the difference between the internal heat production and the heat loss to the actual environment.

Additionally, this concept is extended to allow estimation of The Predicted Percentage Dissatisfied (PPD). This model is also used to estimate the thermal comfort satisfaction of occupants in a space and is defined in terms of the PMV, and adds no information to that already available in PMV. However, it increases as the predicted mean vote moves away from zero in either direction.

# Chapter 3
# Methodology and Implementation

This chapter draws a portrait of the methodology which is used in order to implement this comparison project. In every step the corresponding implemented work task is also presented.

As it is elaborately explained in 2.4 Indoor air quality assessment by CFD, there is a need for implementing the CFD with an instructive methodology of **verification**, **validation**, and **reporting** the indoor environmental CFD simulation.

The **verification** aspect is needed to make sure that relevant physics of the problem are being properly addressed. The **validation** aspect is needed to demonstrate that the CFD user can successfully model problems for which either experimental data or reliable semi-empirical correlations are available. The **reporting** aspect is needed for CFD users to communicate to others the pertinent details of how the analysis was performed and the major results.

In indoor environment modeling, CFD is used to quantitatively predict thermal-fluid physical phenomena. The relevant aspects of this physical phenomena corresponding this project are as followed:

1. Simultaneous heat flows (e.g., heat conduction through the building enclosure, heat gains from heated objects indoors, and solar radiation through the building fenestration)
   Since the mock-up was erected inside of the enclosed area of the laboratory there was no solar radiations (except the radiation from the occupant and other heat sources).

2. Phase changes (e.g., condensation and evaporation of water contents)
   In order to simplify the calculations evaporations from the occupant is not considered in the simulations.

3. Chemical reactions (e.g., combustion in case of a fire)

   This project studied the indoor air quality in normal situations. Studying performance of the PV and ductless PV in case of fire could be considered by the readers as a future complimentary work to this project.

4. Mechanical movements (e.g., fans and occupant movement)

   Throughout this work the occupant is assumed sedentary thus the only source for mechanical air movement will be inlet diffusers of the ventilation systems; DV supply diffuser, PV diffuser, and ductless PV diffuser and air intake box.

The results of the physical experiments which are carried out in the laboratory under controlled condition are also presented. It is a part of the process of the calibration which leads to prepare a base CFD simulation for the final comparison. The process of comparing the performance of different ventilation systems in a space requires a generic base model. In the next step this base CFD model should be calibrated with the aid of measurement results of a physical model with specific boundary conditions.

After producing a reference CFD model it could be adopted for comparison scenarios of this study.

## 3.1 Experimental Set-up

It is essential in the process of the reporting of CFD results to give a detailed description of the experimental design, including the thermal and flow conditions of the test environment. The information provided should also be sufficiently detailed so that other people could repeat the simulation.

### 3.1.1 Experimental Equipment

During the course of measurement two parameters, air temperature and air velocity, were the subject of this study.

Since the indoor air conditions are dealing with very low air speeds the appropriate type of equipment for measuring air velocity in this set of experiments are thermoelectric or hot wire anemometers. Hot Wire Anemometers heat a wire to a specified temperature and then measure the rate of cooling. This rate is proportional to air speed. Thermoelectric

measurement provides fast response times and excellent sensitivity to very low air flows. The ThermoAir6/64 are determining degree of turbulence especially for HVAC applications and are meant to measure flow range of 0.15 - 5m/s with accuracy of ±1,0 % v.E. ±1,5 % v.M.

Since thermistor sensors react quickly to temperature alterations, plus they are being placed without difficulty on the surfaces and make a good contact with them, they were selected for measuring the surface temperatures. In this case Negative Temperature Coefficient (NTC) were the choice. It was tried to dedicate at least one sensor to each wall or window surface, however the total number of sensors could not exceed the amount of logger connections. Eventually six channels have been set aside for walls, ceiling and floor temperatures, three channels for windows, two for air temperature and velocity at reference point, one for outlet air temperature, and ultimately ten for air temperatures and velocities at five points of measurement station.

The measurement station was comprised of five anemometers coupled with thermometers installed in a row on a beam carrying with an adjustable tripod, Figure 4. The whole setup of sensors was connected to three ALMEMO data loggers recording the measured data throughout every step of experiment.



*Figure 4 A view of the measurement station and surface sensors during the test*

### 3.1.2 Calibration of the Sensors

The task of assuring accuracy of measurement is critically important. Prior to experiment, examiner should ensure the reliability of connections and loggers and attempt to calibrate the measuring equipment.

**Thermometers**

To assure temperature accuracy, it is necessary to maintain a temperature reference standards capability. This must include equipment and procedures that permit calibration of operating devices with temperature standards in a way that ensures minimum uncertainty. A climate control chamber, Figure 5 (a), equipped with advanced control system (JUMO IMAGO 500 – Multichannel Process Controller and Program Controller) was used to maintain the temperature and humidity constant for the period of every intended setpoints. Figure 5 (b) show arrangement of the sensors inside the climate control chamber.

The climate control operated one hour in every step of the experiment to bring the indoor air of the chamber to a steady state condition. Two loggers recorded two minutes of measured data by temperature sensors located inside the climate chamber. Setpoints started from 18˚C and raised by 2 degrees increments up to 30°C.

(a)                                    (b)



(c)

*Figure 5 Climate control chamber (a), Position of the sensors (b)*

*An instance of the settings for 18˚C Setpoint (c)*

The accuracy of the reference for thermometers must have an accepted level of uncertainty. In this case for expected error of +/- 1 kelvin it should be in the range of one up to two tenths of degree. As an instance Figure 5 (c) shows that the climate control was able to bring the chamber air precisely to the setpoint.
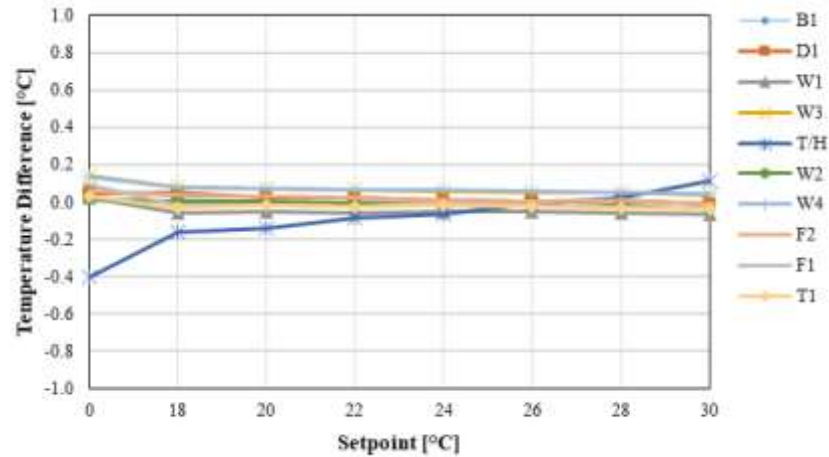
*Figure 6 Temperature Difference between Thermometers and Setpoint*

In Figure 6 it appears the maximum deviation from the setpoint occurs in 18˚C which is less than 0.4 kelvin. Figure 6 shows that all of the relative errors are below 1% which confirms the accuracy of the sensors and assure the examiner to employ them without applying any correction coefficient.
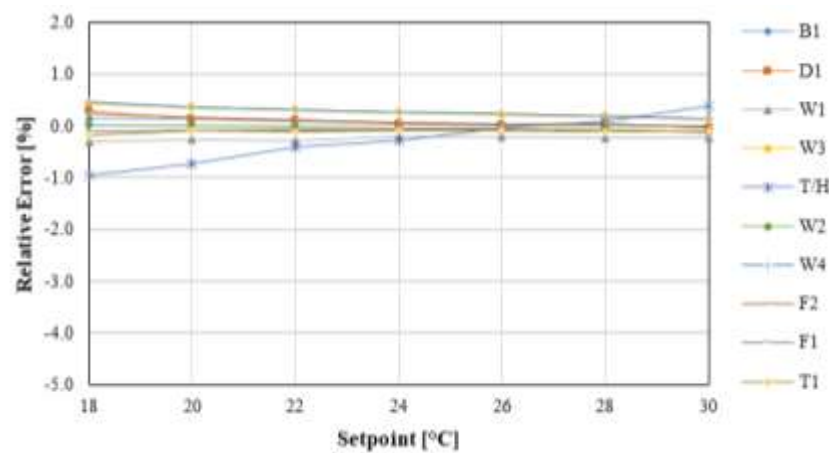


*Figure 7 Relative Error to Setpoint*

**Anemometers**

In view of the fact that calibration of hot wire anemometers demands special equipment, it needs to be implemented by the manufacturer. Employed anemometers in this project were tagged recently calibrated thus, examiner took the accuracy of these equipment for granted and utilized them without applying any correction coefficient.

### 3.1.3 Office Mock-up

A climate control chamber was erected in the laboratory. The room is 3.88m long, 2.91m wide, and 2.99m high. It is furnished in order to simulate an office space to accommodate one workstation, Figure 8. The room has been equipped with DV and a computerized ventilation control system and a number of sensors to monitor inlet and outlet flow temperature and air speed. One 1-way total volume air supply diffuser (length 156 cm, width 17 cm, height 28 cm) was installed in the left end of the room at the opposite side of the the outlet (D 15 cm) which is installed on the ceiling. The room has one wall in common with an adjacent test room with the same size. The other three walls are exposed to the indoor air of the laboratory salon as well as the ceiling and the raised floor.

This space has four openings on each side, two double glazing windows and two windowed doors. Nonetheless, the whole set-up is fully shaded. An attempt was made to make the chamber airtight, although there were still some cracks around the doors which were quite negligible for this experience.



*Figure 8 Experimental Setup and Measurement Grid*

Two hanging luminaires were installed in every one third of the room's length. The presumed workstation consists of a desk, an adjustable office

wheelchair, a desk lamp, laptop PC, and a combo printer. This experimental set-up is supposed to serve to one occupant.

The desk has four simple cylindrical metal legs and no partition on sides. The workstation is equipped with a ductless PV in front side of the desk shown in Figure 9. The ductless PV system consisted of an intake section placed at the floor level, where a commercially available activated carbon filter was fitted, a silencer integrated in the box with an electric fan controlled by a flow controller widget on the desktop, and a pair of adjustable flow guide panels on top of a rotatable arm as supply diffuser. Ductless PV drew in the air supplied across the floor by the DV and transported it to above the desk, close to user's body known as Breathing Zone (BZ).

In order to measure the room under performance of a DV system alone as a reference a fine grid with 270 nodes was designed. In comparison with the previous work, number of measured points increased to improve the CFD simulation calibration to the greatest extend.

Each workstation consisted of a desk, an adjustable chair, a desk lamp (20 W; continuously working during the experimental sessions) and a laptop PC (approx. 50 W). There was a partition (height 1.2 m; length 1.4 m) between the workstations.

The air filter contained 1.1 kg of activated carbon type CKV-3. The intake section limited the intake height to 10cm above the floor. The flow controller located at the desk top provided subjects with individual control over the personalized air flow rate. The test room is located in a large space where the air temperature is controlled to be the same as in the room. The ductless PV system is designed to supply up to 20 l/s.
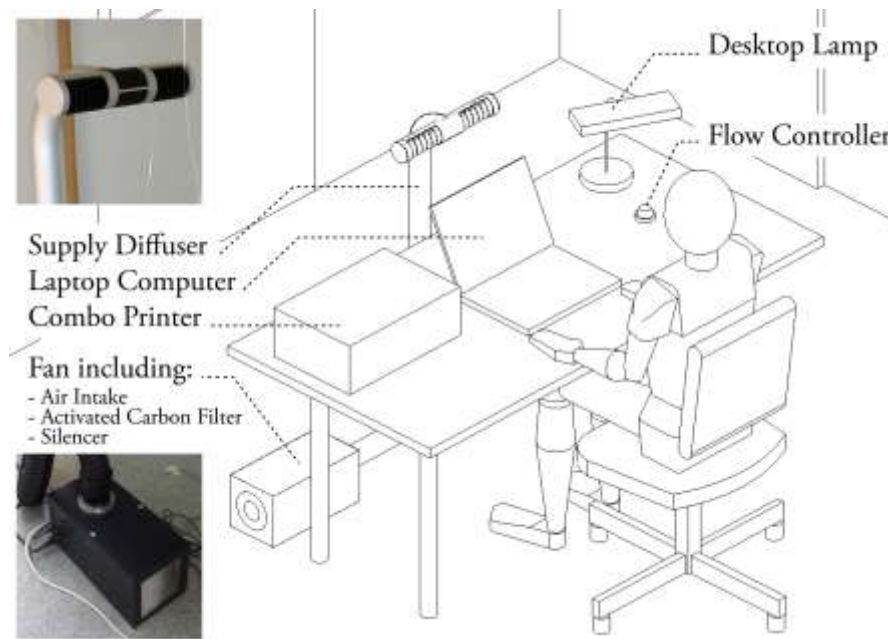
*Figure 9 Ductless Personalized Ventilation*

## 3.2 *Period and interval of measurements*

Once examiner ensured accuracy of the sensors, in the next step needs to check the performance of the system to confirm whether it is able to provide indoor air stability during the test.

To discover the time from startup it takes for the ventilation system to warm up and reach to steady state examiner logged two hours of data of a single experiment in the mock-up. Figure 10 reveals the amount of turbulence detected by each anemometer that is varying significantly until minute 95. After this point, turbulence value does not undergo significant fluctuations and maintain a fixed value. This implies that the system requires an initial time around two hours for warming up.
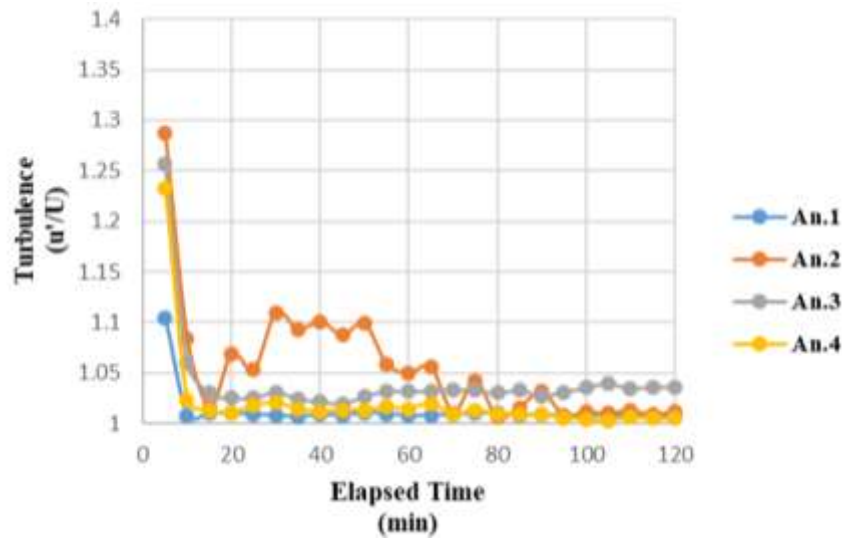
*Figure 10 Turbulence from Startup to 120 Minutes afterwards*

The measurement station has equipped with ntc sensors, which are encapsulated in a protective shield with a steel mesh to let the air penetrate inside and reach to the sensor. As a result, they need a relatively longer time than the other varieties to show actual room air temperature. The station, which holds anemometers and thermometers in the intended positions, needs to relocate 54 times across and along the room. After each movement at the end of each measurement, opening and closing the chamber door leads to an undesired exchange of air with the outside area, which causes heat exchange and thus more turbulence in the flow.

Another experiment was carried out to find out the time it takes for the system to return to steady state after each interruption. Once the system was ready examiner repositioned the measurement station in the same previous spot and logged additionally two hours of data. Figure 11 shows that the system was able to return to steady state condition in less than 18 minutes. Based on this observation it is concluded that after every intrusion into the chamber at least 18 minutes is needed before logging the next step of the experiment. Therefore 20 minutes is considered for the logging intervals.
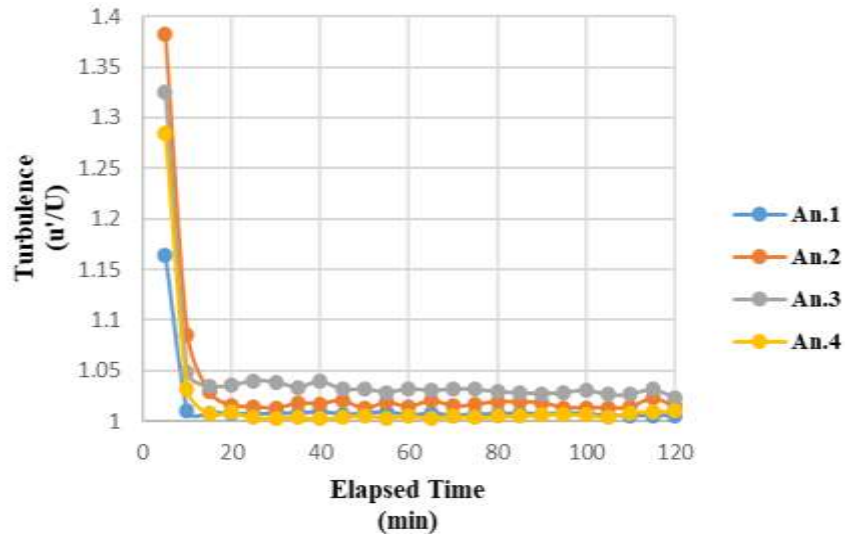
*Figure 11 Turbulence after 2 hours from startup to 120 Minutes afterwards*

## 3.3  DV Supply Air Parameters during Experiment

During the course of the measurements, the office cell in the laboratory ventilated only by DV. The ventilation system, which is connected to an online control and safety system, is continuously monitored to supply a stable airflow rate with steady temperature. Table 3 reports a summary of the data point mean values.

*Table 3 Average of Monitored Air Parameters throughout the Test*

| Exhaust Air Static Pressure [Pa] | Supply Air Static Pressure [Pa] | Supply Airflow Input [m/s] | Return Airflow Input [m/s] | Supply Air Temperature [°C] | Return Air Temperature [°C] |
|---|---|---|---|---|---|
| 157.81 | 99.85 | 0.42 | 0.52 | 20.89 | 27.10 |

Figure 12 illustrates the fluctuations in the air speed which is monitored in the supply and return ducts throughout the experiment. The variations in the aforementioned values, which is shown in terms of percentage in Figure 13, is an indication of capability of the ventilation system to supply a steady flow.
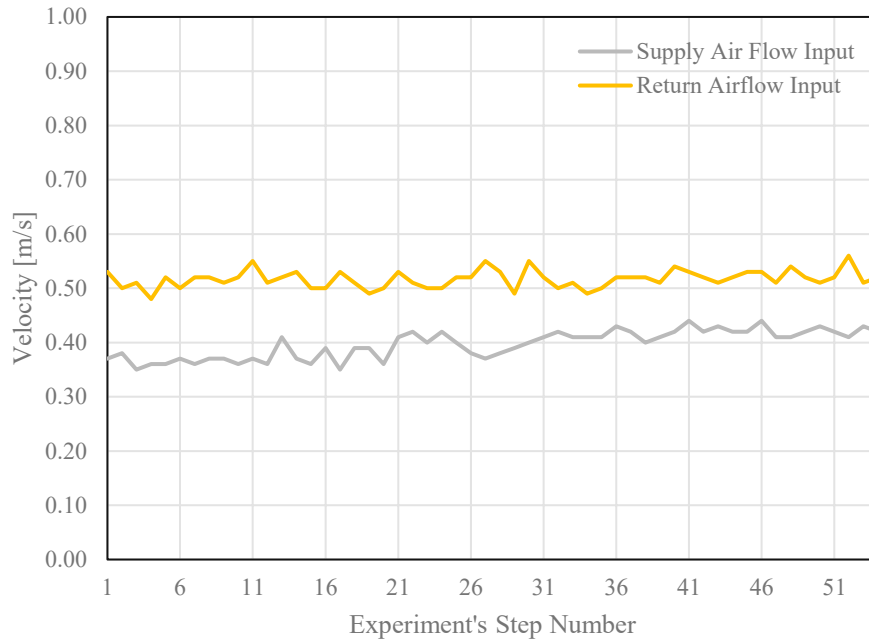
*Figure 12 Variations of Supply and Return Airflow throughout the Experiment*
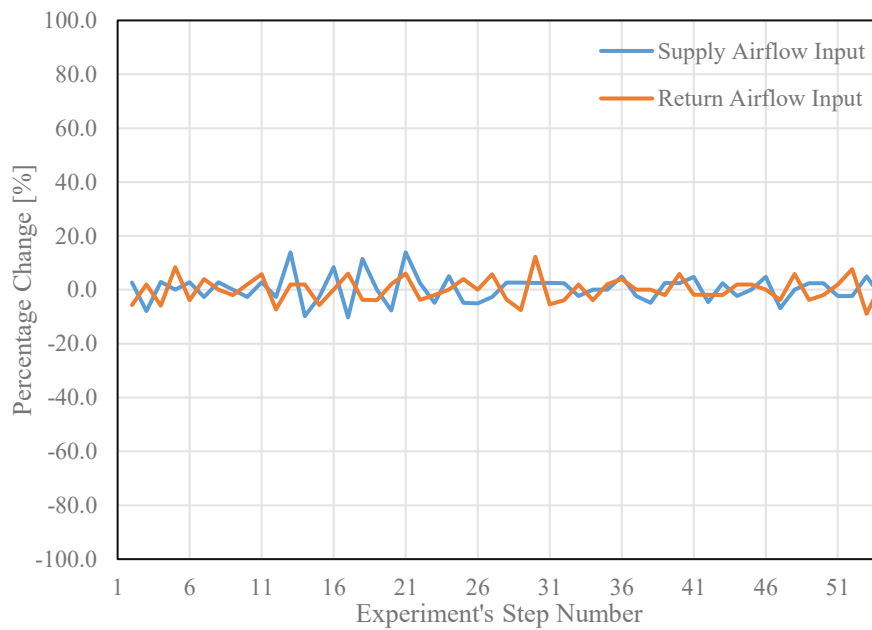


*Figure 13 Percentage Change of Supply and Return Airflow throughout the
Experiments*

Besides the control system, an anemometer and a thermometer were installed
in a fixed position in front of the inlet diffuser to observe the air parameters
as it enters the room. These two sensors monitored the air temperature and
velocity supplied by the DV at each measurement. In addition to the
monitoring points, the surface temperature of 10 point and air temperature at
the outlet are also recorded to provide boundary condition data for CFD

modelling. Table 4 describes the corresponding measured temperatures by all stationary sensors and Figure 14 shows the variation of temperature recorded by these sensors in 52 measurements. The average value from TI sensor is supposed as the reference temperature for calibrating measured Air Temperatures in every experiment, Figure 15.

*Table 4 Temperature Sensor Description*

| Sensor Name | Corresponding Component |
| --- | --- |
| TI | DV Inlet Air Temperature as the Reference |
| W1 to W4 | Surface Temperature of the Surrounding Walls |
| B1 | Surface Temperature of the Floor |
| D1 | Surface Temperature of the Ceiling |
| F1 to F3 | Surface Temperature of the Windows |
| O1 | Outlet Air Temperature |
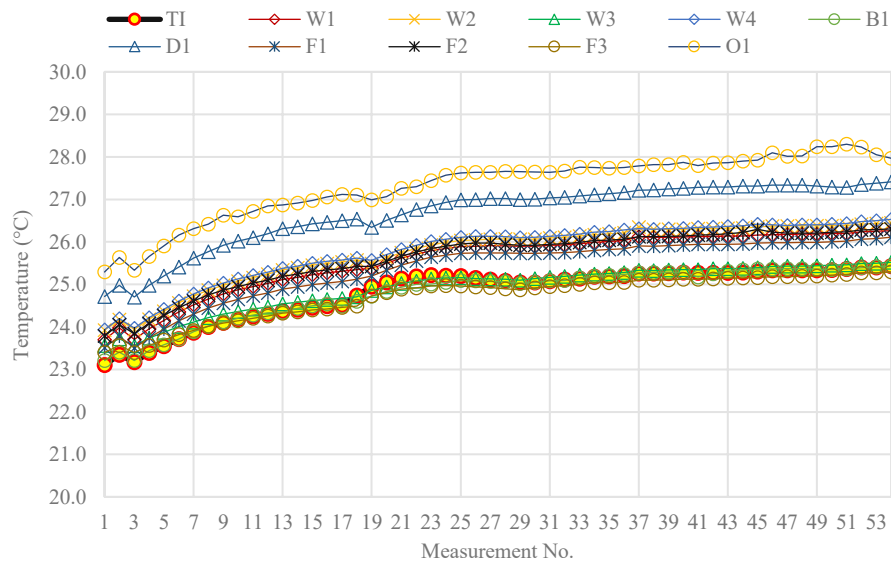


*Figure 14 Variation of the Measured Reference, Surfaces, and Outlet Temperatures*
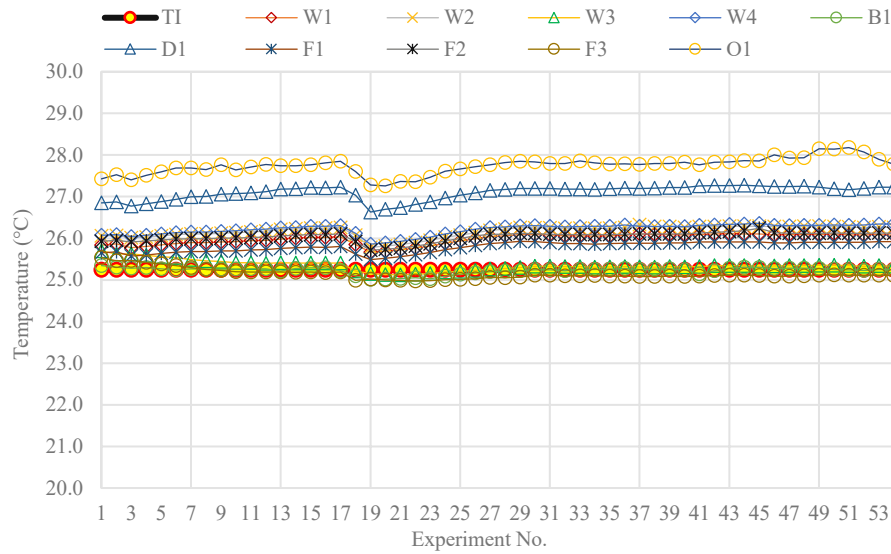
*Figure 15 Calibrated Measured Reference, Surface, and Outlet Temperatures*

## 3.4 CFD Modelling

In the next step the mock-up is modeled in a computational fluid mechanics program. CFD enables scientists and engineers to perform numerical experiments (i.e. computer simulations) in a virtual flow laboratory. Since Autodesk CFD offers free academic license, and not to mention the fact that it is used by professional architects alongside with other programs of Autodesk to provide a complete platform for Building Information Modelling (BIM), it is chosen for this research to develop an alternative method in continue of the previous work done by our colleagues in our institute. Another aspect of this software is providing elaborate tools demanded by mechanical engineers and possibilities for modelling small details of the building with very fine mesh to calculate flow parameters for fluids.

### 3.4.1 Boundary Conditions

Accurate specifications of boundary conditions are crucial in CFD modeling of indoor environments. The boundary conditions indicate how the CFD code user interprets the specific physical phenomena into a computer model or mathematical equations, so that a CFD code can be used to solve the phenomena. A detailed description of the boundary conditions can help others make informed assessments of the quality of the CFD simulation.

## Geometry

The size of the computational domain along with sizes and locations of all the solid objects represented in the model are defined in the geometry setting of a CFD model. The geometries of the available office mock-up in the laboratory is modeled first in Autodesk Revit. The level of details of this model at this stage affects the amount of mesh elements and accordingly computing time of the simulation in the steps. The building components, furniture, and the occupant's mannequin are created in this stage. In the next step this model is exported to Autodesk CFD for further manipulations like the creation of the fluid domain and defining the inlet and outlet surfaces. Although the model should be created in the simplest possible way, but it should represent all of the building characteristics as well as special form features, and should comprise all of the essential elements such as windows and doors in addition the furniture and equipment those would have substantial effect on the flow or heat transfer.

The room is measuring 388cm in length, 291cm in width, and 291cm in height. From north side it is adjacent to another identical room. Since the other room has been ventilated with the same system and had the same indoor air condition during the experiment, it is assumed that these two spaces was in thermal equilibrium, therefore the wall between these two spaces is considered as adiabatic. Nonetheless, the other envelope components as well as walls, ceiling, and floor of the room are modeled as diathermic components. The model contains objects of DV, PV, and ductless PV systems in corresponding scenarios. Two overhead lightings are modeled as two simple boxes suspending 30cm below the ceiling. An office set-up, consisted of all basic conventional electrical equipment, is considered for a single occupant. It is comprised of a desk, small printer, desk lamp, and a laptop computer. An occupant mannequin is placed on an office wheelchair in a seated working position, Figure 16.
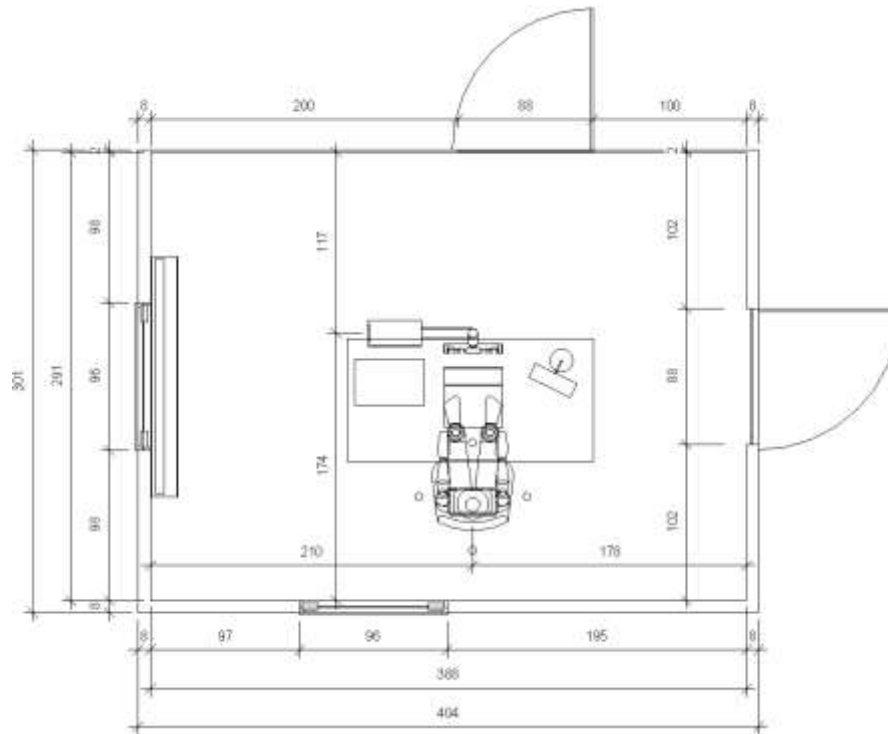
*Figure 16 Geometry layout of DV and ductless PV*

In order to eliminate discrepancies in turbulence, which could be produced by different furniture layouts, a single geometry is used for all cases. This mean for example in PV scenario the ductless PV box has been idle.

In order to create fluid geometry, the Void Fill command in Autodesk CFD is used. The openings of the model, which are shaped particularly for this purpose in CAD stage, are capped now so the software is able to generate automatically a continuous object for fluid from the hollow parts of the objects.

The next step is defining materials of the components. A building may use porous material as insulation. The heat transfer through the insulation material involves conduction, convection, and radiation. Limited computer resources would not allow detailed simulation of the heat transfer process. Therefore, a lumped-parameter model usually is used to combine the heat transfer processes. This model is important for obtaining accurate CFD results for the indoor environment. Table 5 shows a list of materials which are assigned to the building elements and objects of all CFD models.

*Table 5 Materials Assigned to the Model Components in Autodesk CFD*

| Component Name | Material |
|---|---|
| External Walls and Roof | Polystyrene |
| Doors and The Wall between Rooms | Plywood |
| Floor | Wood (Soft) |
| Window Panes | Glass |
| Inlet and Outlet Diffuser | Iron |
| Luminaire Casing | Aluminum |
| Power Supplies | PVC |
| Air | Air (Variable Environment) |

## Walls

Rigid surfaces in an indoor space, such as walls, ceilings, floors, and the furniture surfaces, are all considered as walls. In the region very close to the wall, the airflow is laminar, and often convective heat transfer occurs in this region between the flow and the surface. In Autodesk CFD a film coefficient or convection boundary condition simulates exposure to external flow, without actually modeling the air that surrounds it. The heat transfer between surfaces and the surrounding environment is defined by this factor, hence External wall surfaces that do not have an applied heat transfer boundary condition are treated as perfectly insulated. In this model a film Coefficient of 20 $W/m^2/K$ with Reference Temperature equal to 22°C is applied on all external walls. The external ambient condition during the test in laboratory is assumed to be constant in terms of temperature, external radiative temperature, and convective heat transfer coefficient.

## Inlet

The airflow from a diffuser significantly affects the airflow pattern in a room. The geometry of a diffuser is usually very complicated, therefore approximations are often used in a complete system in order to make the indoor airflow solvable, such as using a simplified geometry for a diffuser. In this study, the perforated surface in the front of the inlet diffuser is modeled as seven rectangular openings, which have the same surface area as the total number of the holes of the physical object. But in contrary it is tried to model the PV diffuser as close as possible to the real object, Figure 18. The reason for this was to achieve a higher resolution in order to be able to investigate the flow in the regions near the occupant in a higher detail.

Apart than the geometry of the inlet diffusers the characteristics of the discharging air to the system defines mostly the whole flow characteristics.

In the first step towards calculating the amount of fresh air supply we need to know the amount of inlet Volume Flow Rate (VFR) and inlet air temperature. These two parameters are predicted by calculating the amount of cooling load and fresh air demand per person. The supply air volume and air temperature provided by the DV system are calculated irrespective of the PV function. It should be also noted that the air volume calculations unlike the MV only the occupied zone is considered. Therefore, the standard heat transfer equation is not applicable. The design procedure of DV is based on an ASHRAE publication 'System Performance and Design Guidelines for Displacement Ventilation' (2003).

The design air volume supplied by a DV system must be capable of meeting both the cooling and minimum ventilation requirements for a given space. In order to determine the cooling design air volume, the type, location and magnitude of all heat loads must be identified. We can classify these loads as $Q_{oe}$ the heat generated by occupants and office equipment, $Q_l$ the generated heat by overhead lighting, and $Q_{ex}$ the heat from the exterior wall and window surfaces including transmitted solar radiation. The office room of this case study is assumed to be equipped with a computer, a monitor, a printer, a desk lamp and overhead lights (hanging ceiling luminaires). All of the surrounding walls include fenestration but since the room is located inside the laboratory and does not expose to the sunlight the Solar and Glass Load is assumed zero. The room will be supplied with a Dedicated Outdoor Air System (DOAS). The values of the aforementioned assumptions for design considerations are enlisted as below:

- Occupancy = 1
- Load per person = 73.3 W
- Overhead lighting load = 21.53 W/m$^2$
- Computer load = 65 W
- Monitor load = 30 W
- Small printer load = 30 W
- Desk lamp load = 40 W
- Solar and glass load = 0 W/m$^2$

In the next seven steps the supply air temperature and volume are calculated with determining the necessary fresh air per person and cooling loads. In the first step the total cooling load, $Q_t$, is calculated by summing up the generated heat from sources and surroundings. Since DV is generally not

recommended for internal heat loads greater than 94.6 W/m², the second step checks this criterion. In the third step the cooling air volume, $V_h$, is determined from heat loads with applied weighting factors. In the fourth step the zone outdoor airflow requirement, $V_{oz}$, and the breathing zone outdoor airflow (cfm), $V_{bz}$, are determined. In the fifth step the supply air volume, $V$, is taken from the larger of either the cooling air volume, $V_h$, or the zone outdoor airflow requirement, $V_{oz}$. The supply air temperature, $T_s$, is always cooler than the room temperature, $T_{sp}$, and in the sixth steps is calculated based on the air temperature at the floor level, $T_f$. And in the seventh step the exhaust air temperature is calculated from total cooling load, $Q_t$, supply air volume, $V$, and supply air temperature, $T_s$.

➢ Step 1, Calculating Total Cooling Load, $Q_t$:

$$Q_t = Q_{oe} + Q_l + Q_{ex} \qquad (5)$$

Where:

> $Q_{oe}$ = Heat generated by occupants, and equipment
> $Q_l$ = Heat generated by overhead lighting
> $Q_{ex}$ = Heat from the exterior wall and window surfaces including transmitted solar radiation

$Q_{oe}$ = person + computer + monitor+ small printer + desk lamp = 238.3 W

$Q_l$ = overhead lighting load × floor area = 240 W

$Q_{ex}$ = solar and glass load × exterior wall area = 0 W

$Q_t$ = 478.3 W

➢ Step 2, Check for Excessive Heat Load:

$Q_t / A \leq 94.6$ W/m²

$A = L \times W$

Where:

> $A$ = floor area (m²)
> $L$ = room length (m)
> $W$ = room width (m)

$Q_t / A = 478.3 / (3.88 \times 2.91) = 42.4$ W/m²

$Q_t / A = 42.4$ W/m² $\leq 94.6$ W/m² ✔

➤ Step 3, Calculating the Cooling Air Volume, $V_h$:

$$V_h = 0.122Q_{oe} + 0.055Q_l + 0.077Q_{ex} \qquad (6)$$

$V_h = 0.122 \times 238.3 + 0.055 \times 240 + 0.077 \times 0$

$V_h = 42.3$ l/s

➤ Step 4, Calculating the Zone Outdoor Airflow for Acceptable Indoor Air Quality:

$$V_{bz} = (R_p \times P_z) + (R_a \times A_z) \qquad (7)$$

Where:

$R_p$ = people outdoor air rate from ASHRAE Standard 62.1 (Table 6-1) = 2.5 l/s.person
$P_z$ = zone population (#) = 1
$R_a$ = area outdoor air rate from ASHRAE Standard 62.1 (Table 6-1) = 0.3 l/s.m²
$A_z$ = zone area (ft²)

$V_{bz} = (2.5 \times 1) + (0.3 \times 3.88 \times 2.91) = 5.9$ l/s

$$V_{oz} = V_{bz} / E_z \qquad (8)$$

Where:

$V_{oz}$ = the zone outdoor airflow requirement
$V_{bz}$ = the breathing zone outdoor airflow
$E_z$ = air change effectiveness from ASHRAE Standard 62.1 (Table 6-2) = 1.2

$V_{oz} = 5.9 / 1.2$

$V_{oz} = 4.9$ l/s

➤ Step 5, Determining the Supply Air Volume, $V$:

$$V = \max \{V_h, V_{oz}\} \qquad (9)$$

$V = \max \{42.5, 4.9\}$

$V = 42.3$ l/s

➢ Step 6, Calculating the Supply Air Temperature, $T_s$:

$$T_s = T_{sp} - 2 - AQ_t / (0.57V^2 + 1.21\, AV) \tag{10}$$

Where:

$\qquad T_{sp}$ = room temperature

$T_{sp} = 22°C$

$T_s = 22 - 2 - 3.88 \times 2.91 \times 478.3 / (0.57 \times 42.3^2 + 1.21 \times 3.88 \times 2.91 \times 42.3)$

$T_s = 17°C$

➢ Step 7, Calculating the Exhaust Air Temperature, $T_e$:

$$T_e = T_s + Q_t / 1.21V \tag{11}$$

Where:

$\qquad T_s$ = Supply Air Temperature
$\qquad Q_t$ = Total Cooling Load

$T_e = 17 + 478.3 / (1.21 \times 42.3)$

$T_e = 26°C$

The calculated parameters of the supplied air by DV for a room with the given indoor air temperature are summarized in the Table 6.

*Table 6 Supplied air parameters by DV*

| $Q_t$ | $T_{sp}$ | $T_s$ | $T_e$ | $V_h$ | $V_{bz}$ | $V_{oz}$ | $V$ |
|-------|----------|-------|-------|-------|----------|----------|-----|
| 478.3 W | 22°C | 17°C | 26°C | 42.3 l/s | 5.9 l/s | 4.9 l/s | 42.3 l/s |

For calculating the parameters of supplied air by DV to the office mock-up under measurement conditions, the same design procedure is employed. In this case, due to the lack of generated heat by the occupants and the equipment, the total cooling load is significantly lower. If the supply air volume is very low and the space does not have high cooling load, the supply air temperature is increased. Correspondingly if the supply air volume is at the maximum setting and the indoor air temperature is still above the setpoint, the supplied air temperature is decreased, with a minimum setpoint

of 17-18. With the previous assumptions of the single occupant office room and the aforementioned exception, the design parameters will be as Table 7.

*Table 7 Supplied air parameters by DV under measurement conditions*

| $Q_t$ | $T_{sp}$ | $T_s$ | $T_e$ | $V_h$ | $V_{bz}$ | $V_{oz}$ | $V$ |
|---|---|---|---|---|---|---|---|
| 243.1 W | 22°C | 17°C | 32°C | 13.4 l/s | 3.4 l/s | 2.8 l/s | 13.4 l/s |

## Outlet

An outlet generally has little impact on room airflow. The conditions set for the outlet can have a significant influence on the numerical stability in many cases. However, the size and form of the outlet diffuser could determine accordingly the amount and direction of air, which exits the system. At the outlet, where a uniform pressure is commonly applied, there must not be any flow features which will conflict with this uniform pressure boundary. A method for defining a surface as an outlet vent in the CFD model is applying a zero pressure to it. In this work, the outlet is located in the opposite side of the DV inlet diffuser on the ceiling, so that conducts the fresh air particles in the longest possible way throughout the room.

Additionally, the flow should be approximately normal to the plane of the outlet. If the outlet boundary is too close to where the flow has to turn, the outlet should be extended so that the flow can align itself, and exit normal to the outlet plane.

## Other Approximations

In the process of making the CFD model the air infiltration rate is assumed zero. In practice however, high values of infiltration rates could affect the flow characteristics to some extent. In this work since the CFD model is based on a mock-up which is enclosed by a bigger room with a rather similar indoor air temperature this this approximation is reasonable.

When a fluid flow is compressible, the fluid density varies with its pressure. Compressible flows are usually high speed flows with Mach numbers greater than about 0.3. Examples include aerodynamic applications such as flow

over a wing or aircraft nacelle as well as industrial applications such as flow through high-performance valves.

Incompressible flows do not have such a variation of density. The key differentiation between compressible and incompressible is the velocity of the flow. A fluid such as air that is moving slower than Mach 0.3 is considered incompressible, even though it is a gas.

**Summary of Applied Boundary Conditions in CFD Simulation**

To simulate the office mock-up with a single occupant the boundary conditions in the CFD software should be defined as followed:

- Heat Generation Sources as Table 8.
- Film Coefficient = 20 W/m$^2$/K, (Reference Temperature = 22°C)
- Inlet Volume Flow Rate = 42 l/s
- Inlet Air Temperature = 17°C
- Outlet Pressure = 0 Pa
- Incompressible Flow
- Heat Transfer and Radiation calculations
- Turbulence Model: k-epsilon

*Table 8 List of heat sources in the office mock-up*

| Item | Total Heat Generation (W) |
|---|---|
| Occupant | 73.3 |
| Computer | 65 |
| Monitor | 30 |
| Small Printer | 30 |
| Desk Lamp | 40 |
| Overhead Luminaires | 2 × 120 |

## 3.4.2 Mesh Characteristics

To prepare a model for CFD analysis, the geometry should be broken up into small pieces called elements. The corner of each element is called a node. The mesh in Autodesk CFD consisted of these elements and their nodes. The calculations are performed at any of these nodes. In three dimensional objects of the model, the elements are Tetrahedral, which is a four sided

volume with triangular faces. On the other hand two dimensional surfaces like walls are triangular flat elements, Figure 17.
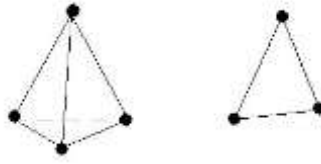


*Figure 17 Mesh elements in Autodesk CFD*
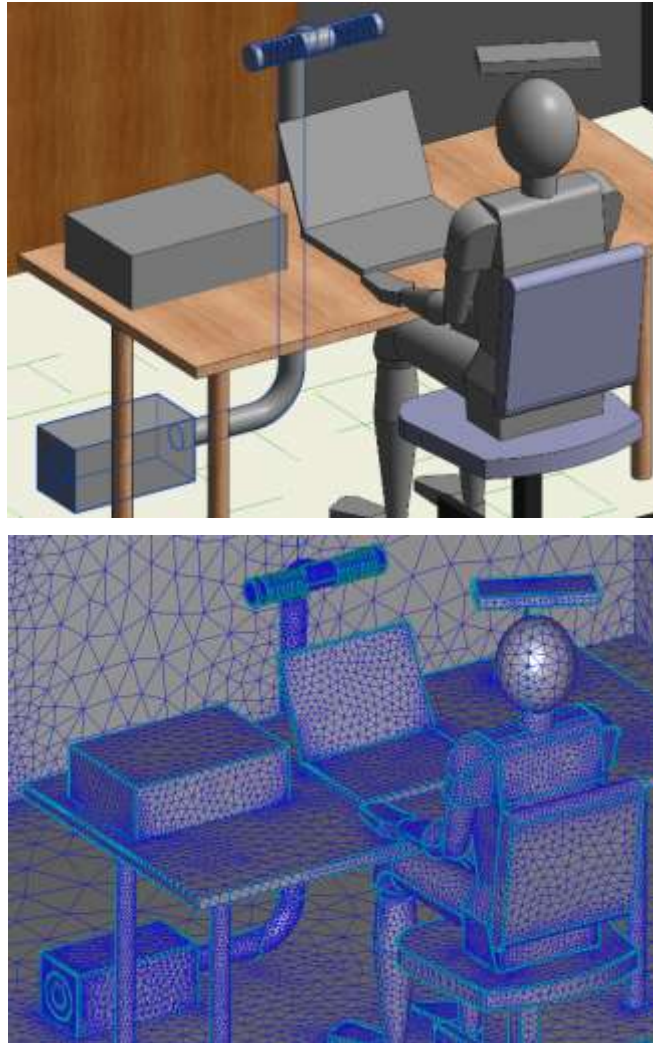


*Figure 18 Office Desk Setup (up), and corresponding Mesh System (down)*

Autodesk CFD performs a comprehensive topological interrogation of the analysis geometry and determines the mesh size and distribution on every edge, surface, and volume in the model. Geometric curvature, gradients, and proximity to neighboring geometry are all considered when assigning element sizes and mesh distributions.

49

### 3.4.3 Solver Parameters of the CFD Simulation Software

Since the concerns of the steady state solution are the constant flow and heat transfer regimes, in this work the steady state solution mode is chosen over the transient mode. This mode is only valid in a simulation where the steady flow phenomenon is generated by constant boundary conditions. Thus, such condition will occur in the constant behavior of a device and assuming fixed objects or a sedentary occupant in the room. This condition could be construed as two describing snapshots of the flow regime in two arbitrary moments which must resemble each other identically. On the contrary, the transient solving method is an iterative process at each time step that is ideal for a time varying flow or heat transfer and it can be interpreted as a sequence of steady state calculations in specific time steps, Figure 19.
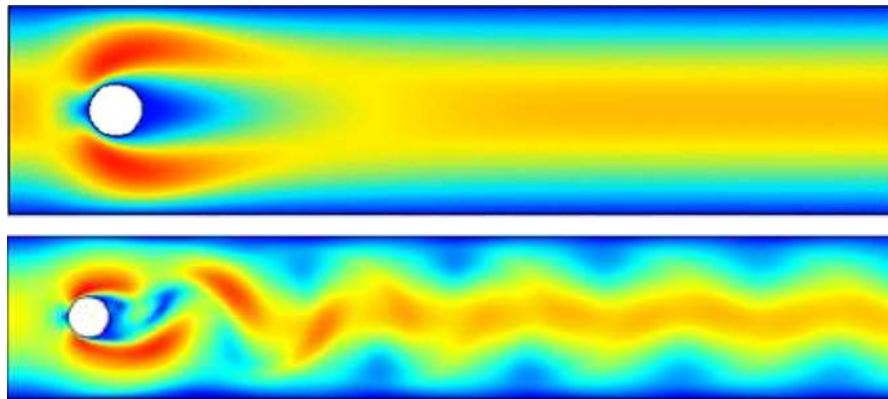


*Figure 19 A flow over Cylinder in Steady State (up)*

*and in Transient (down) (Comsol, 2021)*

Using the transient solving will be necessary when the CFD user wishes to examine a result parameter changing over time. For example, in Motion, Rotating Regions, Free Surface Analyses, Solar Radiation, and Heat Up or Cool Down Analyses. Or, when the flow is inherently transient in nature like forming vortex shedding around a cylinder. Obviously, there will be similar objects such as table legs in the geometrical model of this project, but still since the flow behavior around thiese objects is not the concern of the research, the condition of those regions is understood as a steady state. The other mandatory issue for using the transient solution is when the user has specified non constant boundary conditions or specific device controls, for instance thermostat-controlled fans. In this project all the generated flows,

for instance by the DV inlet diffuser in the laboratory or the internal fan of the ductless PV in CFD models, are controlled to be constant.

In fluid mechanics "Advection" is defined as the transfer of heat or matter by the flow of a fluid, especially horizontally in the atmosphere or the sea. Advection in a CFD software is the numerical mechanism of transporting a quantity, for instance velocity or temperature, through the solution domain. Autodesk CFD provides under solution controls, 5 different schemes for Advection, Table 9.

*Table 9 Advection Schemes*

| ADV1 | Monotone Streamline Upwind |
|------|----------------------------|
| ADV2 | Petrov-Galerkin |
| ADV3 | Flux Based Scheme |
| ADV4 | Mid-Mod Scheme (Petrov-Galerkin Variant) |
| ADV5 | Modified Petrov-Galerkin |

Any of these schemes is programmed for a specific application. ADV1, Monotone Streamline Upwind, which is recommended as a starting point, is a default method for almost all applications. It is a numerically stable for meshes aligned with flow direction; whereas, numerically diffusive for meshes not aligned with flow direction, which works well for geometries with numerous internal blockages. ADV2, Petrov-Galerkin, is moderate numerical stable (less than ADV1), and less numerical diffusive for random meshes. Models with random meshes have large domains, and often feature unrestricted external flow, for example AEC and Displacement Ventilation. After a couple of tries and assistance of the software manual the ADV5 seemed to be the most time efficient and converging scheme in comparison to the other two compatible alternative schemes, thus it is preferred to be selected for the entire of the CFD simulations in this project. ADV5, Modified Petrov-Galerkin, is a more stable variation of ADV2. It is convenient for all application types recommended with ADV2, but commonly produces more globally conservative results. According to the software developer, ADV5 has demonstrated improvements over ADV2 in natural convection and in the accuracy of recirculating and secondary flows, which here in this project occurs in the ductless PV model.

Every single simulation has been run for at least 100 iterations to achieve convergence in every calculated factor. It implies, the software iterates the

calculation for all the flow parameters until reaching the convergence. Since the steady state solving method is employed, thus the number of inner iterations should be 0 as default. Figure 20 displays an example of the convergence plot of one of the scenarios in this project.
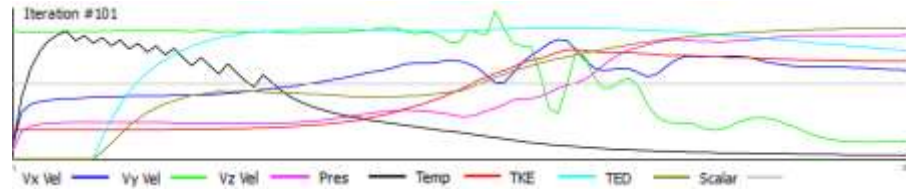


*Figure 20 Example of the Convergence of the Calculated Parameters in a Simulation*
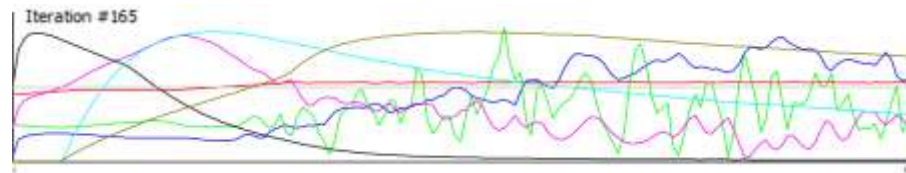


*Figure 21 Example of Non-Converging Solution*

Result quantities which are calculated and observed during entire scenarios are as follows:

*Table 10 Result Quantities*

| Basic Flow Values | Fluid Properties | Miscellaneous |
|---|---|---|
| • Velocity | • Density | • Shear Stress<br>• Local mean age (LMA)<br>• Wall Heat Flux<br>• Wall Film Coefficient<br>• Thermal Comfort |

*Table 11 Thermal Comfort Factors*

| Factor | Value | Unit |
|---|---|---|
| Metabolic Rate | 60 | $W/m^2$ |
| Clothing | 0.61 | clo |
| Humidity | 76 | % |

Under physics settings of the "Solve" control the flow was presumed incompressible, and the gravity direction was defined as the vector of (0, 0, -1).

Heat Transfer and Radiation calculations were also implemented in all the simulations during this work, admitting, solar heating calculations were not enabled. The radiation model uses an appropriate view factor calculation, which provides an accurate energy balance as it enforces reciprocity between solids. Temperature and energy balance accuracy are ensured for geometries with widely varying feature sizes. Radiative heat transfer through transparent media is also supported as well as geometric symmetry.

Since almost all flows in AEC applications are turbulent the Turbulence calculations were applied during the simulations. The Autodesk CFD offers 10 different turbulence models as well as "k-epsilon", variations of hybrid models of "k-omega SST (Shear Stress Transport)", "RNG", "Low Re k-epsilon", "Mixing Length" and "Eddy Viscosity". K-epsilon is typically more accurate than the constant eddy viscosity model, but computationally more intensive and slightly less robust. It is not as resource comprehensive as the RNG model, but still gives good results. It is a general-purpose model that performs well across many applications as well as AEC. In this series of simulations k-epsilon model produced the most legitimate results too. It is essentially a two equation, linear Eddy viscosity RANS approach. It attempts to model the turbulence throughout the flow domain where it effectively changes the viscosity and connectivity based on what the turbulence changes inside the flow domain. The admirable aspects and deficiency of this model are:

Pros:

- Robust for a wide range of models
- Long History of Industrial Benchmarking
- Reduced wall mesh requirements

Cons:

- Large adverse pressure gradients (e.g. flow profile over a wing)
- Difficulty in predicting accurate separation points
- Large Swirling Flows
- Sensitive to mesh refinement
- Not accurate for high Prandtl Number (liquids) wall heat flux prediction

One of the methods for overcoming a few deficiencies of the k-epsilon model is the scalable wall function, which is also offered by the Autodesk CFD.

This trait enhances the accuracy issue of the k-epsilon model, for example, by increasing the sensitivity of the model to the mesh refinements. And regarding the last point of the cons, and since heat exchange between air and liquid is not the concern in this study, therefore, there will be no perturb about using the k-epsilon turbulence model.

There are three additional and important parameters to set achieving an appropriate turbulence model. Making changes to "Auto Startup", "Turb/Laminar Ratio" and "Turbulence Intensity" could affect the convergence of the solution and the results drastically.

The Auto Startup, which is found in the Turbulence window, controls the Automatic Turbulent Start-Up (ATSU) algorithm. This algorithm goes through several steps to attain turbulent flow solutions. The algorithm starts by running 10 iterations using a constant eddy viscosity model, so the k and epsilon equations are not solved. As an initial guess with this solution, the two-equation turbulence model is started. At iteration 10, a spike in the convergence monitoring data will appear for the "k" and "epsilon" equations. Other steps are then taken to gradually appear at the converged result. These steps may involve spikes in the convergence monitoring data at iterations 10, 20 and 50. After 50 iterations, the ATSU will be turned off automatically. If Lock On is selected, the ATSU stays on during the entire analysis until the user manually turns it off. If there are convergence difficulties after iteration 50 (divergence within 10 iterations), then Lock On should be enabled. If the ATSU is turned on, at least 200 iterations have to be run to ensure convergence of the turbulent flow solution. An extended version of the ATSU will be activated in case Extend is marked. This method is handy for difficult analyses, particularly compressible analyses.

The Turb/Laminar Ratio is the ratio of the effective (turbulent) viscosity to the laminar value. It is employed to estimate the effective viscosity at the beginning of the turbulent flow analysis. The effective viscosity is 2-3 orders of magnitude larger than the laminar value in most turbulent flow analyses. For all the other turbulence models (K-Epsilon, RNG, Low Re Number), the specified value is the starting point or initial value of the eddy viscosity.

The Turbulence Intensity Factor, which is found in the advanced settings of the Turbulence window, controls the amount of turbulent kinetic energy in

the inlet stream. The recommended value is 0.05 and should rarely exceed 0.5.

Since the mock-up is located inside of the laboratory room it is not exposed to any solar radiation, the last consideration about solution settings before running the simulation in this work was Solar Heating calculations; therefore, the solar heating option left disabled during the simulations.

### 3.4.4 Comparison Scenarios

The CFD base model consists of a room with furniture obstacles, solar load, and heat loads generated by occupants and other equipment sources. However, due to the placement of the office mock-up in an enclosed space, solar calculations are not required in this project.

Preformance of Ducted and Ductless PVs are the subject of comparison in this project. Since Ductless variation is supposed to work in conjunction with DV, the performance of the DV system is assessed seperately. On the other hand, a possibility for Ductless PV system to work along with DV is considered. Thus five different scenarios are defined (Table 12, A) to simulate the performance of those ventilation systems, supplying an equal amount of outdoor fresh air for better indoor air quality and cooling load.

Comparing different combinations with the same amount of air handling (literally the same load), gives a better understanding about ventilation system performance.

In the B section of Table 12, four alternatives of the new DV diffuser prototype are presented. Alternatives 1 to 4 were the most distinctive variations among 10 different ones.

*Table 12 List of Simulation Scenarios*

| A. Standard Diffusers | |
|---|---|
| A1 | DV |
| A2 | DV + High-speed Ductless PV |
| A3 | DV + Low-speed Ductless PV |
| A4 | Ducted PV |
| A5 | DV + Ducted PV |

| B. Alternative Inlet Diffusers of DV + Ductless PV (High Speed) | |
|------|-------------------------------------------|
| B1 | DV (Inlet Diffuser Alt. 1) + Ductless PV |
| B2 | DV (Inlet Diffuser Alt. 2) + Ductless PV |
| B3 | DV (Inlet Diffuser Alt. 3) + Ductless PV |
| B4 | DV (Inlet Diffuser Alt. 4) + Ductless PV |

The Solver Manager of the chosen CFD program provides the possibility of running many different scenarios in a queue. This feature not only accelerates numerous runs of simulations, but also facilitates the procedure of exporting the results as well as minimizing the level of user errors in similar projects.

### 3.4.5 Ducted and Ductless PV CFD Model

The CFD models of these scenarios are based on the calibrated model. The geometry of furniture, a human mannequin, and personalized ventilation equipment are added. It should be noted as well that the internal fan model needs to be defined in material section of the software. Two $120^{mm}$ fans with 27.8 l/s and 49.3 l/s are selected for Ductless PV air intake box.

**Ducted**

Geometry of the PV diffuser is modeled according to the available version in the laboratory. Figure 18 shows level of geometry detail and mesh resolution of the PV diffuser.

Two scenarios are designed to investigate the performance of ducted PV in two conditions of individual operation and in conjunction with DV. This comparison yields results to assess if ducted PV system is individually capable of providing acceptable IAQ for occupants in a room.

In scenario A4 it is assumed the designed supply air volume, V, is entirely delivered by PV under individual operation of the system, whereas in scenario A5, which ducted PV operates in conjunction with DV, this amount is distributed between the two systems. In the latter case 20 percent of the supply air is handled by DV and 80 percent by ducted PV.

**Dcutless**

In these scenarios in addition to the performance of the displacement ventilation a ductless PV creates a shortcut for fresh air to reach to the occupant without encountering the convective plume. Intake fan of ductless PV vacuums the fresh air from 10cm above the floor, transfers it through the duct and eventually releases it to the BZ. In this study two different speeds assigned to the ductless PV to investigate the effect intake fan on the DV. To model these two states, it is needed to assign different fans to the corresponding geometry in the CFD model. Two 120mm direct current fans from Comair Rotron with 27.8 l/s and 49.3 l/s flow rates were chosen for low-speed and high-speed scenarios respectively. The model number and specification of the fans are as follows:

- Comair Rotron Flight II 120$^{mm}$ 2000 RPM, 27.8 l/s
- Comair Rotron Flight II 120mm 3500 RPM, 49.3 l/s

In the CFD simulation it is also assumed that the intake fan does not generate heat due to low wattage and high efficiency of ball bearing DC fans. It should be noted that in Autodesk CFD the properties of the internal fan/pump should be assigned in the materials section before proceeding to the boundary conditions.

## 3.5 *Physical Measurement Results and CFD Model Calibration*

Velocity magnitudes and temperatures are measured in heights of 10, 60, and 110 centimeters from the floor. By placing the measurement station, the beam which carries the temperature and velocity sensors and data logger, perpendicular to the diffuser's face it was possible to carry out measurements in more nodes throughout the room. This method let adding two more rows next to the side walls of the climate chamber. The measured air parameters near to the walls would help to draw a better conclusion about the accuracy of the CFD simulation. However, handling large number of the measured values could lead to user errors and is rather impossible manually. For this purpose, the assistance of a numerical computing environment (i.e. MATLAB) comes in handy. The MATLAB scripts, which are written for this purpose, are found in appendix 6.2.

Figure 22 and Figure 23 compare the measured Air Temperature and Velocities. The linear correlation in these charts is an indication of the similarities between the indoor air flow characteristics of the office mock-up and the CFD simulation. The significant improvement in the $R^2$ values to around 0.75 implies the success in the calibration efforts. Moreover, the cumulative graph of Air Velocity relative errors, Figure 26, show that the median of the distribution of relative errors decreased from 45% in initial model to 25% in the calibrated model. In addition, the cumulative graph of Air Temperature errors illustrates only 3% of the data in calibrated model have relative errors greater than 1 %, Figure 27.

In the calibrated model, 95% of both calculated Air Velocity and Air Temperature rates have an absolute error less than 0.01 m/s and 0.1°C, Figure 24 and Figure 25. This magnitude of error is acceptable for many common applications of air flow field data in indoor environmental studies such as PMV calculations and human perception of the indoor climate (Loomans, 1998).

The calibration process is achieved by applying a series of changes in the model as well as correcting component's materials, changing the advection scheme from ADV1 (Monotone Streamline Upwind) to ADV2 (Modified Petrov-Galerkin), increasing the resolution of the mesh size in regions with higher detail and decreasing it in regions with less importance, and the most influencing factor, changing the geometry of the inlet diffuser. The front porous surface of the DV inlet diffuser is modeled as a simple rectangular opening in the initial model, which is later replaced with seven rectangles in order to make it possible dividing the amount of inlet VFR in seven different values based on the measured Air Velocities and assigning them separately to each opening correspondingly, Figure 28.
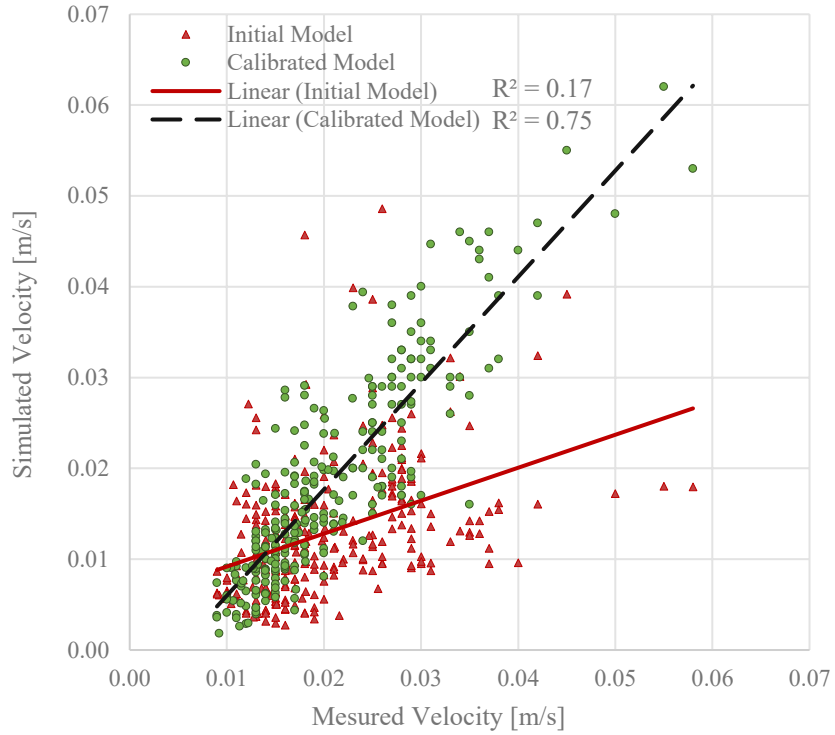
*Figure 22 Measured versus Simulated Air Velocities*

*in Initial and Calibrated Model*
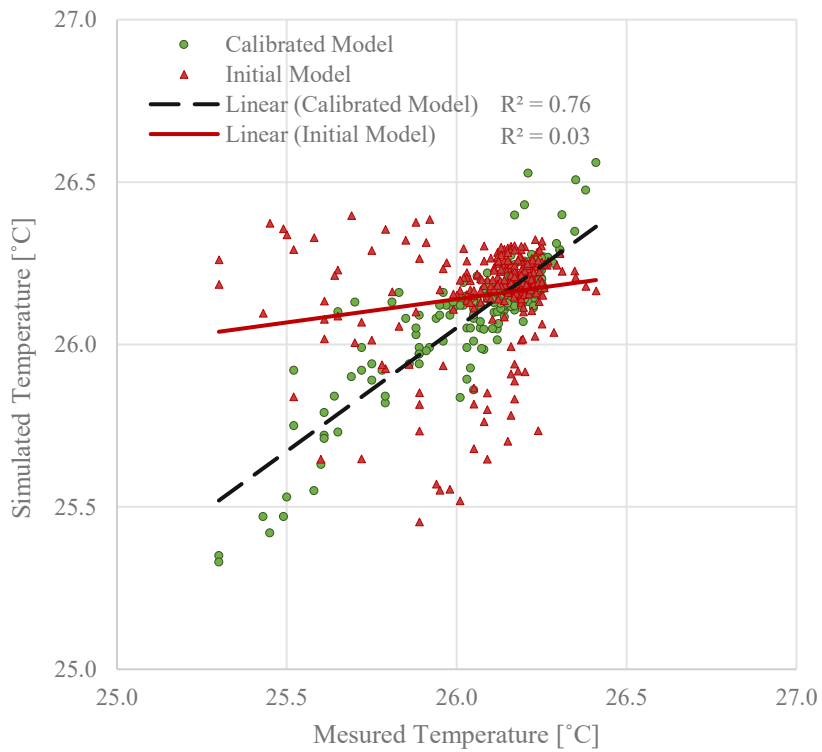


*Figure 23 Measured versus Simulated Air Temperatures*

*in Initial and Calibrated Model*
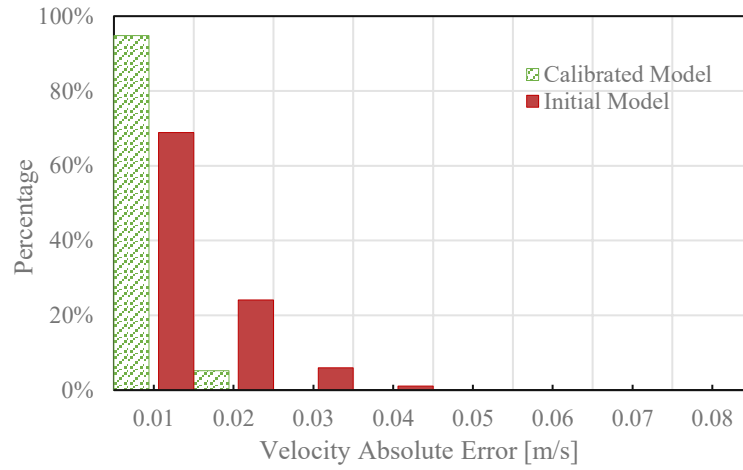
*Figure 24 Air Velocity Absolute Error Distributions*

*in Initial and Calibrated Model*
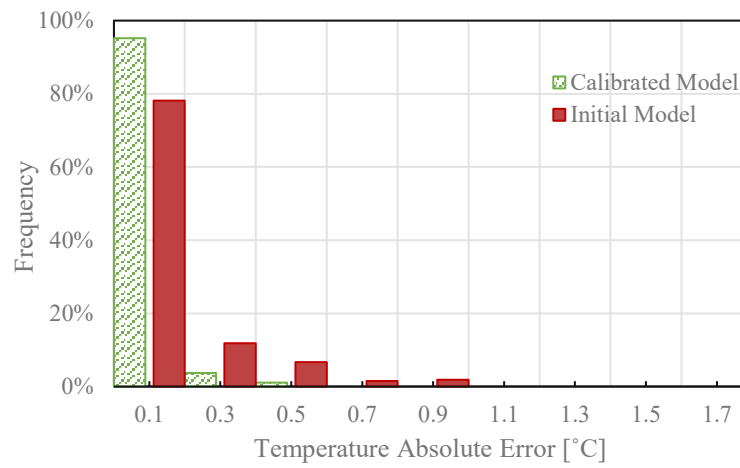


*Figure 25 Air Temperature Absolute Error Distributions*

*in Initial and Calibrated Model*
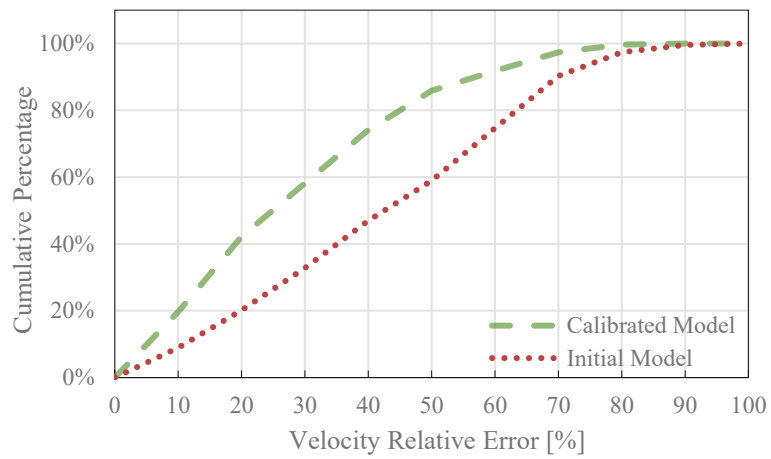
*Figure 26 Cumulative Distributions of Air Velocities Relative Errors*

*in Initial and Calibrated Model*
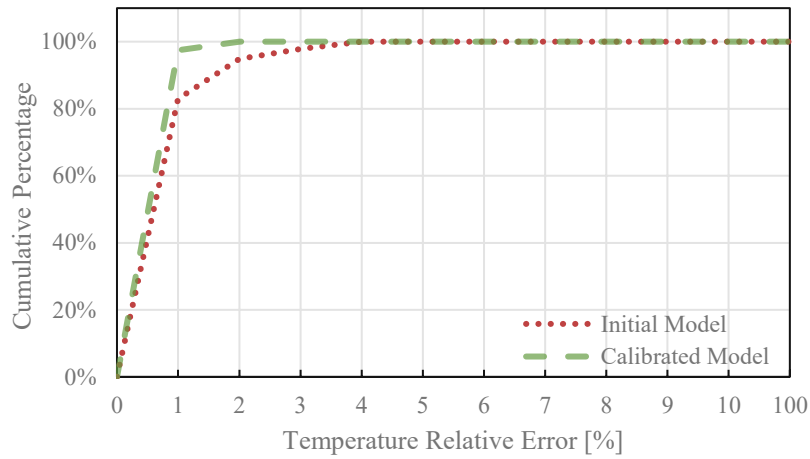


*Figure 27 Cumulative Distributions of Air Temperature Relative Errors*

*in Initial and Calibrated Model*
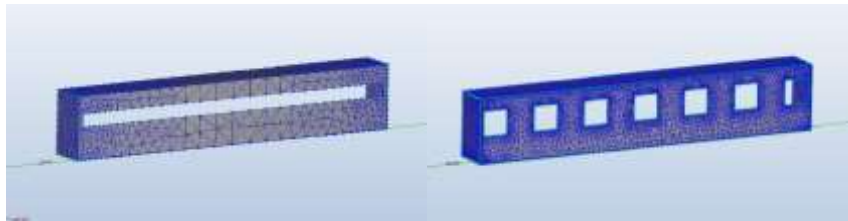


*Figure 28 Geometry Improvement of the DV Inlet Diffuser*

The *x* and *y* axis of the following diagrams indicating the coordinates of the sensors. The [0,0] point is assumed to be in the center of the DV inlet diffuser attached to its front surface. For better understanding the orientation of the results see Figure 8.

Figure 29 and Figure 30 show correspondingly the air velocity and air temperature results, from measurements, initial and calibrated CFD model in y = -1.0m and 0.0m and 1.0m. These diagrams display the improvements in the calibrated model.

The diagrams of Figure 31 to Figure 36 describe the air velocities in three heights resulted alternately from measurement and calibrated CFD simulation. Air velocity iso lines of the Figure 32, in the range of x = 0.1m to 0.6m, verify the close similarity of the near zone air flow to the measurements in the calibrated model.
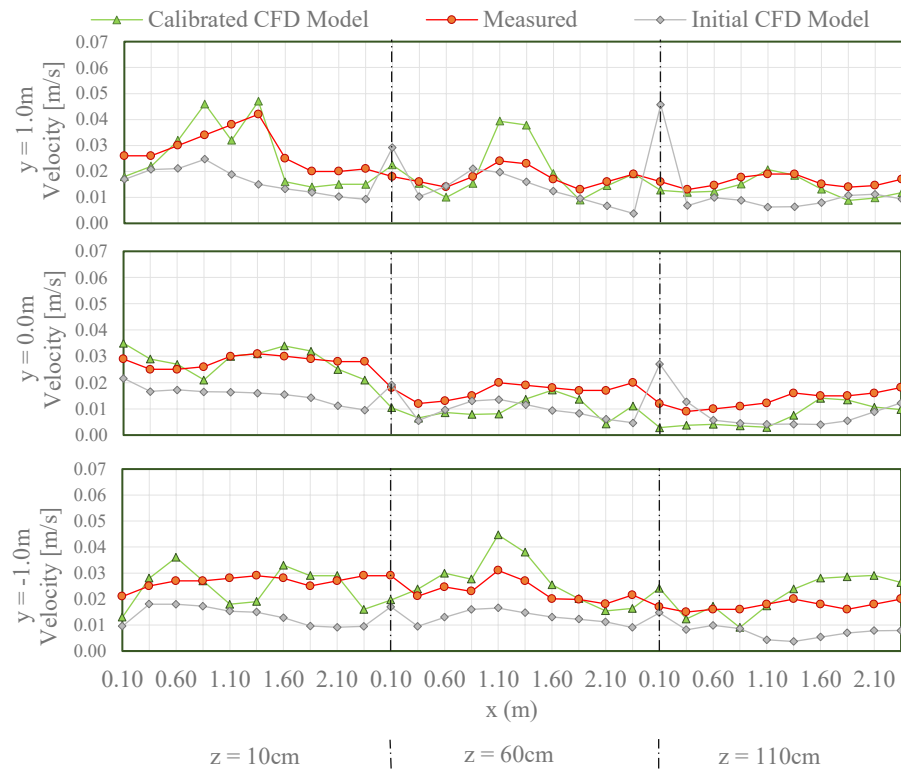


*Figure 29 Air Velocities from Measurements, Initial and Calibrated CFD Model*
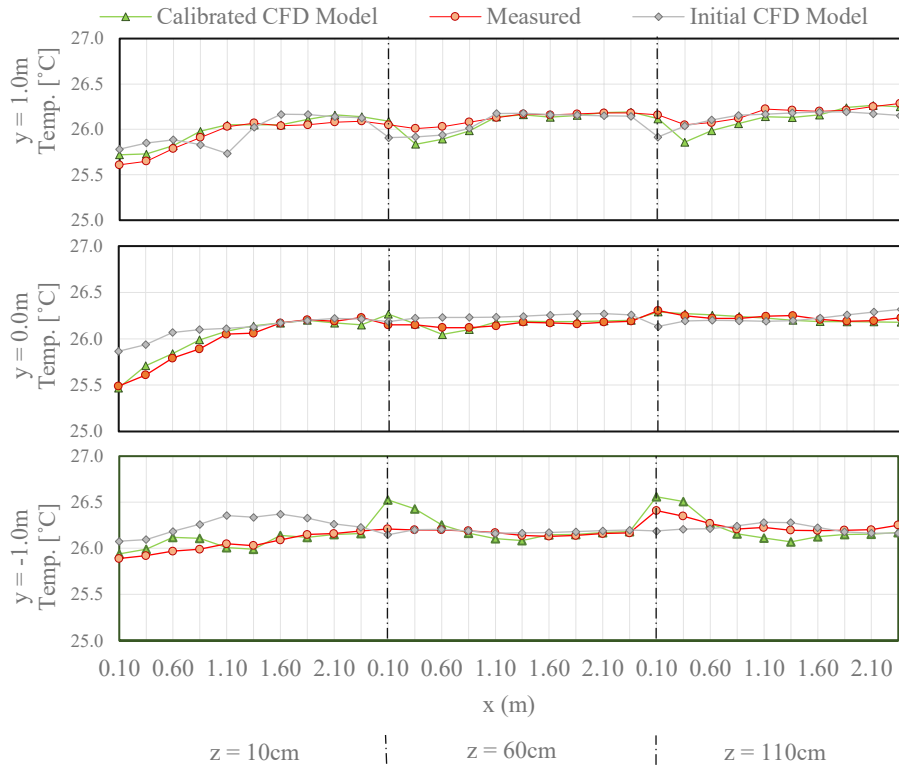
*Figure 30 Temperatures from Measurements, Initial and Calibrated CFD Model*
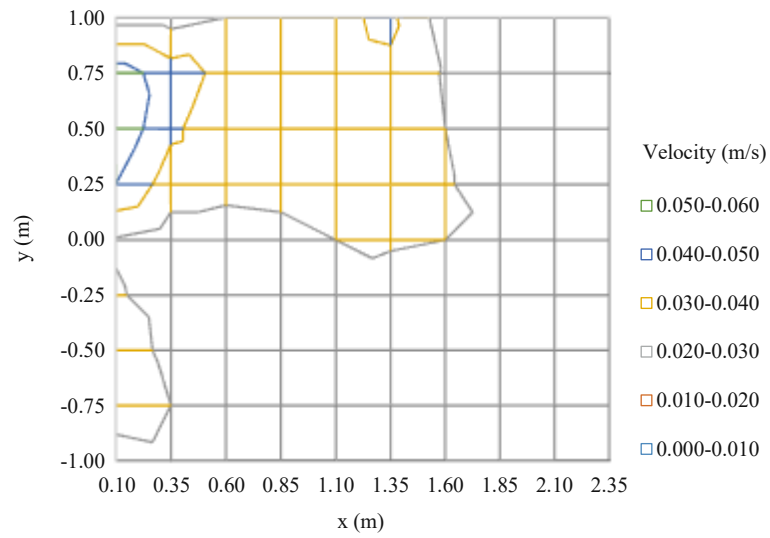
*Figure 31 Measured Air Velocities in 10cm above the floor*
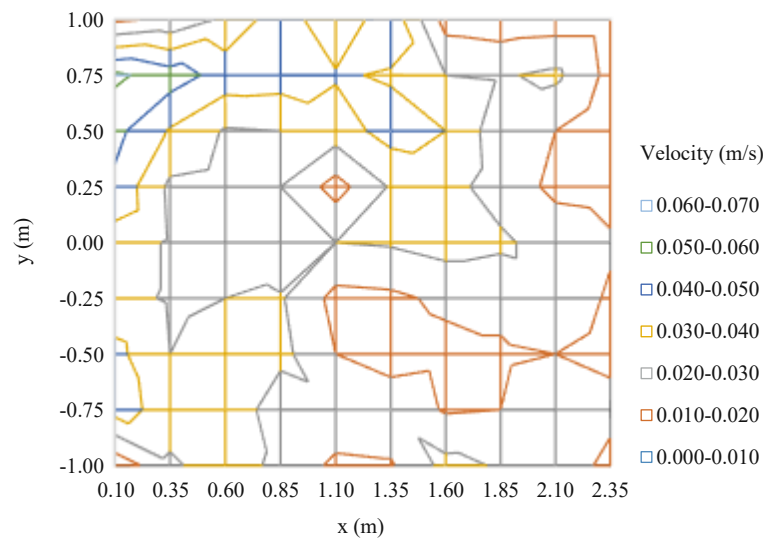


*Figure 32 Simulated Air Velocities in 10cm above the floor*
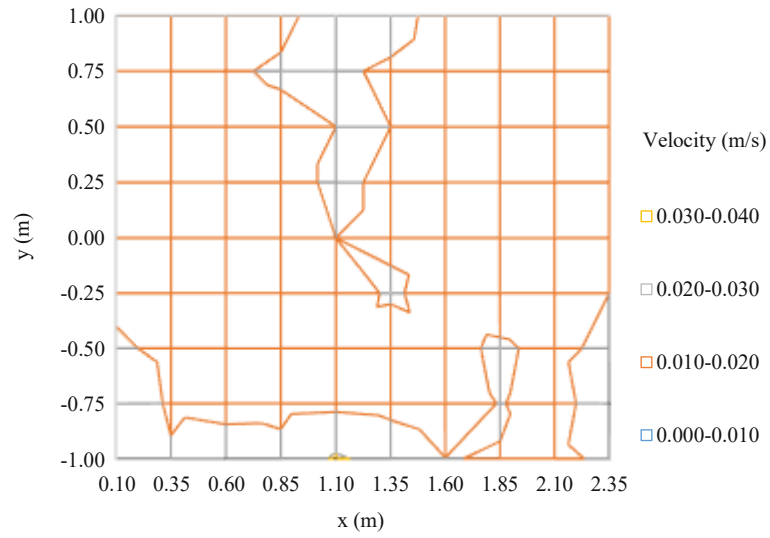
*Figure 33 Measured Air Velocities in 60cm above the floor*
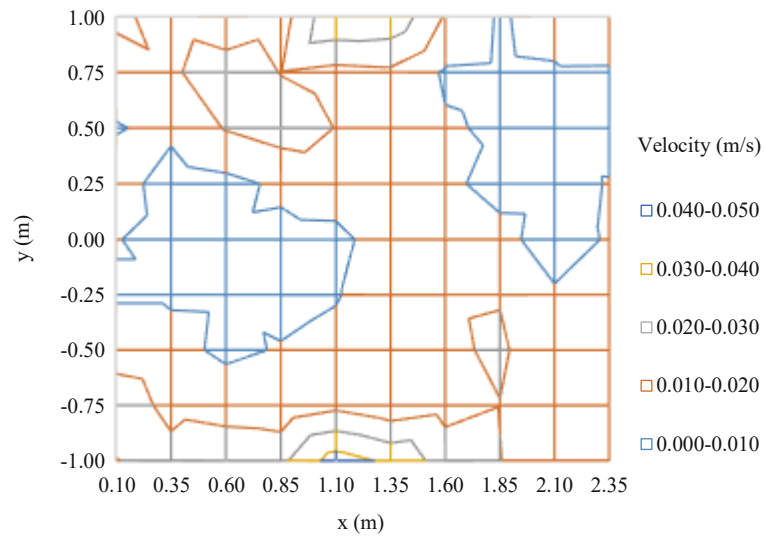


*Figure 34 Simulated Air Velocities in 60cm above the floor*
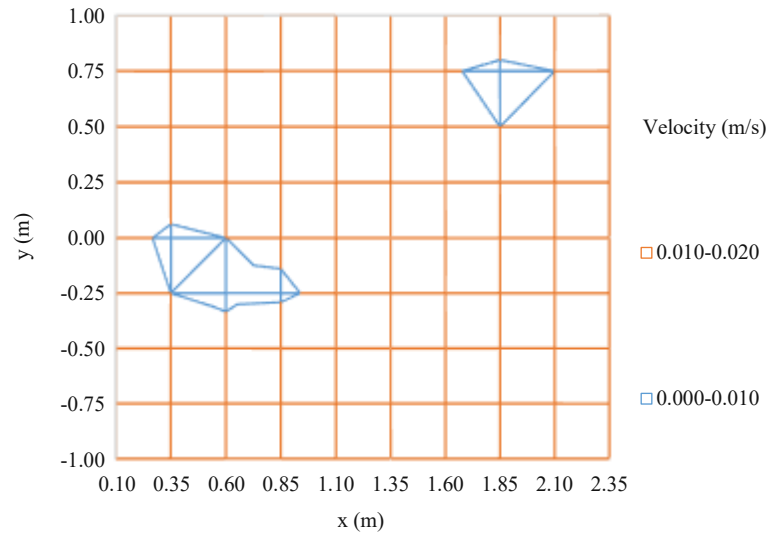
*Figure 35 Measured Air Velocities in 110cm above the floor*
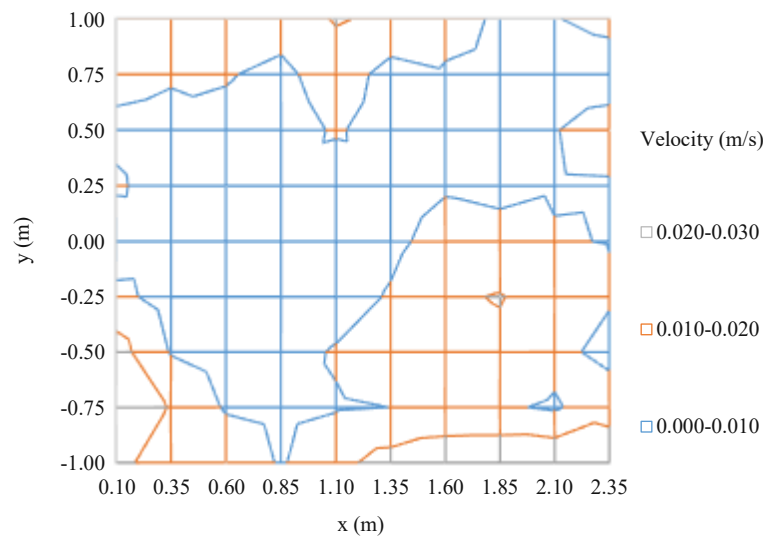


*Figure 36 Simulated Air Velocities in 110cm above the floor*

Figure 37 to Figure 42 illustrate the Air Temperature values in three heights resulted alternately from measurement and CFD simulation. These diagrams imply an acceptable correlation between iso thermal lines from simulations and measurements, even though lines do not match perfectly by overlaying and there is a 0.1˚K temperature difference in some cases.
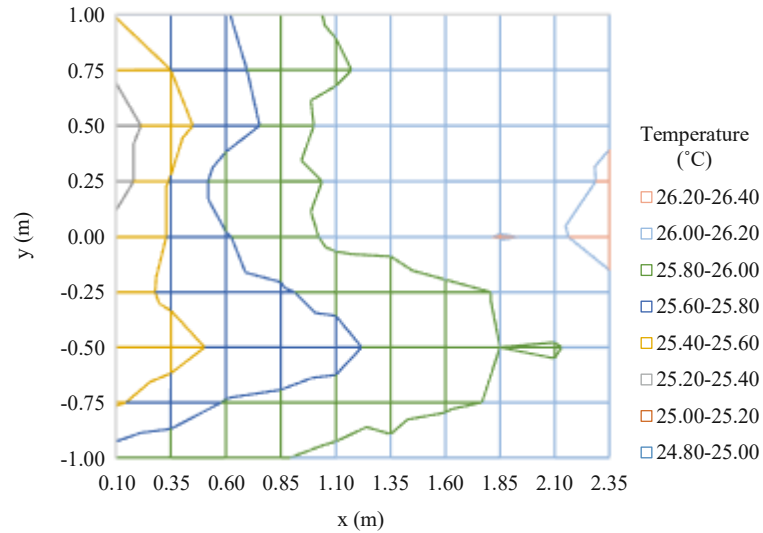


*Figure 37 Measured Air Temperatures in 10cm above the floor*
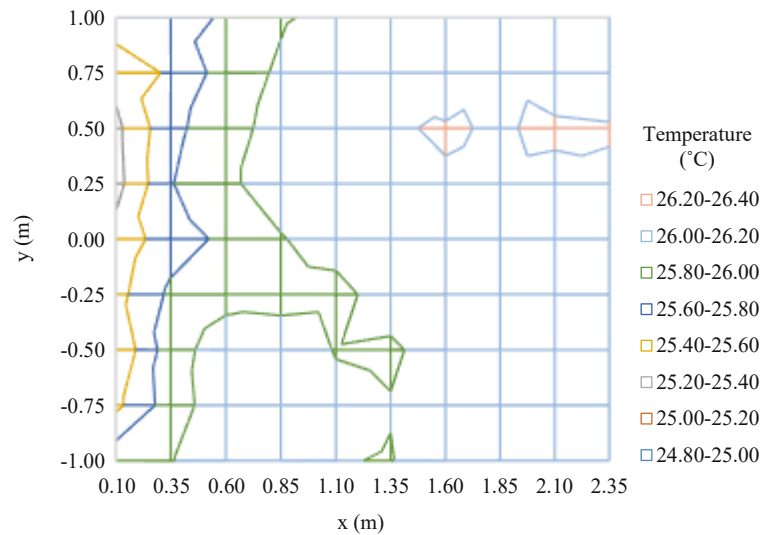


*Figure 38 Simulated Air Temperatures in 10cm above the floor*
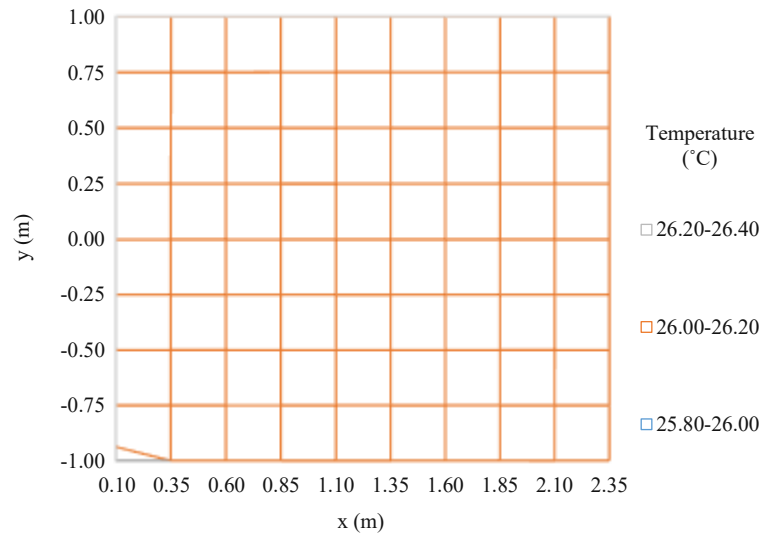
*Figure 39 Measured Air Temperatures in 60cm above the floor*
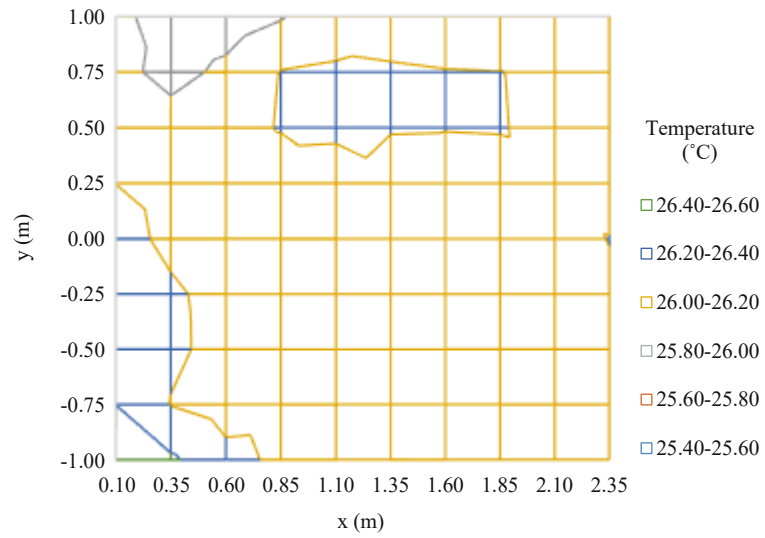


*Figure 40 Simulated Air Temperatures in 60cm above the floor*
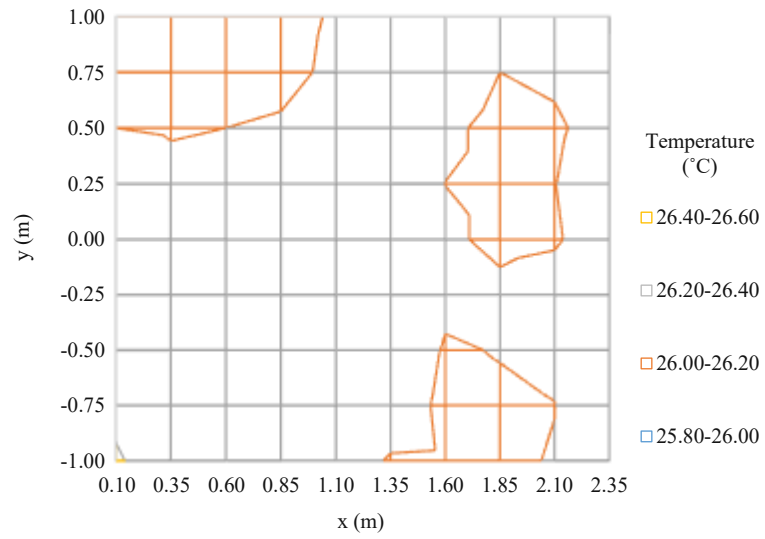
*Figure 41 Measured Air Temperatures in 110cm above the floor*
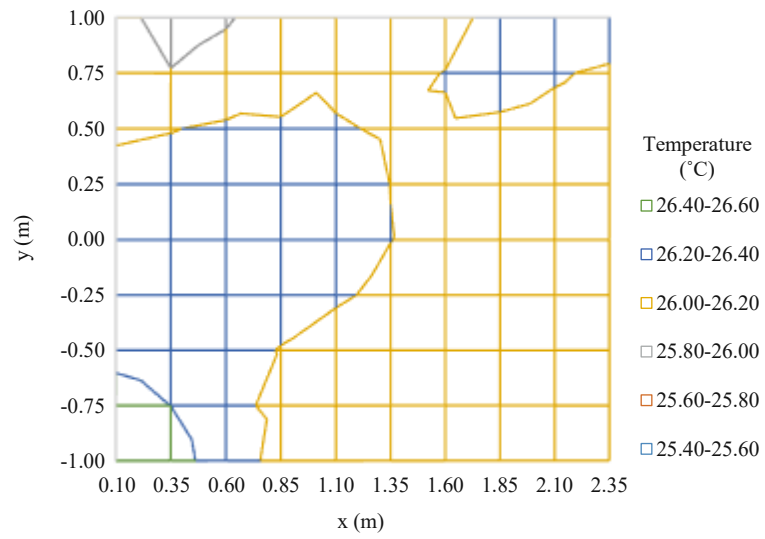
*Figure 42 Simulated Air Temperatures in 110cm above the floor*

# Chapter 4
# Results and Discussion

In this chapter results of the CFD simulations which are presented in the previous chapter are reported and afterwards in the discussion it is tried to reflect the yielded findings.

## *4.1 Results*

In the next pages, the results of CFD simulations is presented in two forms of graphical diagrams and line charts. The colors on the section planes (Figure 44 to Figure 61) represents profiles of LMA, air velocity, or air temperature. The aforementioned profiles of air variables are created in two A-A and B-B sections Figure 43 to investigate the air quality in the BZ of the occupant. In addition to the profiles, the colors on the human mannequin represent either Predicted Mean Vote (PMV) or Percentage Persons Dissatisfied (PPD) scale. In diagrams which contain either LMA or Velocity profiles, the color representation on the human mannequin indicates PMV scale. On the other hand, diagrams with temperature profiles are coupled with PPD scale on the mannequin. In all diagrams arrows on the section plane denote three-dimensional air velocity vectors and have all the same length. Their complementary purpose, for example in diagrams with velocity profile, is showing the flow direction at the corresponding position; and in those with LMA profile is revealing the movement of air particles towards their next position.
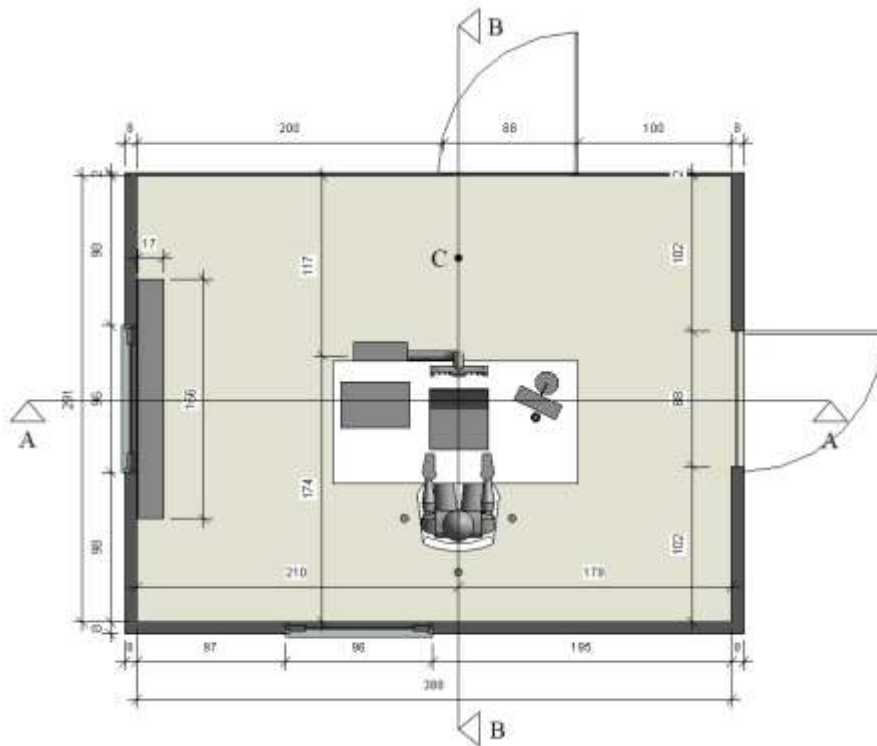
*Figure 43 Office Room Setup for CFD Simulations*

### 4.1.1 Scenario A1 (DV)

In this scenario the office cell is ventilated only with displacement ventilation. Figure 44 and Figure 45 illustrate LMA profile in the occupant's position. These diagrams show that the indoor air formed separate layers in the height of the room. The layers near to the floor have lower age of air and near to the ceiling are older. The temperature profiles are also in accordance with the fact that the indoor air has become stratified in the height of the room, Figure 48 and Figure 49. This confirms the DV system is designed properly and handles the heating sources of the office room. Velocity vectors and air speed magnitude in section A-A, Figure 47, show the air is flowing on the floor from inlet diffuser towards the end of the room and raising up as it hits the occupant. The fresh air is nevertheless able to reach to the end of the room. Figure 46 to Figure 49 display areas above the heat sources have higher air velocity and temperatures. This shows the thermal plume is formed around these objects and warm air is rising up.

Figure 45 show throughout the room up to 80cm above the floor air particles have LMA values less than 240 seconds. This signifies DV is able to provide

fresh air in this zone. Figure 44 reveals that around the occupant in the BZ, 110cm above the floor, LMA values are less than 180 seconds and lower the rest of the room in this height. It is as well an indication of effective removal of contaminants produced by occupant from BZ. It can be inferred that a stationary occupant at any place of the room could attract the airflow towards itself and benefit the fresh air in its position.

In the unoccupied zone - heights above 110cm - the air particles have LMA values higher than 300 seconds. Despite working principle of DV, Figure 45 shows there is also a region of stagnant air with LMAs higher than 420 seconds above the near zone in upper left of the profile, which indicate air quality is very poor in this region. The area near the outlet position have LMAs around 360 seconds which suggests it take 6 minutes in average from an air particle to be discharged from DV inlet diffuser, travel in the room and finally exits from the outlet. However, in the Breathing Zone (BZ) near to the occupants and heat sources on the desk the air tends to be less stagnant. Due to convective (thermal) flows with DV, contaminants will flow to the upper zone, thus DV provides better IAQ. Velocity diagrams also ascertain this fact, Figure 46 and Figure 47. The surface color of the human mannequin in the latter pictures, which shows PMV values, express that the occupant experiences a minor discomfort in this scenario. The blue feet region indicates cool feeling in the ankle level in contrast with yellow chest and back. It suggests that in practice the occupant will feel slightly cold in lower body and slightly warm in upper body.

Temperature diagrams (Figure 48 and Figure 49) show the air around the head of the occupant is 3˚C warmer than the air in the feet zone. This temperature difference could become even bigger if the occupant was in a standing position. In the latter diagrams, the occupant colors represent Percentage Persons Dissatisfied. It is visible that in most parts of the body the PPD is less than 10%.
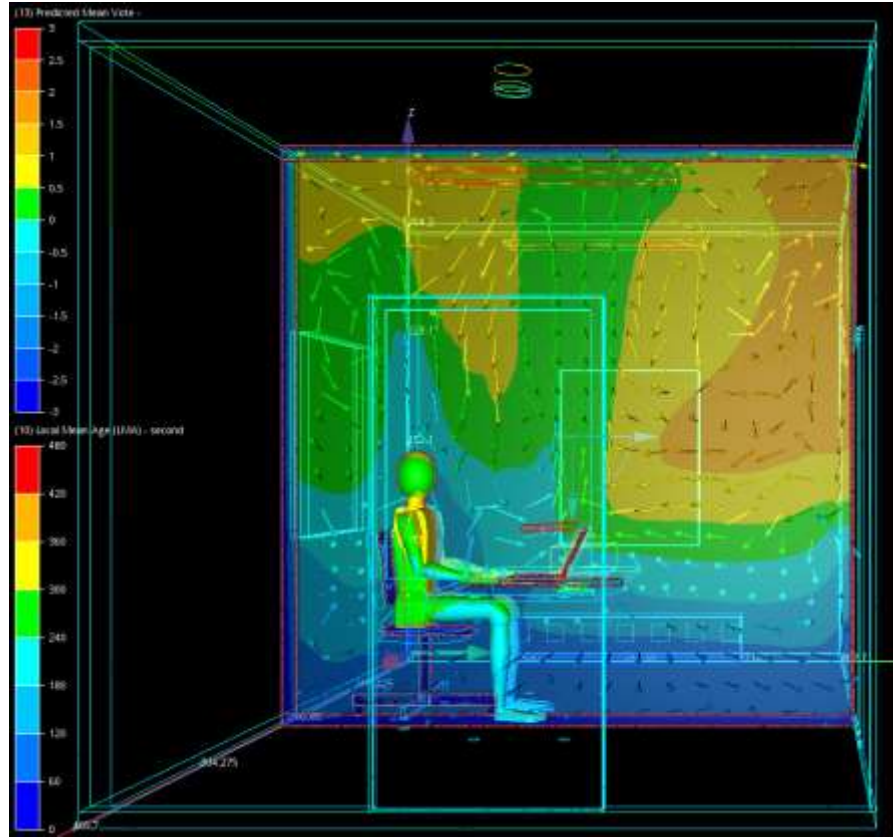
*Figure 44 Profile of LMA together with PMV scale on the mannequin,*

*DV Scenario, Section B-B*
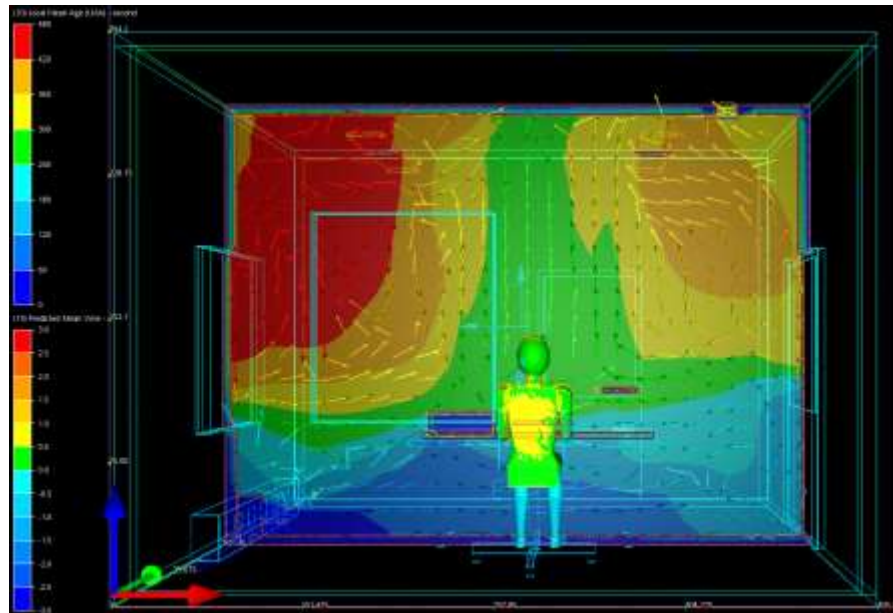


*Figure 45 Profile of LMA together with PMV scale on the mannequin,*

*DV Scenario, Section A-A*

73
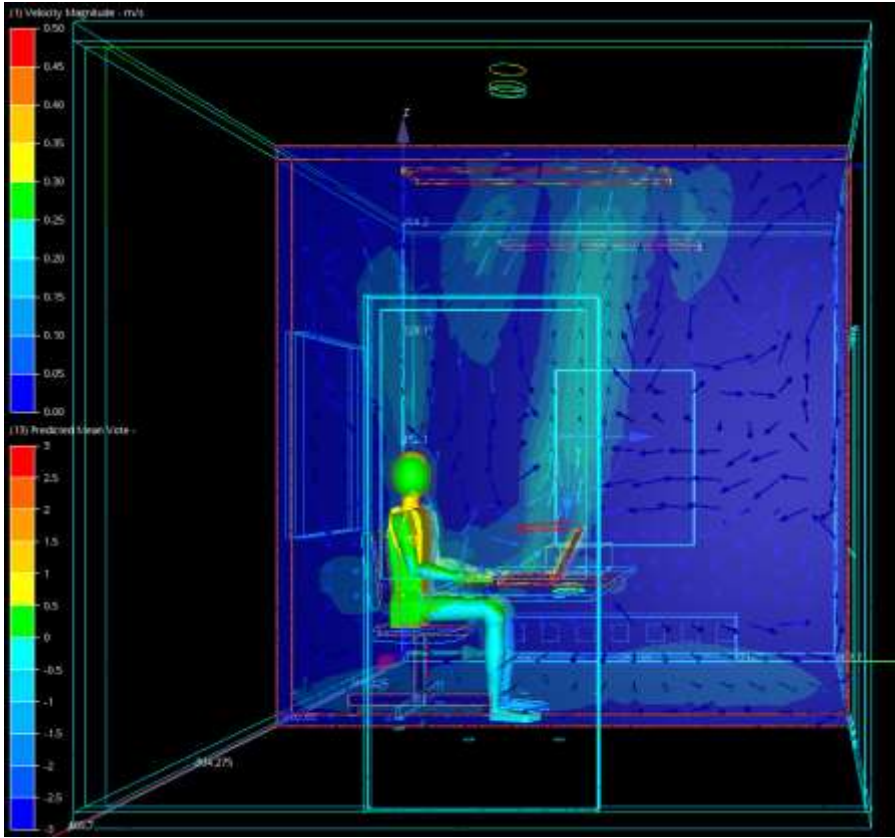
*Figure 46 Profile of Air Velocity together with PMV scale on the mannequin,*

*DV Scenario, Section B-B*
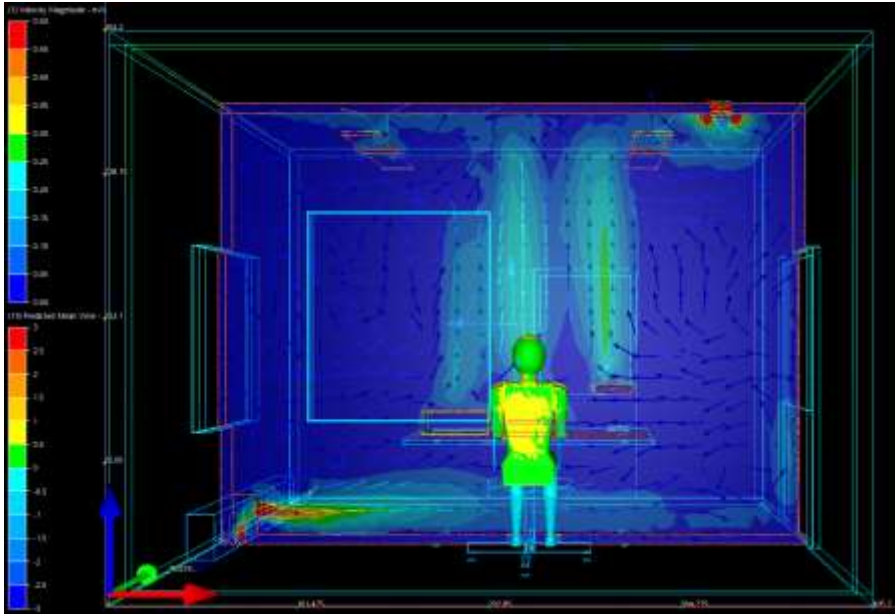


*Figure 47 Profile of Air Velocity together with PMV scale on the mannequin,*

*DV Scenario, Section A-A*
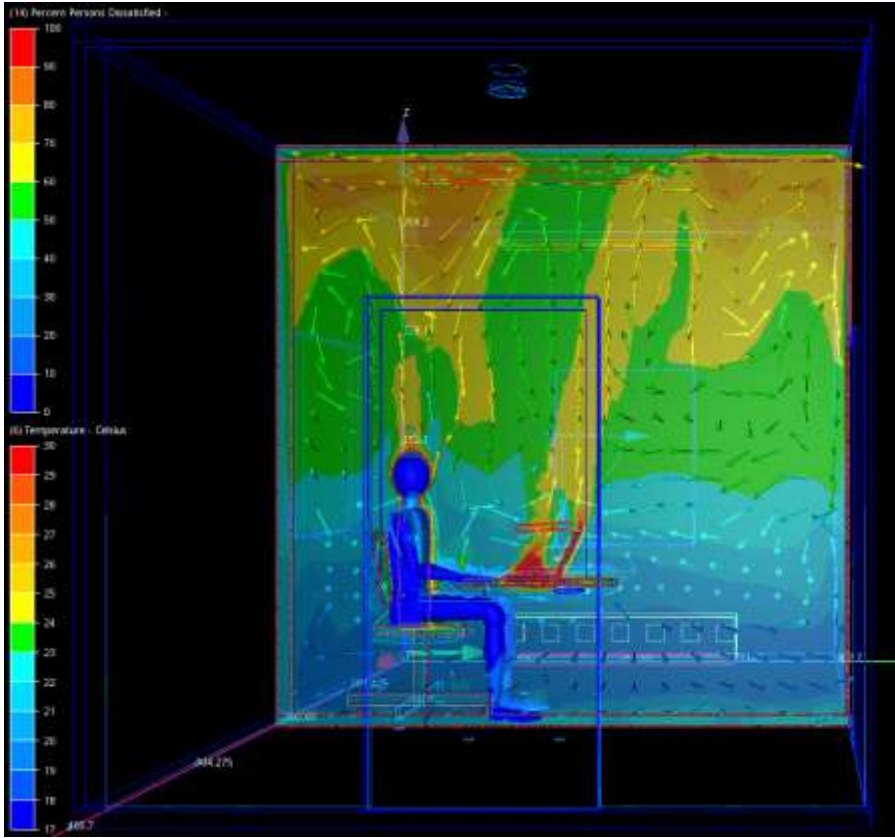
*Figure 48 Profile of Air Temperature together with PPD scale on the mannequin,*
*DV Scenario, Section B-B*
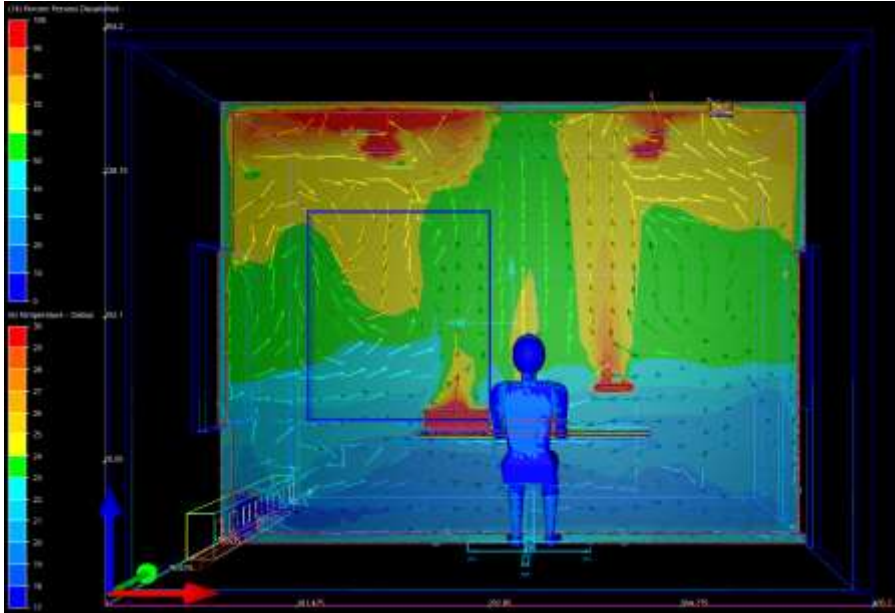


*Figure 49 Profile of Air Temperature together with PPD scale on the mannequin,*
*DV Scenario, Section A-A*

## 4.1.2 Scenario A2 (DV + Low-speed Ductless PV) and A3 (DV + High-speed Ductless PV)

As described in 3.4.5, in these scenarios a ductless PV system operates in parallel to assist the performance of DV by transferring air directly from ankle level to the breathing zone of the occupant.

Comparing LMA results in section A-A, Figure 51, suggest that fresh air supply by DV has been disturbed by vacuuming large volumes of air from ankle level in high-speed ductless PV scenario. In this state the fresh air cannot reach to the end of the room and regions near to the door have LMAs greater than 300 seconds. Temperature profiles in Figure 61 confirms as well this finding and indicates moreover that in high-speed scenario layers with stratified temperature could not form, which is one of the requirements for a DV system to remove contaminants properly from space. Additionally temperature profile and velocity vectors in section A-A, Figure 55, illustrate the air after being discharged from the DV inlet tends to rise instead of forming a layer of cool fresh air on the floor.

Figure 50 shows LMA values in occupant's BZ are at least 120 seconds higher than the low-speed case. LMA profiles in both sections display a stagnant region of air particles above the desk near the ceiling with values higher than 420 seconds. Furthermore, maximum LMA value of DV + low-speed DV scenario has been decreased by 60 seconds compared to individual operation of DV which is an indication for higher efficiency of the system in this state.

Investigating Figure 54 and Figure 55 suggest forming thermal plumes on top of personal computer and occupants' head is disrupted by high volumes of cool air discharged to the BZ. Thus, the produced contaminants in this region cannot rise up towards the outlet and is mixed instead with the indoor air. This phenomenon can also be observed in velocity and Temperature profiles. On the other hand, the high speed of ductless PV intake escalated the height of air layer with 23°C from 110cm to 260cm. Therefore, it resulted reduction of the air temperature in BZ by 5°C.

Figure 54 illustrate cold regions of air with 17°C in front and back of the occupant in high-speed scenarios versus 22°C in low-speed. High speed of the intake fan results a level of discomfort for occupant. Color scale on the mannequin confirms this fact too by showing PPD of 50 % and PMVs greater than 1 in chest and back areas. It should also be noted that in low-speed scenario mannequin displays -0.5 PMV scale on the feet whereas +0.5 in the high-speed scenario. Hence high speed of the ductless PV can reduce the cold feet sensation slightly.
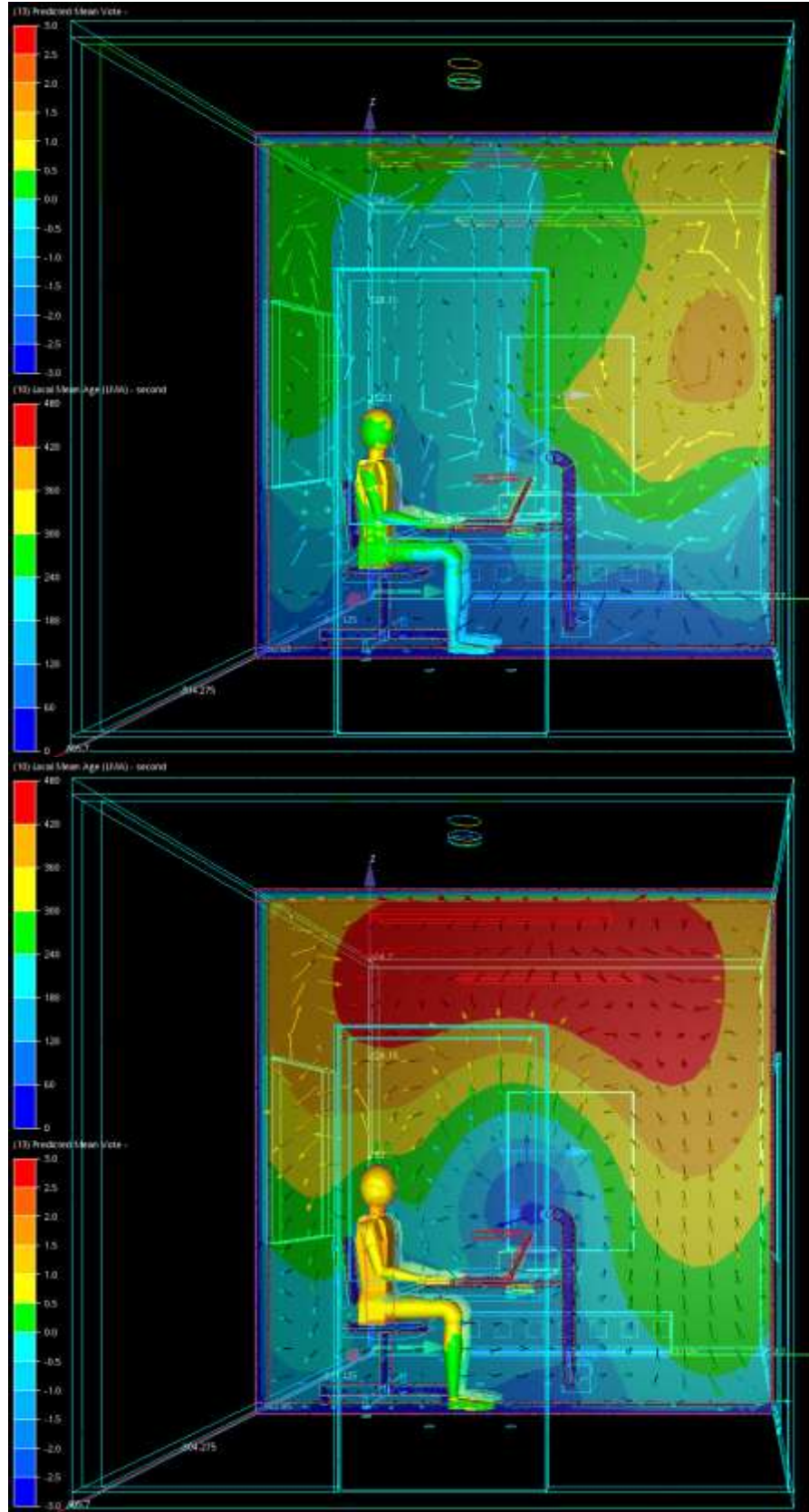
*Figure 50 Profile of LMA together with PMV scale on the mannequin,*

*DV + Low Speed (up) and High Speed (down) Ductless PV scenarios, Section B-B*
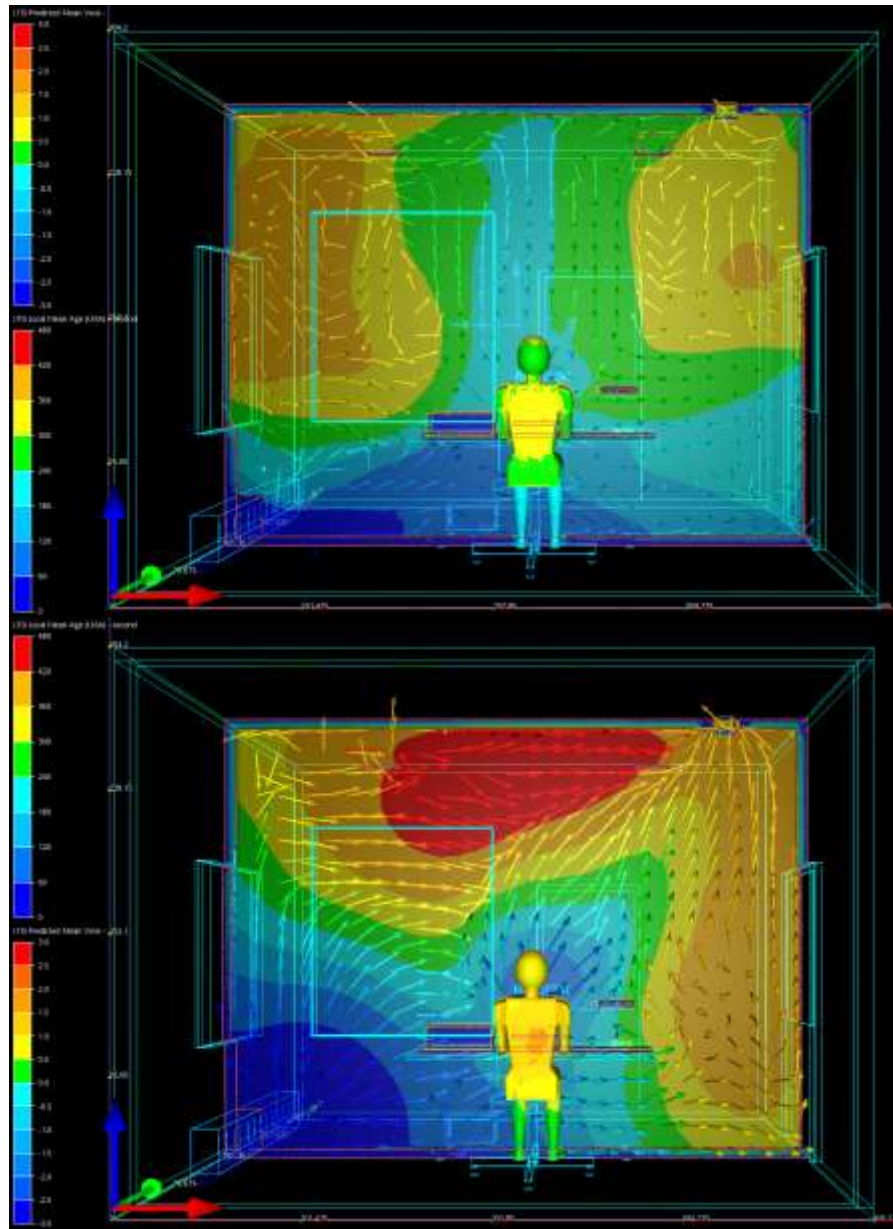
*Figure* 51 *Profile of LMA together with PMV scale on the mannequin,*

*DV + Low Speed (up) and High Speed (down) Ductless PV scenarios, Section A-A*
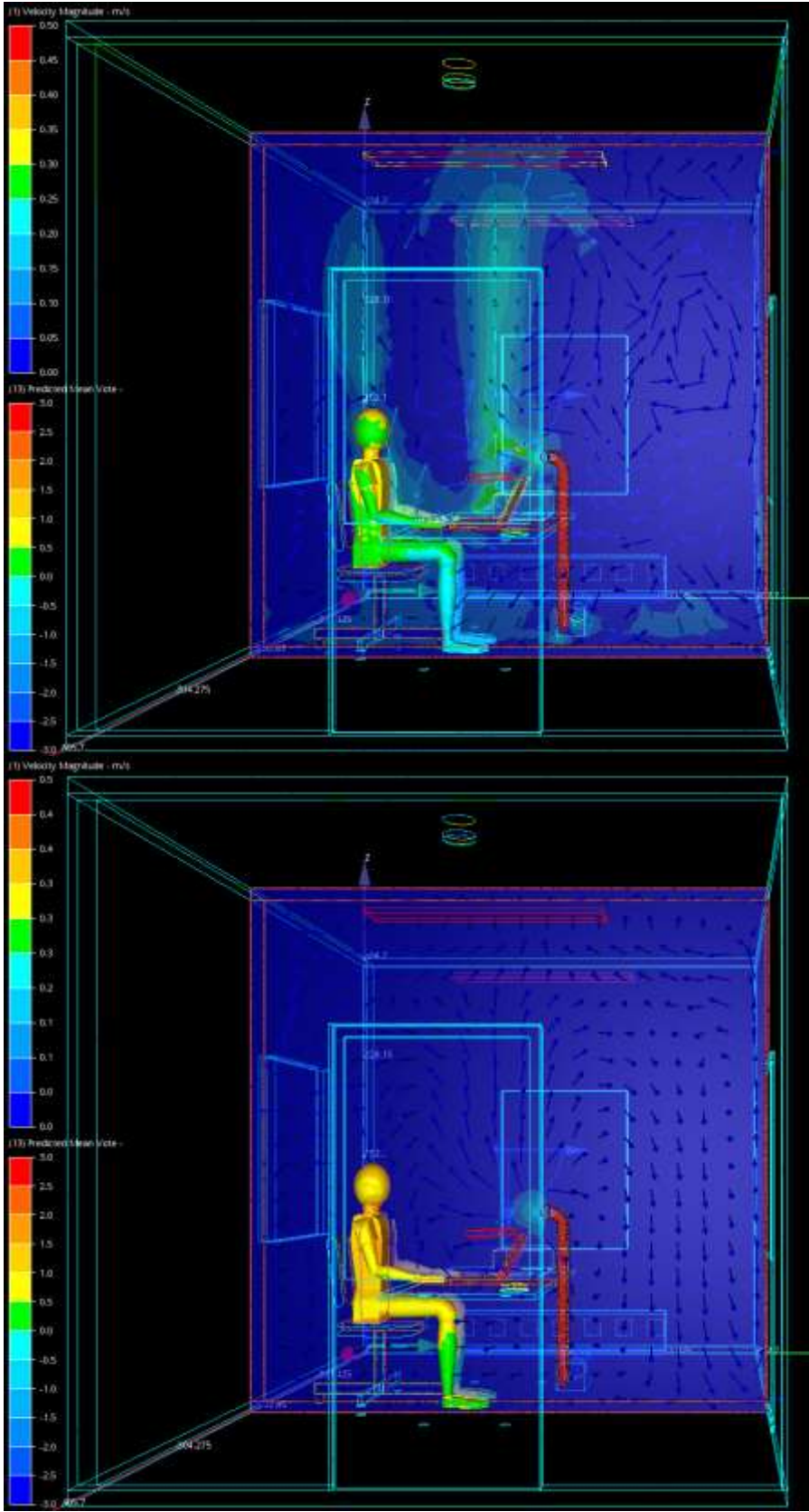
*Figure* 52 *Profile of Air Velocity together with PMV scale on the mannequin,*

*DV + Low Speed (up) and High Speed (down) Ductless PV scenarios, Section B-B*
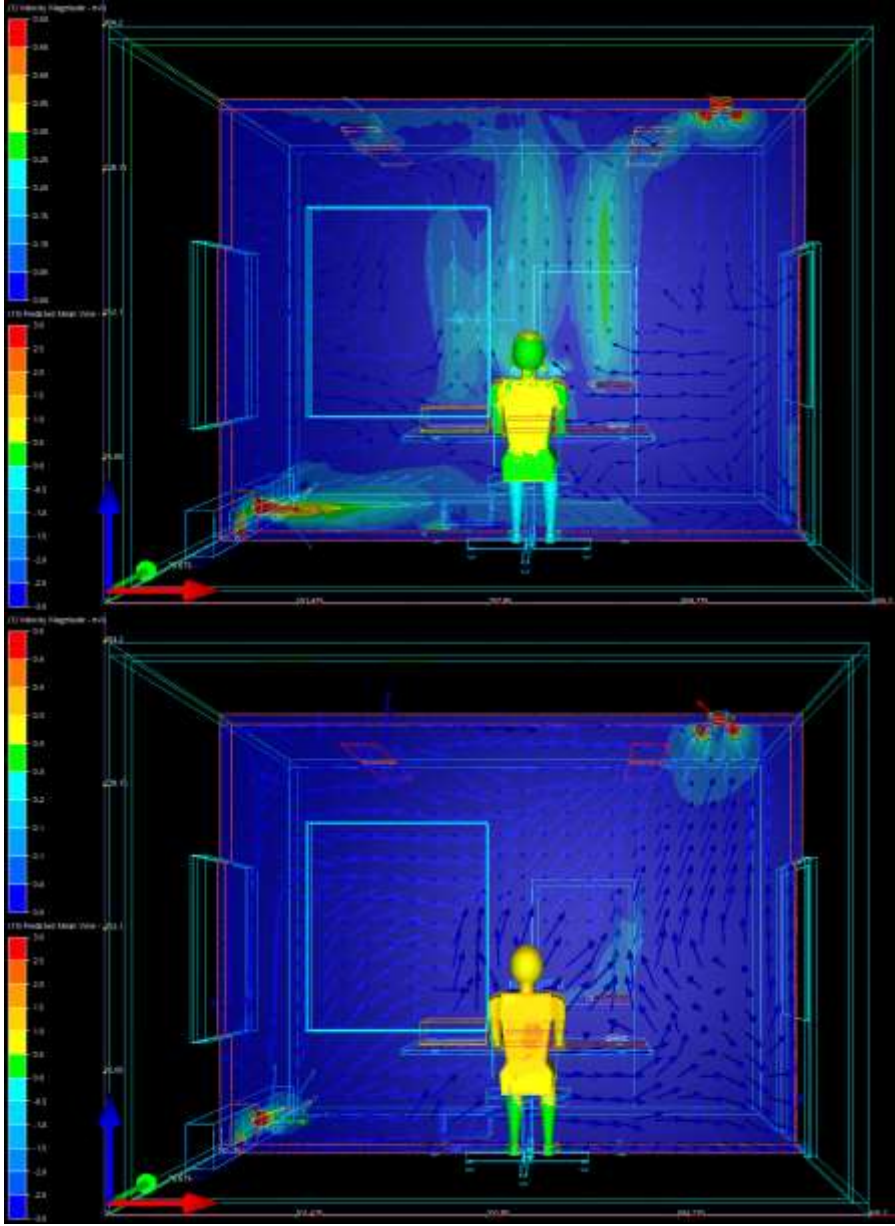
*Figure* 53 *Profile of Air Velocity together with PMV scale on the mannequin,*

*DV + Low Speed (up) and High Speed (down) Ductless PV scenarios, Section A-A*
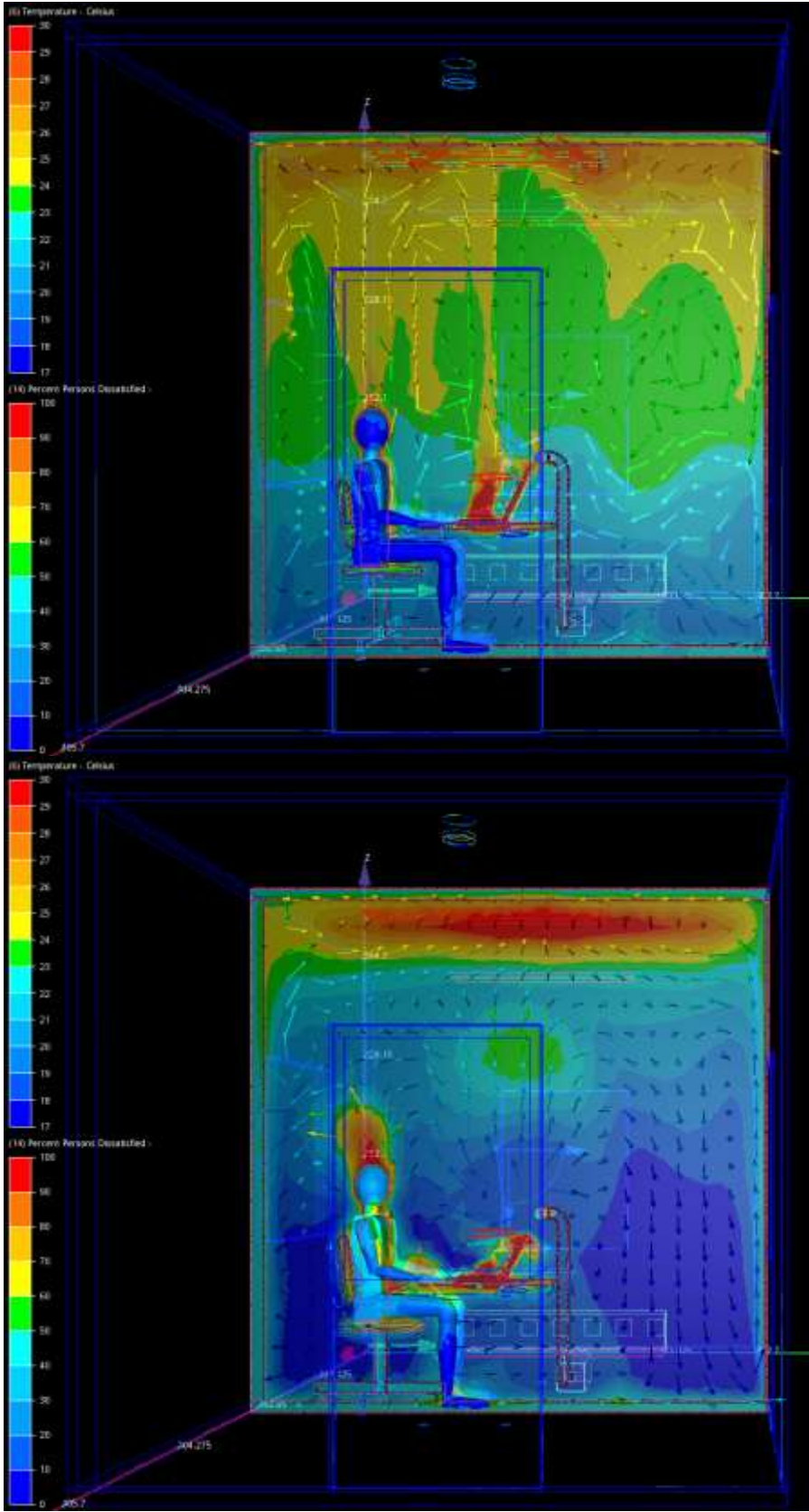
*Figure* 54 *Profile of Air Temperature together with PPD scale on the mannequin,*

*DV + Low Speed (up) and High Speed (down) Ductless PV scenarios, Section B-B*
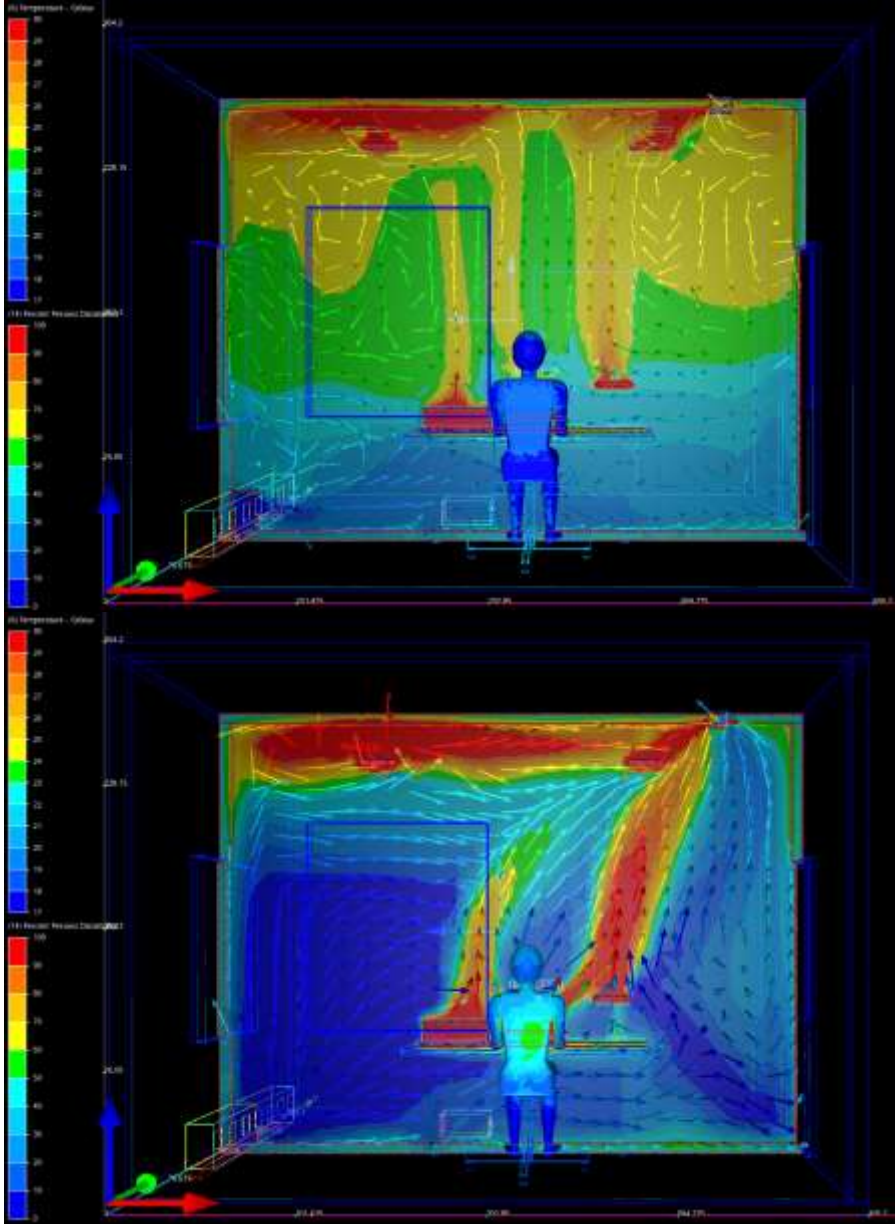
*Figure 55 Profile of Air Temperature together with PPD scale on the mannequin,*

*DV + Low Speed (up) and High Speed (down) Ductless PV scenarios, Section A-A*

### 4.1.3 Scenario A4 (Ducted PV) and A5 (DV + Ducted PV)

As described in 3.4.5, two scenarios are designed to investigate the performance of ducted PV in two conditions of individual operation and in conjunction with DV. In this state 20 percent of the supply air is handled by DV and 80 percent by ducted PV.

In case of individual operation of ducted PV, it appears all regions have 60 seconds younger local mean air, Figure 56 and Figure 57. It could be observed that both cases are the most effective in terms of removing contaminants from Breathing Zone among all scenarios. Since the Ducted PV provides fresh air directly to the BZ the radius of the region with LMAs less than 120 seconds is visibly broader comparing to the all other scenarios. In ducted PV scenario this region is extended from floor to 180cm height. This could be due to higher VFR of fresh air discharged to the BZ. Furthermore, Figure 57 shows that LMA values of air particles in the outlet position of ducted PV scenario is less than 240 seconds. However, the regions behind the PV diffuser have high LMAs, thus containing high levels of contaminants.

ASHRAE standards 1992, ISO 1984 require PMV ≤ 0.5 for an office environment. Velocity profiles in Figure 58 illustrate air speeds higher than 0.5 m/s in front of the occupant. The high velocity region is larger especially in ducted PV scenario. In the CFD model the mannequin's position is, nevertheless, in a region with air speeds less than 0.05 m/s. In practice occupant may seat in a different position for instance leaning forward to the desk and experience the discomfort which is caused by high speed of air from PV diffuser. ASHRAE (Glicksman & Chen, 2003) recommends a maximum face velocity of 0.2 m/s for regularly occupied commercial spaces.

Figure 60 shows that the air temperature in front of the mannequin is 25˚C versus 19˚C in the back of its head. This temperature asymmetry may result in discomfort for the occupant. The PPD is 50% in the back of the mannequin confirms this fact, Figure 61. This will lead to a warm feeling and sweating in posterior part the body. A PMV value greater than 1 in Figure 57 is also in compliance with this notion.

Temperature profiles illustrate ducted PV results in significantly lower air temperatures among all the scenarios. Figure 60 and Figure 61 suggest the system has a good capability for cooling down the room despite its shortcomings. It appears in both sections that the generated heat by human mannequin and electrical equipment on the desk is dissipated successfully. However, the system is still not effective with the accumulated heat near to the ceiling generated by high wattage overhead lighting.

It seems level of provided IAQ under individual operation of ducted PV system depends on its orientation in the room and room size. Direction and magnitude of the air velocity, together with relatively uniform air temperature throughout the room imply that better designs of this system has the potential for providing acceptable IAQ and human comfort in small spaces.
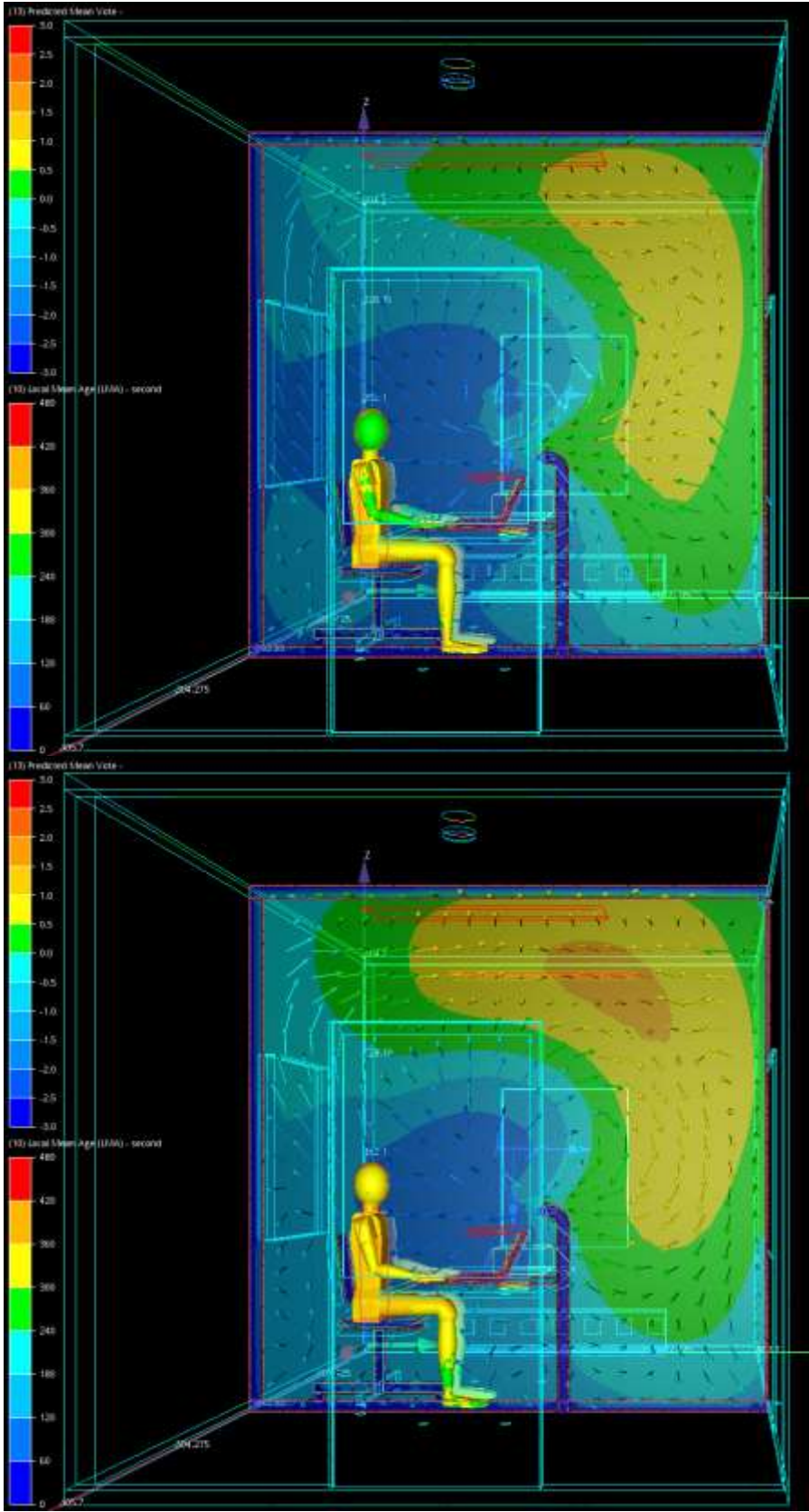
*Figure 56 Profile of LMA together with PMV scale on the mannequin,*

*Ducted PV (up) and DV + Ducted PV (down) scenarios, Section B-B*
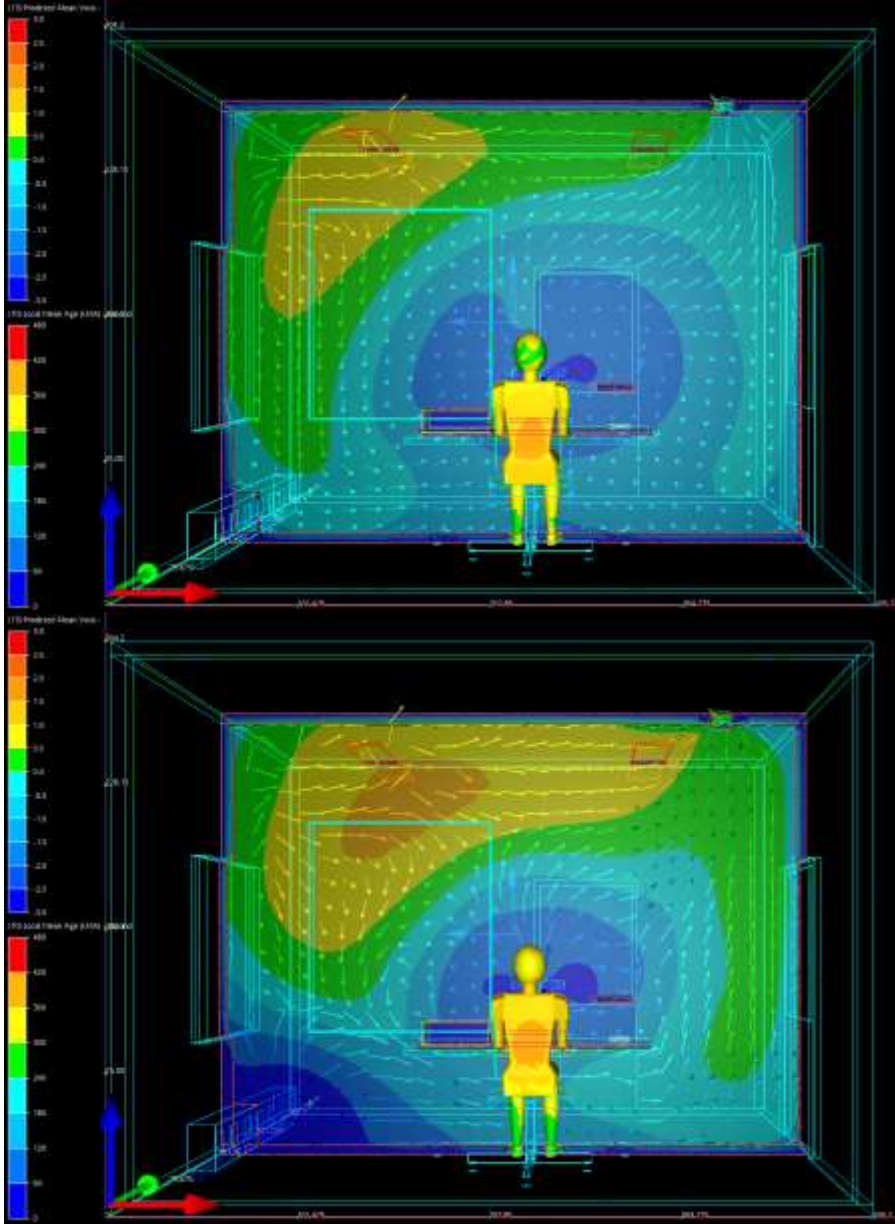
*Figure 57 Profile of LMA together with PMV scale on the mannequin,*

*Ducted PV (up) and DV + Ducted PV (down) scenarios, Section A-A*
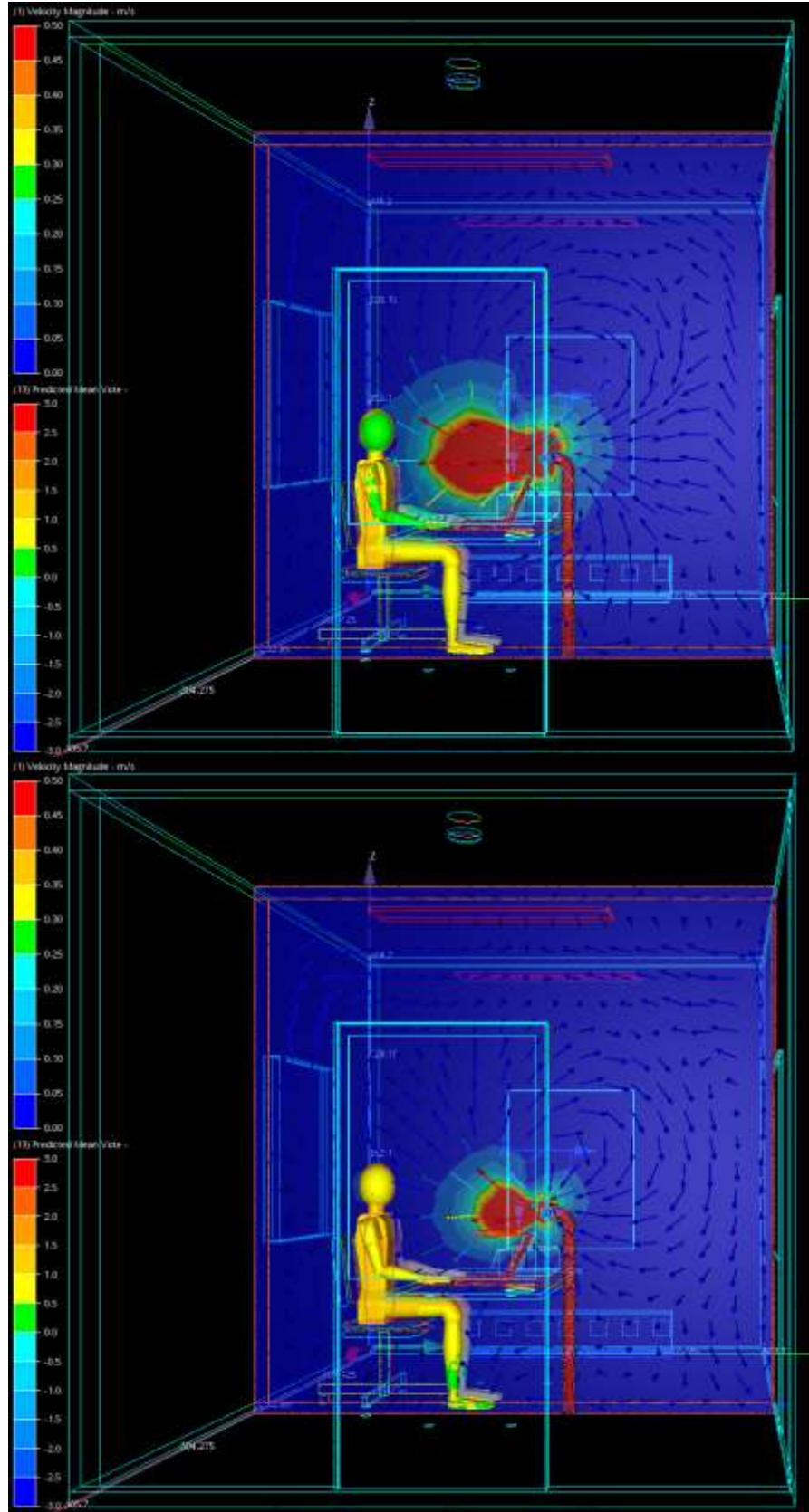
*Figure 58 Profile of Air Velocity together with PMV scale on the mannequin,*

*Ducted PV (up) and DV + Ducted PV (down) scenarios, Section B-B*
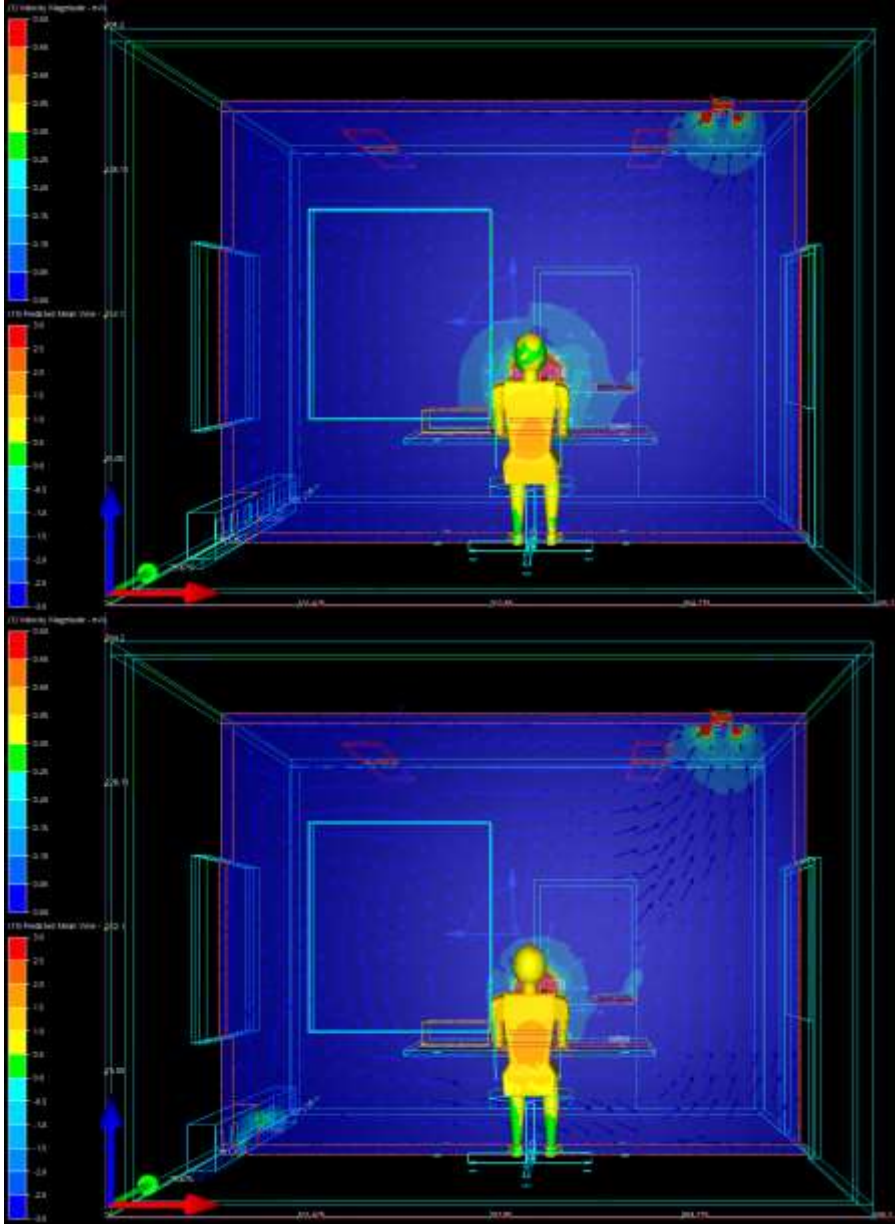
*Figure* 59 *Profile of Air Velocity together with PMV scale on the mannequin,*

*Ducted PV (up) and DV + Ducted PV (down) scenarios, Section A-A*
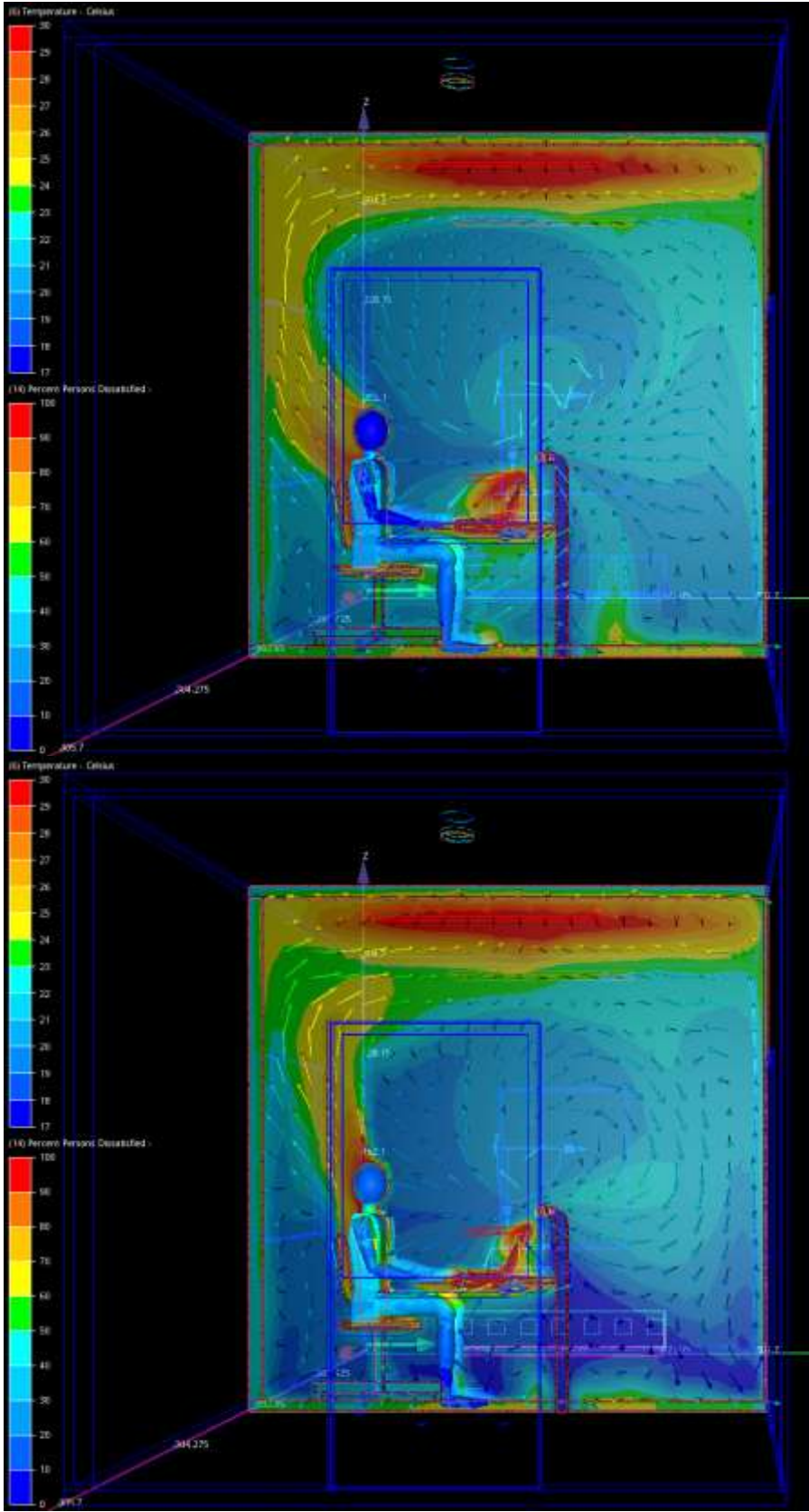
*Figure* 60 *Profile of Air Temperature together with PPD scale on the mannequin,*

*Ducted PV (up) and DV + Ducted PV (down) scenarios, Section B-B*
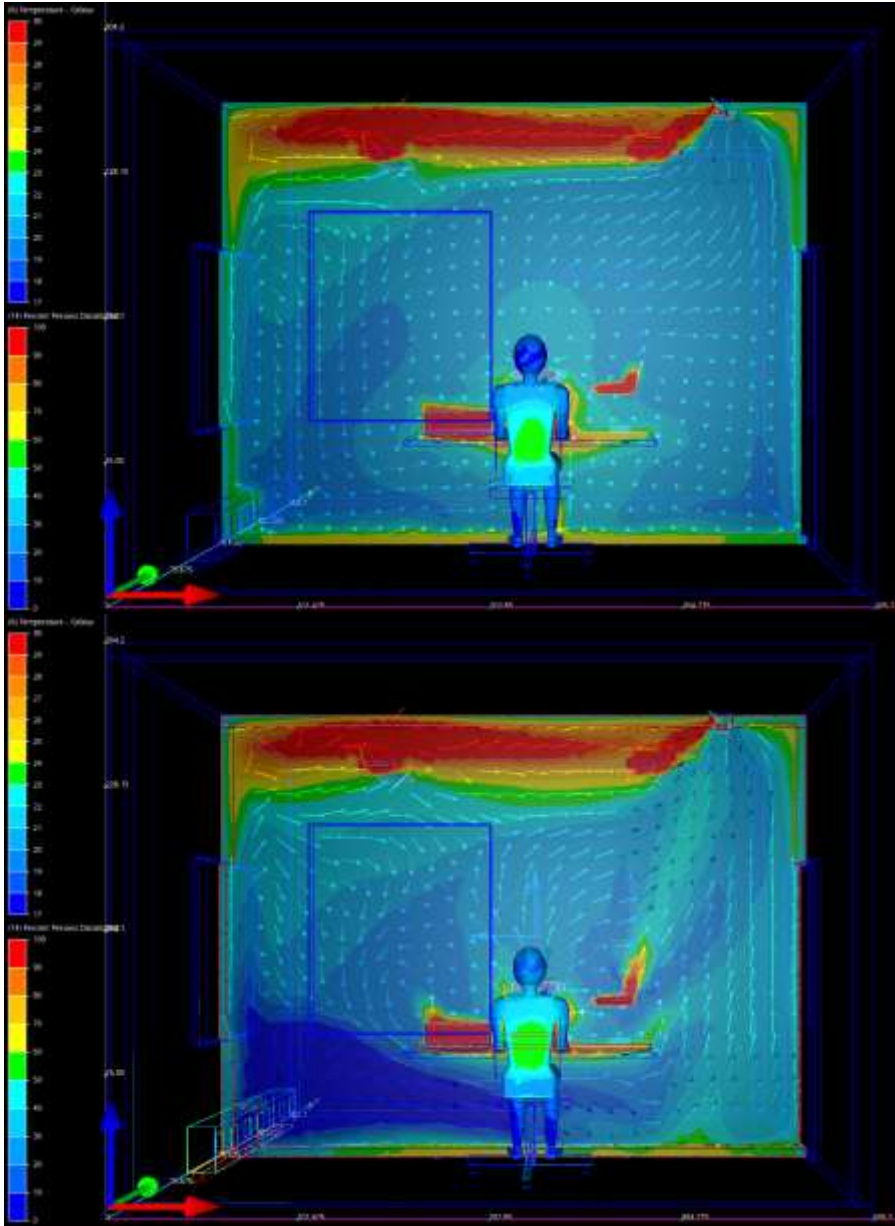
*Figure* 61 *Profile of Air Temperature together with PPD scale on the mannequin,*

*Ducted PV (up) and DV + Ducted PV (down) scenarios, Section A-A*

## 4.1.4 Scenarios B1 to B4 (Alternative Inlet Diffusers of DV + Ductless PV)

The results of a previous study, which also carried out in the office mock-up of this project, revealed air speeds in 10cm above the floor are not uniform (Taheri, et al., 2016). Likewise in this project air speed measurements in front of DV inlet diffuser confirms that air velocities in y = 0.25 to 0.75m are in average 0.01 m/s higher than in y = -0.25 to -0.75m, Figure 31. This difference is also detectable in the center of the room. It is suspected that this asymmetry is due to the design of the DV inlet diffuser. This fact aroused suspicion that the nonuniformity in distribution pattern of diffuser could diminish the effectiveness of ductless PV system. To answer this hypothesis, four prototypes are designed for the inlet diffuser of DV, Figure 62. New diffusers have the same length as the one installed in the laboratory mock-up. In order to reduce turbulence inside the chamber and ease of the product construction, author suggested cylindrical shape. In addition, a flow guide is designed in the center of the air chamber to distribute air evenly to sides, Figure 63.Each alternative has a row of small holes in the front. Alternative 1 has circular openings with equal diameter whereas the others with varying sizes from 5 to 8mm. The reason for having holes with different sizes along the tube is to diffuse air with various pressures.
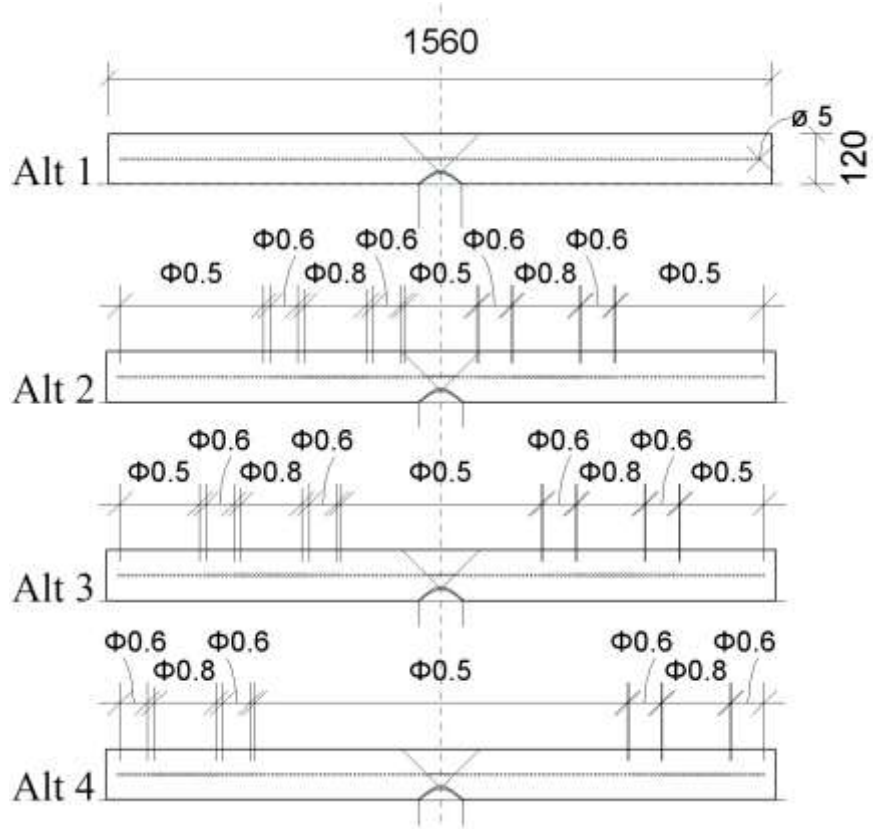
*Figure 62 DV Alternative Diffusers*
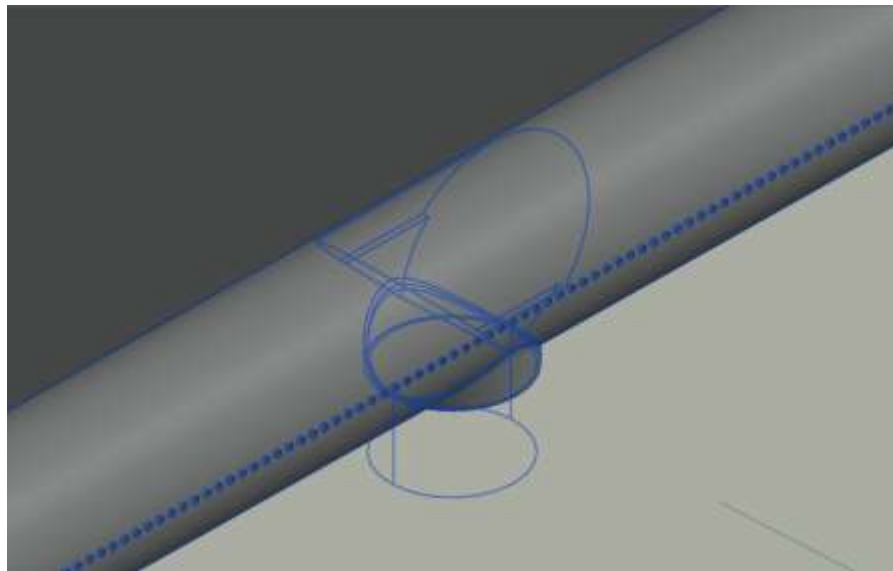


*Figure 63 Close-up of DV Alternative Diffusers*

To investigate diffusing efficiency of alternative diffusers they are replaced with the default DV diffuser and compared with *DV + High-speed Ductless PV* scenario.

Figure *64* compares LMA profiles of alternative diffusers with the existing one in section A-A. As diagrams show new design of the diffuser could not effectively improve the performance of ductless PV in terms of providing fresh air in room and removing contaminants from space. It is worth noticing that in scenarios B1 to B4 the area of stagnant air particles, LMAs greater than 420 seconds, is wider to some extent than the scenario with original DV supply diffuser. The dark blue region, which indicates the discharge range of fresh air, LMAs less than 60 seconds, is also decreased noticeably. However, LMAs in the outlet's position and in the breathing zone in front of the occupant has been remain unaffected, which imply there is no difference between the efficiencies of new DV supply diffusers and the default one.

Temperature profiles show no alteration not only in section A-A but also in section B-B. They show as well temperature gradient is not affected in the position of outlet as a result of diffuser substitution. Velocity profiles are also in compliance with LMA profiles. They show variations merely in the acceleration region of DV diffuser and not in the velocity decay region. These diagrams are not presented in this report for the sake of conciseness.
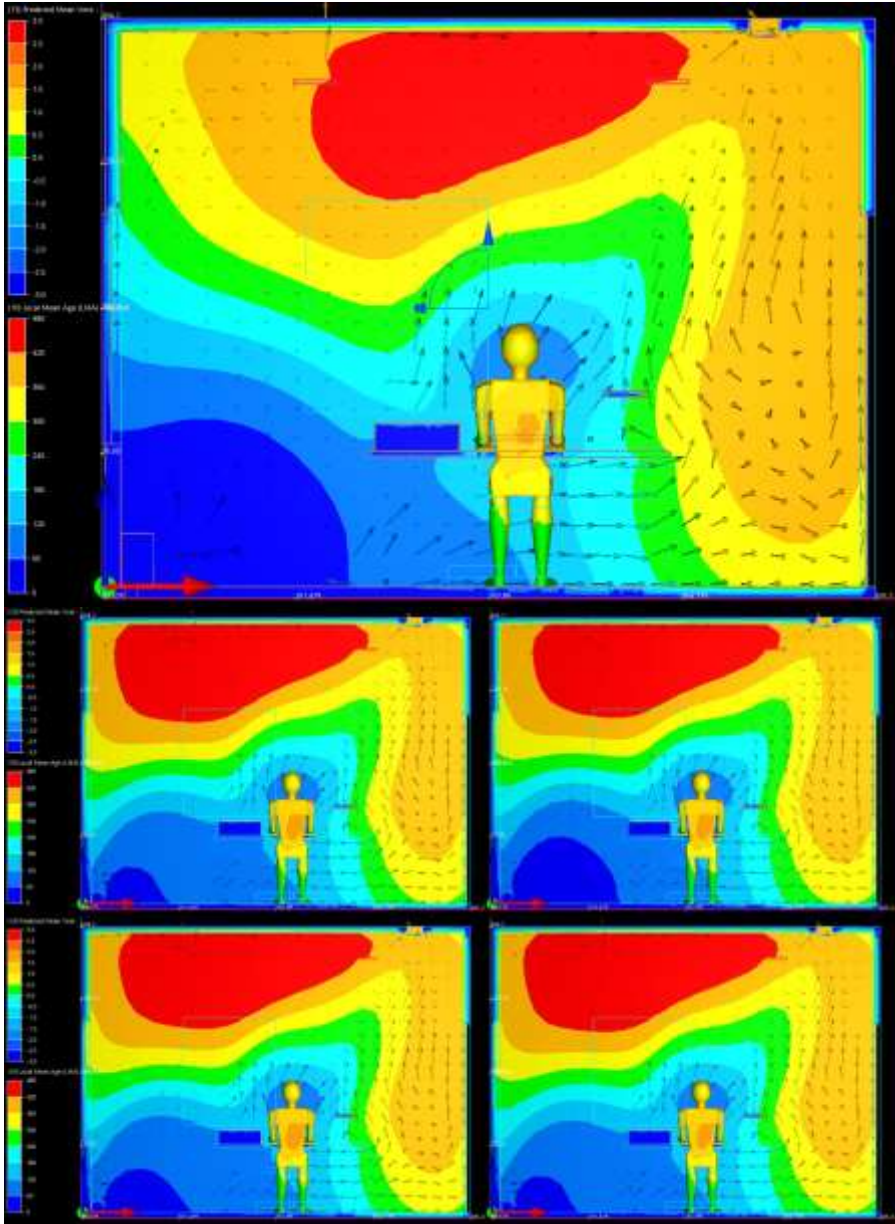
*Figure* 64 *Profile of LMA together with PMV scale on the mannequin,*

*Actual Diffuser (Up), Dif. Alt.06 (Center Left), Dif. Alt.07 (Center Right), Dif.*

*Alt.08 (Down Left), and Dif. Alt.09 (Down Right) in Section A-A*

## *4.2 Discussion*

Comparison of PPD and PMV results on the mannequin shows that both ducted and ductless PV alter the stratified temperature zone around the occupant. As a result, the occupant feels warmer in the back. Figure 65 compares PMV scale on the mannequin side by side in scenarios A1 to A5. This illustration shows that higher amounts of VFR discharged from either ducted or ductless PV can lead to discomfort in the position of occupant. However, these systems assist in reducing temperature gradient. ASHRAE Standard 55-2010 recommends that for good thermal comfort the temperature difference between the head and foot level of a standing person should not exceed 3°K. In a stratification zone assume that the temperature gradient will be less than 1.8°K/m. Compliance with these requirements will assure acceptable thermal comfort levels for 95% or more of the occupants.

Investigating LMA profiles show ducted PV can produce best results in the office mock-up. It shows this system has a better ability to remove contaminants from space. The maximum observed LMA values in this case is 120 seconds in average younger than the other models.

It is observed ductless PV, working in the low velocity mode, is able to improve ventilation effectiveness of DV. Figure 66 and Figure 67 show it can slightly improve the overall LMA values too without disturbing the pattern of supplied fresh air distribution by DV. However, it reduces the velocity decay region. Apropos, some additional simulations, which carried out in order to determine the minimum speed of ductless PV intake fan, showed decreasing its speed to smaller quantities than what is defined in low speed scenario not only does not deliver adequate air into the BZ but also decreases the LMA values in this region.

(1)                (2)                (3)                (4)                (5)
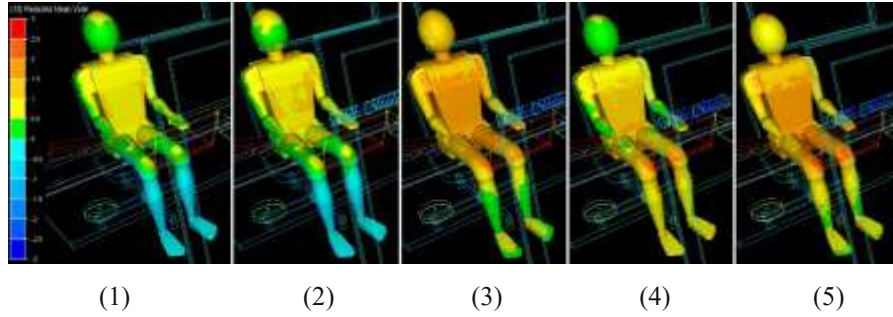
*Figure 65 PMV on the mannequin in DV (1), DV + Low-speed Ductless PV (2),*
*DV + High-speed Ductless PV (3), Ducted PV (4), and DV + Ducted PV (5)*
*scenarios*



(1)                (2)                (3)                (4)                (5)
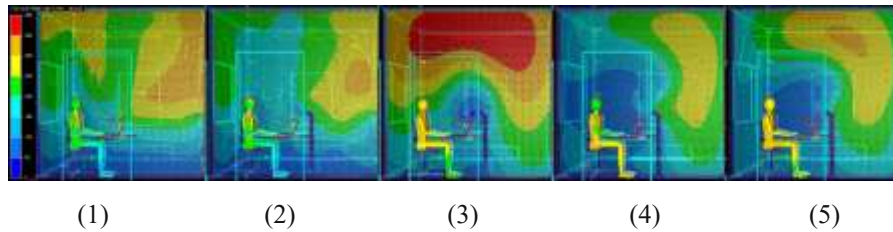
*Figure 66  LMA (on the section plane) and PMV (on the mannequin) in DV (1),*
*DV + Low Speed Ductless PV (2), DV + High Speed Ductless PV (3), Ducted PV*
*(4), and DV + Ducted PV (5) scenarios in Section B-B*
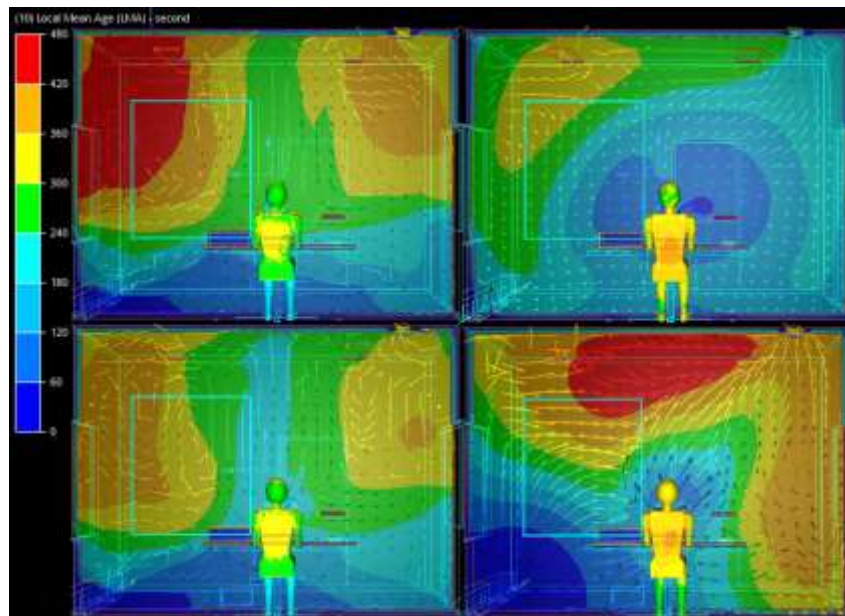


*Figure 67 LMA (on the section plane) and PMV (on the mannequin) in DV (up*
*left), Ducted PV (up right), DV + Low Speed Ductless PV (down left), and DV +*
*High Speed Ductless PV (down right) scenarios in Section A-A*

The line chart of Figure 68 displays air temperatures from A1 to A5 scenarios in 110cm above the floor in section B-B. The sudden temperature change in y = 60cm indicates the occupant's position. This diagram reveals that in ducted PV, DV + ducted PV, and DV + high-speed ductless PV, air temperature in 110cm above the floor around occupant's position is in average 3˚K lower than the other cases. This can be an indication of better cooling performance in these three scenarios and can be due to delivering higher amounts of fresh air to the BZ.

Figure 69 displays air temperatures from floor to ceiling in occupant's position. These line charts show in DV and DV + low-speed ducted PV air temperate variations are minimum among all scenarios. This condition is also in Figure 70 which compares air temperatures in point C (see also Figure 43).

Figure 71 reveals that in ducted PV scenario temperature stratification is not occurred in the outlet's position. It appears in scenario A5 ducted PV disturbed the air temperature stratification in outlet's position which is a sign of lower efficiency of air contaminant removal at this point. It is also perceivable that the exhaust air temperature, $T_e$, only in DV and DV + low-speed ductless PV scenarios is reached to 26˚C which is the designed value.
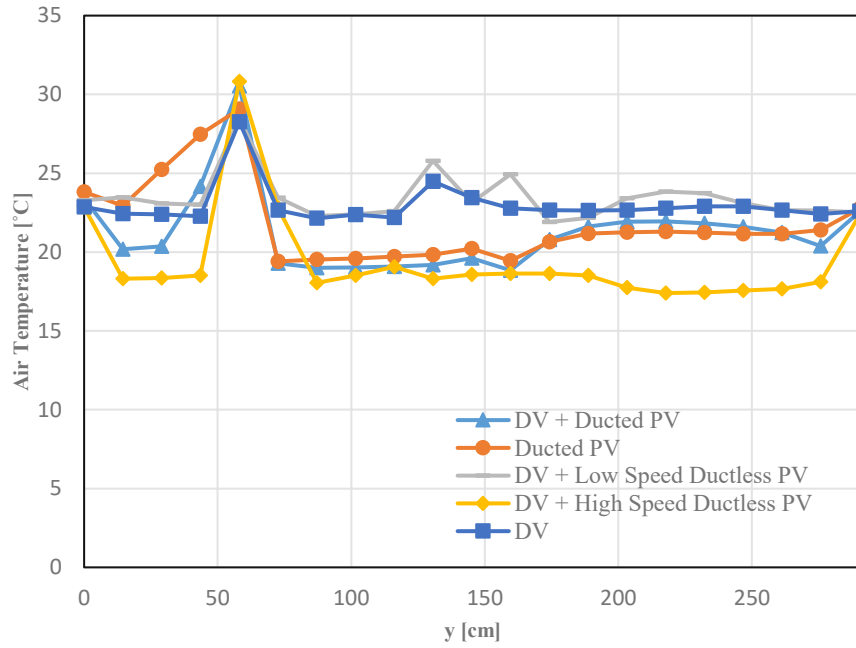
*Figure 68 Air Temperature in 110cm above the Floor in Section B-B*
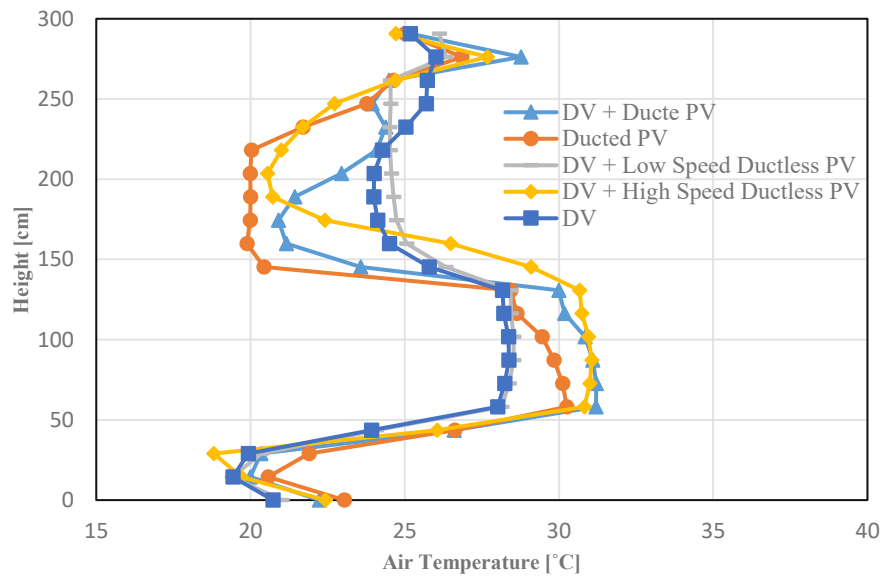


*Figure 69 Air Temperature in Occupant's Position*
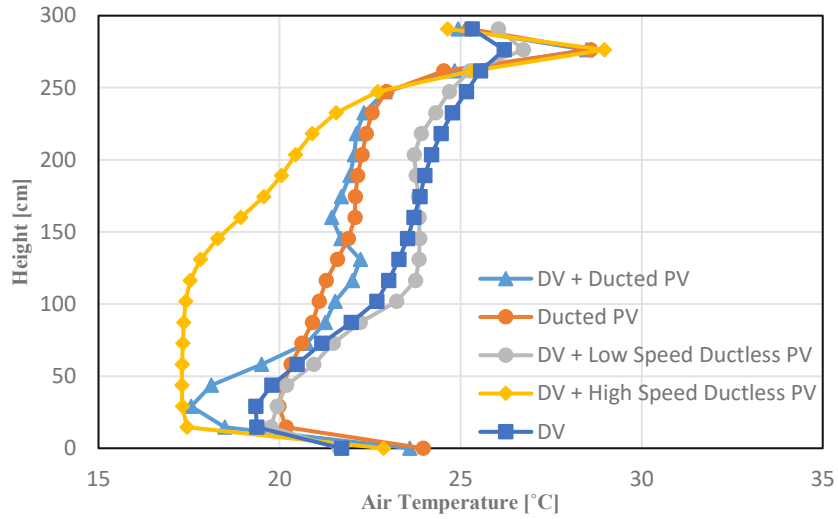
*Figure* 70 *Air Temperature in Point C*
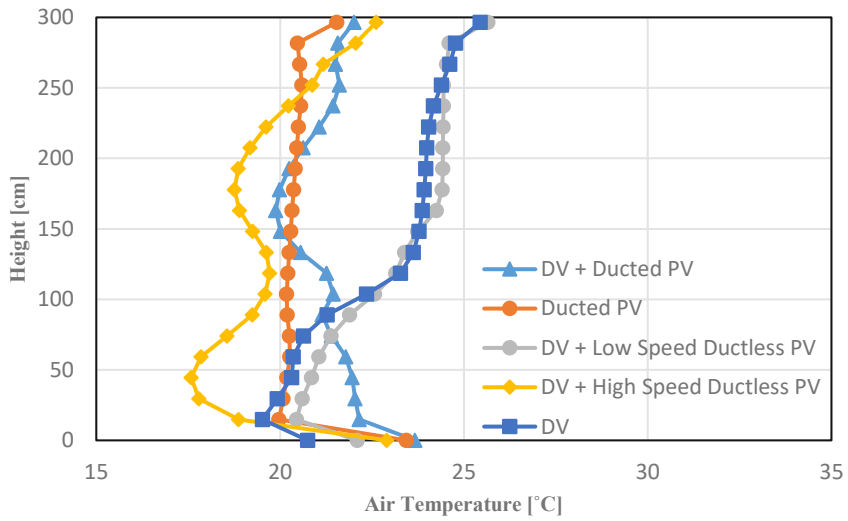


*Figure* 71 *Air Temperature in Outlet's Position*

# Chapter 5
# Conclusion

It is tried in this chapter to draw a conclusion and give concrete answers to questions of the author in the beginning of this work and assess the hypothesis which led to implement this research work.

## 5.1  Contributions

This theses was an attempt to compare the ducted and ductless variations of PV systems with each other using quantitative methods and disambiguate the uncertainties about their performances.

In the previous chapter the regional air flow characteristics as well as air velocity, direction, temperature and LMA were considered to analyze the performance of the ventilation systems in the predefined scenarios. Calculated LMA values were employed to reveal the previous and next conditions of the air particles and evaluate the efficiency of the systems in terms of providing fresh air in the intended parts of the occupied zone and removing pollutants from space.

Various scenarios were defined to represent an office setup designed for an occupant under performance of the intended ventilation systems. In the A series the CFD models were created based on the parts from the ventilation system manufacturer (Standard DV supply diffusers). These scenarios consist of five alternatives which are: DV, DV + high-speed ductless PV, DV + low-speed ductless PV, ducted PV, and DV + ducted PV. In the B series the CFD models were created based on the proposed geometry for DV supply diffuser. Four prototypes of inlet diffuser were replaced in the "DV + high-speed ductless PV" scenario to provide a basis for studying the effect of air distribution efficiency of DV in the acceleration region on the performance of ductless PV.

Comparison of PPD and PMV results on the mannequin showed that both ducted and ductless PV disturb the stratified temperature zone provided by DV system around the occupant. Thus, in practice the occupant may feel warmer in the back and is likely to suffer from air temperature asymmetry. Experiments showed that high amounts of VFR from either ducted or ductless PV could cause discomfort to the occupant. Among all of the defined scenarios in this case ducted PV had the lowest LMA values. It suggests this system generally has a superior ability to remove contaminants comparing to DV or ductless PV. Results of ductless PV scenario showed that this system is able to improve the efficiency of DV system by delivering optimum amounts of volume flow rate. Moreover, it has been shown that it can slightly improve the overall LMA values without disturbing the fresh air distribution throughout the space, nonetheless, it shortens slightly the velocity decay region of DV. Apropos, it is concluded that decreasing the speed of ductless PV fan to smaller quantities than what is studied in low speed scenario does not bring about any enhancement in the efficiency of DV system. Profiles in section B-B, reveals that in three scenarios of ducted PV, DV + ducted PV, and DV + low-speed ductless PV, the air temperatures in 110cm above the floor and around occupant's position are in average 3˚K lower than the other cases. In those three scenarios, fresh air is supplied in comparison with a higher VFR directly to this level.

It has also been illustrated that DV and DV + low-speed ductless PV scenarios could provide narrowest temperature stratification in occupant's position. However, it appears the other scenarios have better situation in other spots of the room.

The strengths and weaknesses of the studied systems which are revealed through the CFD simulations suggest the practicality of this tool in analyzing of the ventilation systems by visualizing the air flow patterns in the design phase of the AEC applications. The ability to foresee the implications of any modification in the geometry or boundary conditions prior to the implementation of the project allows engineers to study extreme situation that are difficult to reproduce in the laboratory. However, the complexity of the modeling and configuration of variables in a CFD program demands essential fluid dynamic knowledge and some level of experience in order to preclude its users from producing false and misleading results.

# Chapter 6

# Appendices

## *6.1   Nomenclature*

| | |
|---|---|
| $\upsilon$ | kinematic viscosity of the fluid |
| $A_z$ | Zone floor area |
| ADV | Advection |
| AIAA | the American Institute of Aeronautics and Astronautics |
| ATSU | Automatic Turbulent Start-Up |
| BIM | Building Information Modeling (Management) |
| BZ | Breathing Zone |
| ACE | Air Change Effectiveness |
| AEC | Architecture, Engineering and Construction |
| ASHRAE | American Society of Heating Refrigeration and Air-conditioning Engineers |
| ASHRAE HOF | ASHRAE Handbook Of Fundamentals |
| CFD | Computational Fluid Dynamics |
| DOAS | Dedicated Outdoor Air System |
| DV | Displacement Ventilation |
| $E_z$ | Air change effectiveness |
| VFR | Volume Flow Rate |
| HVAC | Heating, Ventilation and Air-Conditioning |
| IAQ | Indoor Air Quality |
| ISO | the International Organization for Standarization |
| L | A characteristic linear dimension |
| LES | Large-Eddy Simulations |
| LMA | Local Mean Age |
| MV | Mixing Ventilation |
| NTC | Negative Temperature Coefficient |
| PPD | The Predicted Percentage Dissatisfied |
| PMV | Predicted Mean Vote |
| PV | Personalized Ventilation |
| $P_z$ | Zone population |
| $Q_{ex}$ | Heat from the exterior wall and window surfaces including transmitted solar radiation |
| $Q_l$ | Heat generated by overhead lighting |
| $Q_{oe}$ | Heat generated by occupants, and equipment |

| | | |
|---|---|---|
| $Q_t$ | | The total cooling load |
| $R_p$ | | People outdoor air rate |
| $R_a$ | | Area outdoor air rate |
| $Ra$ | | Rayleigh Number |
| $RANS$ | | Reynolds averaged Navier-Stokes |
| $Re$ | | Reynolds Number |
| $SST$ | | Shear Stress Transport |
| $T_e$ | | The exhaust air temperature |
| $T_s$ | | The supply air temperature |
| $T_{sp}$ | | Room temperature |
| $T_{TconvU}$ | | Time scale for thermal transport via convection at speed U |
| $T_{Tdiff}$ | | Time scale for thermal transport via diffusion |
| $U$ | | Flow speed |
| $V$ | | The supply air volume |
| $V_{bz}$ | | The breathing zone outdoor airflow |
| $V_h$ | | The cooling air volume |
| $V_{oz}$ | | The zone outdoor airflow requirement |

## *6.2 Codes*

1. This code reads the measured values out of the files produced by ALMEMO loggers and calculates the average of the corresponding value.

```
%
%Reading measured values from excel file.
format longEng
filename1 = 'Mem-N2-G00-20160503-A2590-4S-6-48-
H12050499-L6-06.xls';
sheet1 = 'Pg1';
xlRange0 = 'A7:C368';
Data = xlsread(filename1, sheet1, xlRange0);
[a,b] = size(Data);

% Defining the headers
Headers = {'Meas.','Date & Time','Temp.01 °C'};
sheet2 = 'results';
xlRange1 = 'A1';
xlswrite(filename1,Headers,sheet2,xlRange1);

% Calculating the Averages

n = 1;
m = 1;
l = 1;

while n < a
    date1 = Data(n,1);
    date2 = Data(n+1,1);
    % Calculating The Average of each measurment
    while abs((date2-date1)) < 2.3148e-05
        subdata = Data(m:n+1,2);
        if n >= a-1
            break
        end
        n = n+1;
        date1 = Data(n,1);
        date2 = Data(n+1,1);
    end
    meas{l} = mean(subdata);
    % Writing The Measurement Number
    xlRange1 = sprintf('A%d',l+1);
    xlswrite(filename1,l,sheet2,xlRange1);
    % Writing The Time
    xlRange2 = sprintf('B%d',l+1);
    xlswrite(filename1,Data(l,1),sheet2,xlRange2);
%!!!!!!! Time is not precise !!!!!!
    % Writing The Average of Measurement
    xlRange3 = sprintf('C%d',l+1);
```

```
    xlswrite(filename1,meas{l},sheet2,xlRange3);
    if n >= a-1
        break
    end
    n = n+1;
    date1 = Data(n,1);
    date2 = Data(n+1,1);
    l = l+1;
    m = n;
end
```

2. This code reads out the measured data from files with "xls" extensions produced by ALMEMO data loggers and calculates the average of every measuremnet. The output will be written down back in a new sheet, named results, of the same spreadsheet.

```
% This script reads out the measured data from
ALMEMO data loggers .xls
% files and calculates the average of every
measuremnet. The output will be
% written down back in a new sheet, named results,
of the same
% spreadsheet. Input file should be replaced with
the content of filename1
% variable.


% Reading measured values from excel file.
filename1 = 'Mem-N2-G00-20160503-A2590-4S-6-48-
H12050499-L6-06.xls';
[Data,txt] = xlsread(filename1);
[a,b] = size(Data);
[c,d] = size(txt);

% Defining the headers
Headers{1} = 'Meas.';
Headers{2} = 'Date & Time';
i = 1;
for i = 1:d-2
    Headers{i+2} = txt{6,i+2};
end
sheet2 = 'results';
xlRange1 = 'A1';
xlswrite(filename1,Headers,sheet2,xlRange1);

% Calculating the Averages

n = 1;
m = 1;
l = 1;
i = 1;
```

```
while n < a
    date1 = Data(n,1);
    date2 = Data(n+1,1);

    % Calculating The Average of each measurment
    while abs((date2-date1)) < 2.3148e-05
        i = 1;
        for i = 1:(b-1)
            subdata{i} = Data(m:n+1,i+1);
        end

        if n >= a-1
            break
        end
        n = n+1;
        date1 = Data(n,1);
        date2 = Data(n+1,1);
    end
    % Writing The Results of The Previous Loop

    % Writing The Measurement Number
    xlRange1 = sprintf('A%d',l+1);
    xlswrite(filename1,l,sheet2,xlRange1);
    % Writing The Time
    xlRange2 = sprintf('B%d',l+1);
    meastime = datestr(Data(m,1),'mmmm dd, yy
HH:MM:SS AM');

xlswrite(filename1,{meastime},sheet2,xlRange2);

    i = 1;
    for i = 1:(b-1);
        meas{i} = mean(subdata{i});
    end
        % Writing The Average of Measurement
        xlRange3 = sprintf('C%d',l+1);
        xlswrite(filename1,meas,sheet2,xlRange3);

    if n >= a-1
        break
    end

    n = n+1;
    date1 = Data(n,1);
    date2 = Data(n+1,1);
    l = l+1;
    m = n;
end
```

3. This code is used to define the coordination of the monitor points and surface temperature sensors in the Autodesk CFD program.

```
from CFD import Setup
from CFD import Results

def main():
    study = Setup.DesignStudy.Create()
    scenario = study.getActiveScenario();
    results = scenario.results()
    results.activate()
    mp1 = Results.MonitorPoint.Create(results,
"N1", 37, 5.350000e+01, 10)
    mp2 = Results.MonitorPoint.Create(results,
"N2", 62, 5.350000e+01, 10)
    mp3 = Results.MonitorPoint.Create(results,
"N3", 87, 5.350000e+01, 10)
```

To avoid repetition the similar commands for nodes N4 to N269 are not written here.

```
    mp270 = Results.MonitorPoint.Create(results,
"N270", 262, 2.535000e+02, 110)
    mp271 = Results.MonitorPoint.Create(results,
"W1", 8, 250, 130)
    mp272 = Results.MonitorPoint.Create(results,
"F1", 3.3, 153, 136)
    mp273 = Results.MonitorPoint.Create(results,
"W2", 180, 299, 130)
    mp274 = Results.MonitorPoint.Create(results,
"W3", 396, 250, 130)
    mp275 = Results.MonitorPoint.Create(results,
"F3", 399, 153, 136)
    mp276 = Results.MonitorPoint.Create(results,
"W4", 220, 8, 130)
    mp277 = Results.MonitorPoint.Create(results,
"F2", 153, 3.3, 145)
    mp278 = Results.MonitorPoint.Create(results,
"B1", 202, 153, 0)
    mp279 = Results.MonitorPoint.Create(results,
"D1", 202, 153, 291)
    mp280 = Results.MonitorPoint.Create(results,
"O1", 346, 151, 291)
main()
```

4. This code is used for the post calculations on the produced data by Autodesk CFD.

```
% This script reads out the produced data by
AutodeskCFD and reorganize it
% in an excel spreadsheet.
```

```matlab
filename1 = 'DV - mock-up - 5 - 7sectioned -
Sc11.xlsx';
sheet1 = 1;
[Data,txt] = xlsread(filename1,sheet1);

% Extracting values of 10cm
n = 1;
r = 9;
for i = 1:9

    for j = 1:10
    VT10(r,j) = Data(4*n-3,1)/100;
    VT10(r,j+10) = Data(4*n-2,1);
    n = n+1;
    end
    r = r-1;
end
sheet3 = '10cm';
xlRange1 = 'C6';
xlswrite(filename1,VT10,sheet3,xlRange1);

% Extracting values of 60cm
r = 9;
for i = 1:9

    for j = 1:10
    VT60(r,j) = Data(4*n-3,1)/100;
    VT60(r,j+10) = Data(4*n-2,1);
    n = n+1;
    end
    r = r-1;
end
sheet4 = '60cm';
xlRange1 = 'C6';
xlswrite(filename1,VT60,sheet4,xlRange1);

% Extracting values of 110cm
r = 9;
for i = 1:9

    for j = 1:10
    VT110(r,j) = Data(4*n-3,1)/100;
    VT110(r,j+10) = Data(4*n-2,1);
    n = n+1;
    end
    r = r-1;
end
sheet5 = '110cm';
xlRange1 = 'C6';
xlswrite(filename1,VT110,sheet5,xlRange1);

% Writing summary data in a separate sheet.
```

```matlab
for i = 1:270
    
    Vsum(i,1) = Data(4*i-3,1)/100;
    Tsum(i,1) = Data(4*i-2,1);
end

sheet7 = 'Histogram';
xlRange1 = 'B4';
xlRange2 = 'F4';
xlswrite(filename1,Vsum,sheet7,xlRange1);
xlswrite(filename1,Tsum,sheet7,xlRange2);

% Transposing measured data in two columns

sheet2 = 'Meas. Data';
MeasData = xlsread(filename1,sheet2);

n = 1;
r = 9;
for i = 1:9
    
    for j = 1:10
        
        MDV(n) = MeasData(r,j);
        MDT(n) = MeasData(r,j+10);
        n = n+1;
    end
    r = r-1;
end

r = 19;
for i = 1:9
    
    for j = 1:10
        
        MDV(n) = MeasData(r,j);
        MDT(n) = MeasData(r,j+10);
        n = n+1;
    end
    r = r-1;
end

r = 29;
for i = 1:9
    
    for j = 1:10
        
        MDV(n) = MeasData(r,j);
        MDT(n) = MeasData(r,j+10);
        n = n+1;
    end
    r = r-1;
end
```

```
% Writing measured data
MDV = MDV.';
MDT = MDT.';
sheet8 = 'Histogram';
xlRange1 = 'C4';
xlRange2 = 'G4';
xlswrite(filename1,MDV,sheet8,xlRange1);
xlswrite(filename1,MDT,sheet8,xlRange2);
clear;
clc;
```

# Chapter 7
# References

AIAA, 1998. *Guide for the Verification and Validation of Computational Fluid Dynamics Simulations.* AIAA G-077-1998 ed. Reston, Virginia: s.n.

ASHRAE, 2001. *Energy Standard for Buildings Except Low-Rise Residential Buildings.* ASHRAE Standard 90.1 ed. s.l.:American Society of Heating, Refrigerating and Air-Conditioning Engineers, Inc..

Baker, A. & Gordon, E., 1997. Computational Fluid Dynamics—A Two-Edged Sword. *ASHRAE.*

Bauman, F. S., Zhang, H., Arens, E. A. & Benton, C. C., 1993. Localized comfort control with a desktop task/ambient conditioning system: laboratory and field measurements. *ASHRAE Transactions,* Volume 99, part 2, pp. 733-749.

Bordass, B. & Leaman, A., 2009. *An overview of post-occupancy evaluation,* Glasgow, UK: The Lighthouse.

Cermak R., M. A. F. L. K. O., 2006. Performance of Personalized Ventilation in Conjunction with Mixing and Displacement Ventilation. *HVAC&R Research,* Volume 12, pp. 295-311.

Chen, Q., 1997. Computational Fluid Dynamics for HVAC—Successes and Failures. *ASHRAE Transactions.*

Chen, Q. & Srebric, J., 2002. A procedure for verification, validation, and reporting of indoor environment CFD analyses. *HVAC&R Research,* Volume 8, pp. 201-216.

Comsol, 2021. *https://www.comsol.com/.* [Online] Available at: https://www.comsol.com/blogs/which-turbulence-model-

should-choose-cfd-application/
[Accessed 21 November 2021].

Comsol, 2021. *https://www.comsol.com/.* [Online]
Available at: https://www.comsol.com/blogs/characterizing-flow-choosing-right-interface/
[Accessed 21 November 2021].

Dalewski, M., Vesely, M. & & Melikov, A. K., 2012. *Ductless personalized ventilation with local air cleaning.* Brisbane, Australia, International Society of Indoor Air Quality and Climate, pp. 1-6.

Glicksman, L. & Chen, Q., 2003. *System Performance Evaluation and Design Guidelines for Displacement Ventilation.* Atlanta, GA: ASHRAE.

H.B.AWBI, 1991. *Ventilation of Buildings.* Taylor & Francis e-Library, 2003. ed. New York: Routledge.

Halvoňová B., M. A., 2010. Performance of "ductless" personalized ventilation in conjunction with displacement ventilation: Impact of disturbances due to walking person(s). *Building and Environment,* Volume 45, pp. 427-436.

Halvoňová B., M. A., 2010. Performance of "ductless" personalized ventilation in conjunction with displacement ventilation: Impact of intake height. *Building and Environment,* Volume 45, pp. 996-1005.

Halvonová B., M. A., 2010. Performance of Ductless Personalized Ventilation in Conjunction with Displacement Ventilation: Impact of Workstations Layout and Partitions. *HVAC&R Research,* Volume 16, pp. 75-94.

Kaczmarczyk J., M. A. F. P. O., 2004. Human response to personalized ventilation and mixing ventilation. *Indoor Air, International Journal of Indoor Environment and Health,* pp. 17-29.

Kwok, A. G., 2000. *Thermal Boredom.* Cambridge, UK, s.n., pp. 640-641.

Ladeinde F, Nearon M., 1997. CFD Applications in the HVAC&R Industry. *ASHRAE,* Volume 39(1), p. 44.

Launder, B. & Spalding, D., 1974. The Numerical Computation of Turbulent Flows. *Computer Methods in Applied Mechanics and Engineering,* 3(2), pp. 269-289.

Lesbirel, M., 2012. *LEED post-occupancy surveys: Designing a survey for maximum return,* USA: Brown University.

Loomans, M., 1998. *The Measurement and Simulation of Indoor Air Flow.* Ph.D. thesis ed. Eindhoven, The Netherlands: Eindhoven University of Technology.

Martin, P., 1999. Using CFD in the Real World. *ASHRAE Journal,* pp. 41(1):20-25..

Nielsen, et al., 2007. *Chair with Integrated Personalized Ventilation for Minimizing Cross Infection.* Helsinki, Finland, FINVAC ry.

Nielsen, P. V., 1995. Vertical Temperature Distribution in a Room with Displacement Ventilation. *Aalborg: Dept. of Building Technology and Structural Engineering. (Indoor Environmental Technology),* R9509(48), p. 1.

Niu, J., Gao, N., Phoebe, M. & Huigang, Z., 2007. Experimental study on a chair-based personalized ventilation systems. *Building and Environment,* Volume 42, pp. 913-925.

PADILLA-MARCOS , M., MEISS , A. & FEIJÓ-MUÑOZ , J., 2017. Proposal for a Simplified CFD Procedure for Obtaining Patterns of the Age of Air in Outdoor Spaces for the Natural Ventilation of Buildings. *Energies,* 10(9), p. 1252–1269.

Post, N., 1994. Airflow Models Gaining Clout. *ENR,* pp. 233:22-25.

Taheri, M., Schuss, M., Fail, A. & Mahdavi, A., 2016. *A performance assessment of an office space with displacement, personal, and natural ventilation systems.* Newcastle, s.n., pp. 89-100.

Taheri, M., Schuss, M., Lechleitner, J. & Mahdavi, A., 2016. *Application of calibrated CFD models for the assessment of a displacement ventilation system.* Dresden, BauSIM.

Titus-HVAC, 2021. *https://www.titus-hvac.com/.* [Online] Available at: https://www.titus-

hvac.com/file/9915/displacement_guidelines2018.pdf

[Accessed 21 November 2021].

Wiercinski, Z. & Skotnicka-Siepsiak, A., 2008. Application of CFD for temperature and air velocity distribution calculation in a ventilated room. *Task Quarterly,* Volume 12, pp. 303-312.

Wilcox, D., 1994. *Turbulence Modeling for CFD.* California: DCW Industries, Inc..

## *7.1 Tables*

## 7.2 Figures